



UNIL | Université de Lausanne

Unicentre

CH-1015 Lausanne

<http://serval.unil.ch>

Year : 2022

Probing the conformational flexibility of the Munc18-1/Syntaxin-1a complex

Stefani Ioanna

Stefani Ioanna, 2022, Probing the conformational flexibility of the Munc18-1/Syntaxin-1a complex

Originally published at : Thesis, University of Lausanne

Posted at the University of Lausanne Open Archive <http://serval.unil.ch>

Document URN : urn:nbn:ch:serval-BIB_447E0040C32C8

Droits d'auteur

L'Université de Lausanne attire expressément l'attention des utilisateurs sur le fait que tous les documents publiés dans l'Archive SERVAL sont protégés par le droit d'auteur, conformément à la loi fédérale sur le droit d'auteur et les droits voisins (LDA). A ce titre, il est indispensable d'obtenir le consentement préalable de l'auteur et/ou de l'éditeur avant toute utilisation d'une oeuvre ou d'une partie d'une oeuvre ne relevant pas d'une utilisation à des fins personnelles au sens de la LDA (art. 19, al. 1 lettre a). A défaut, tout contrevenant s'expose aux sanctions prévues par cette loi. Nous déclinons toute responsabilité en la matière.

Copyright

The University of Lausanne expressly draws the attention of users to the fact that all documents published in the SERVAL Archive are protected by copyright in accordance with federal law on copyright and similar rights (LDA). Accordingly it is indispensable to obtain prior consent from the author and/or publisher before any use of a work or part of a work for purposes other than personal use within the meaning of LDA (art. 19, para. 1 letter a). Failure to do so will expose offenders to the sanctions laid down by this law. We accept no liability in this respect.



UNIL | Université de Lausanne

Faculté de biologie
et de médecine

**Department of fundamental neurosciences
Department of computational biology**

***Probing the conformational flexibility
of the Munc18-1/Syntaxin-1a complex***

Thèse de doctorat ès sciences de la vie (PhD)

présentée à la

Faculté de biologie et de médecine
de l'Université de Lausanne

par

Ioanna STEFANI

Master of Research in Protein Structure and Function

Jury

Prof. Thomas Hügle, Président
Prof. Dirk Fasshauer, Directeur de thèse
Prof. Matthijs Verhage, Expert du comité
Prof. Julia Santiago Cuellar, Experte du comité

Lausanne
2022



UNIL | Université de Lausanne

Faculté de biologie
et de médecine

Ecole Doctorale

Doctorat ès sciences de la vie

Imprimatur

Vu le rapport présenté par le jury d'examen, composé de

Président·e	Monsieur	Prof.	Thomas	Hügler
Directeur·trice de thèse	Monsieur	Prof.	Dirk	Fasshauer
Expert·e·s	Monsieur	Prof.	Matthijs	Verhage
	Madame	Prof.	Julia	Santiago Cuellar

le Conseil de Faculté autorise l'impression de la thèse de

Ioanna Stefani

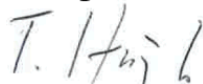
Master - Mres in protein structure and function, University of Bath, Royaume-Uni

intitulée

**Probing the conformational flexibility
of the Munc18-1/Syntaxin-1a complex**

Lausanne, le 18 février 2022

pour le Doyen
de la Faculté de biologie et de médecine


Prof. Thomas Hügle

Acknowledgements

I would like to express my deep gratitude to *Prof. Dirk Fasshauer*, my research supervisor and mentor, for his patient guidance and enthusiastic encouragement throughout my doctoral training. Thank you for trusting me with the project, leading me towards independence and molding my scientific character.

I extend my gratitude to *Prof. Julia Santiago Cuellar* and *Prof. Matthijs Verhage* for accepting to participate in my thesis committee, their interest and advice throughout the project. I also thank *Prof. Thomas Hügler* for accepting to chair my committee.

I am thankful to *Dr Justyna Iwaszkiewicz* of the Protein Modelling Facility of UniL for her guidance on the homology modeling and *Dr David Moi* from Dessimoz group for his help with Alphafold.

I am deeply thankful to all laboratory members throughout the years for the guidance, stimulating discussions and especially the fun moments at the lab, the office, and the coffee breaks. Many thanks to *Yves Mingard*, *Dr Frédérique Varoqueaux*, *Dr Emilie Neveu*, *Dr Dany Khalifeh*, *Dr Mykola Dergai*, *Dr Carlos Pulido*, *Yasmine Genolet*, *Michela Dall'Angelo*, *Iman Bentahar*, *Akansha Mehta*, *Susie Grandemange*, *Dominique Trauffer*, *Luca Truscello*, *Tristan Regazzoni* and *Rosanna Pescini*, for the help, the friendships as well as cultural, language and culinary experiences. Special thanks to *Deepak Yadav* for all the previous as well as his help with anything terminal-related and for proofreading this manuscript.

I would also like to thank my colleagues from both departments for sparking moments of joys every day. Thank you to the DNF ones: *Akrivi*, *Alejandro*, *Andrea*, *Andrian*, *Arnau*, *Bilal*, *Camille*, *Carlos*, *Gil*, *Lara*, *Laura*, *Lise*, *Ludovic*, *Magda*, *Massimo*, *Nadia*, *Nuria*, *Romain*, *Tamara*, *Theodora*, and the DBC ones, from the office, coffee, outreach, ping-pong, hiking, skiing and spinning groups: *Adriaan*, *Arvind*, *Barbara*, *Danielle*, *Debora*, *Diogo*, *Diana*, *Divyanshu*, *Florian*, *Kaido*, *Lisa*, *Marco*, *Marie*, *Marion*, *Mariona*, *Marta*, *Michelle*, *Robin*, *Simone*, *Sven*, *Theo* and *Vincent*.

Many thanks to my friends in Lausanne: *Dimitra*, *Eirini*, *Georgia*, *Giannis*, *Jason*, *Sanne*, *Sevi*, *Stephanie*, in Cyprus: *Andreani*, *Christina*, *Despo*, *Louiza*, *Maria*, *Maria* and *Savvia*, and around the globe: *Gogo*, *Heba*, *Maria*, *Maria*, *Olga*, *Petroula*, *Vaso*, *Vefa*, for their friendship, in proximity and distance.

Thanks to all my previous teachers and mentors: *Mrs Poullidou*, *Mrs Rayia*, *Mr Chatzimichael*, *Mr Zacharikos*, *Mr Sakkas*, *Mrs Zarkouloudi*, *Prof Boukouvala*, *Prof Fakis*, *Prof Glykos*, *Prof Katsani* and *Prof Licchesi*, each of whose contribution throughout my education helped me grow to who I am today. "I am indebted to my father for living, but to my teacher for living well" - *Alexander the Great*.

Finally, my heartfelt thanks to my family, my parents *Astero* and *Christos*, and my sister *Antri*, for their lifelong support, at personal and career level, as well as the financial support of my studies. *Ευχαριστώ* for teaching me the values of education and always chasing my dreams. *Ευχαριστώ* for being there!

“Beauty—be not caused, said Emily Dickinson. It is.

In one way she was wrong. The scattering of light over a long distance creates a sunset. The crashing of ocean waves on a beach created by tides, which are themselves the results of gravitational forces exerted by the sun and the moon and the rotation of the Earth. Those are causes.

The mystery lies in how those things become beautiful.”

-Matt Haig, The Humans.

To anyone who takes time to read further than this

Abstract

Munc18-1, a protein of the Sec1/Munc18-1 (SM) protein family, is interacting with high affinity with Syntaxin-1a, a neuronal SNARE protein. Neuronal SNARE proteins constitute the core machinery that drives the fusion of neurotransmitter-loaded synaptic vesicles with the plasma membrane. The tight interaction between Munc18-1 and Syntaxin-1a controls neurotransmitter release. However, biochemically this interaction inhibits SNARE complex formation, because Syntaxin-1a is locked in a closed conformation by Munc18-1. In this conformation, the SNARE domain of Syntaxin-1a is bound inside the central cavity of Munc18-1. It remains unclear whether Syntaxin-1a must leave the tight grip of Munc18-1 to adopt an open conformation that can then assemble into a SNARE complex or, whether, Munc18-1 remains bound, renders Syntaxin-1a open and by this facilitates SNARE complex formation. The latter scenario implies that the Munc18-1/Syntaxin-1a complex must be able to undergo conformational changes, a notion that is supported by Syntaxin-1a mutations that bypass the inhibitory activity of Munc18-1. Such changes might be triggered by additional factors such as Munc13 or induced by post-translational modifications. However, the mechanism of the conformational changes of the Munc18-1/Syntaxin-1a complex have remained elusive so far. To shed more light on these putative conformational changes, I have investigated the effects of several point mutations in Syntaxin-1a on its interaction with Munc18-1 using biochemical and biophysical approaches. I also examined whether these mutations can bypass the inhibition of SNARE complex formation that is exerted by Munc18-1. Lastly, I created a homologous 3D model which shows the structural changes during the conformational transitions. The results from this study suggest that Syntaxin-1a opens up while in complex with Munc18-1.

Résumé

Munc18-1, une protéine de la famille des Sec1/Munc18-1 (SM) protéines, se lie avec une grande affinité à Syntaxin-1a, une protéine qui appartient au complexe neuronal SNARE. Les protéines du complexe SNARE forment la machine principale qui permet la fusion des vésicules contenant le neurotransmetteur avec la membrane plasmique. L'interaction entre Munc18-1 et Syntaxin-1a contrôle le relâchement du neurotransmetteur. Cependant, biochimiquement, cette interaction inhibe la formation du complexe SNARE. Cela s'explique car Syntaxin-1a est bloquée en conformation fermée par Munc18-1. Dans cette conformation, le domaine SNARE de Syntaxin-1a est lié à l'intérieur de la cavité centrale de Munc18-1. Il n'est pas clair si Syntaxin-1a doit se détacher de Munc18-1 pour adopter une conformation ouverte permettant ensuite la formation du complexe SNARE, ou si Munc18-1 reste lié, rendant Syntaxin-1a ouvert et facilite ainsi la formation du complexe SNARE. Ce dernier scénario implique que le complexe Munc18-1/Syntaxin-1a doit être capable de subir des changements de conformation, ce qui est soutenu par les mutations de Syntaxin-1a qui contournent l'activité inhibitrice de Munc18-1. Ces changements pourraient être déclenchés par des facteurs tels que Munc13 ou induits par des modifications post-traductionnelles. Cependant, le mécanisme des changements de conformation du complexe Munc18-1/Syntaxin-1a est resté insaisissable jusqu'à présent. Afin d'éclaircir ces changements de conformation putatifs, j'ai étudié les effets, de manière biochimique et biophysique, de plusieurs mutations ponctuelles dans Syntaxin-1a qui changent son interaction avec Munc18-1. J'ai également examiné si ces mutations peuvent contourner l'inhibition de la formation du complexe SNARE qui est exercée par Munc18-1. Enfin, j'ai créé un modèle 3D homologue qui montre les changements structurels au cours des transitions de conformation. Les résultats de cette étude suggèrent que Syntaxin-1a s'ouvre lorsqu'elle est en complexe avec Munc18-1.

List of abbreviations

ATP	Adenosine Tri Phosphate
DNA	Deoxyribonucleic acid
Dnase	Deoxyribonuclease
DTT	Dithiothreitol
<i>E. coli</i>	Escherichia coli
EDTA	Ethylene Diamine Tetraacetic Acid
ER	Endoplasmic reticulum
FAD	Flavin adenine dinucleotide
GA	Golgi Apparatus
GTP	Guanosine Tri Phosphate
H3	SNARE domain of syntaxins
Habc domain	regulatory domain of syntaxins
IPTG	Isopropyl- β -D-Thiogalactoside
Koff	Dissociation rate
LB	Luria Bertani
LE	L165A/E166A mutant of Syntaxin-1a
Munc18	Mammalian uncoordinated protein 18
NAD	Nicotinamide adenine dinucleotide
NADP	Nicotinamide adenine dinucleotide phosphate
NSF	N-ethylmaleimide Sensitive Factor
OD	Optical Density
OG	Oregon green 488 maleimide
PAGE	Polyacrylamide Gel Electrophoresis
PMSF	Phenyl-methyl-sulphonyl-fluoride
RT	Room Temperature
SDS	Sodium Dodecyl Sulfate
SM	Sec1/Munc18 protein family
SNAP	Soluble NSF Association Proteins
SNAREs	Soluble N-ethylmaleimide-sensitive factor Attachment protein Receptors
Syb	Synaptobrevin2, R SNARE
Syb 1-96^{*28}	Syb (1-96) labeled at Cys28 with Oregon Green dye
Syx	Syntaxin, Qa-SNARE
Syx1a^{*1}	Syx1a (1-262) labelled at Cys1 with Oregon Green dye
Syx1a^{*186}	Syx1a (1-262) labelled at Cys186 with Oregon Green dye
Syx1aΔLinker^{*1}	Syx1a (1-262) Δ 161-182 labelled at Cys1 with Oregon Green dye
Syx1aΔLinker^{*186}	Syx1a (1-262) Δ 161-182 labelled at Cys186 with Oregon Green dye
Syx1aΔLE^{*186}	Syx1a (1-262) L165A/E166A labelled at Cys186 with Oregon Green dye
TEMED	N,N,N',N'-Tetramethylethylene diamine
TGN	trans-Golgi network
TR	Texas Red 520 maleimide
Tris	Tris(hydroxymethyl)-aminomethane
UV	Ultraviolet
Vps	Vacuolar protein-sorting
wt	wild-type
ΔN	Δ (1-25) mutant of Syntaxin-1

Table of contents

ACKNOWLEDGEMENTS	2
ABSTRACT	I
LIST OF ABBREVIATIONS	I
TABLE OF CONTENTS.....	I
LIST OF FIGURES.....	A
LIST OF TABLES	B
1. INTRODUCTION	1
1.1 PRESYNAPTIC FUSION MACHINERY.....	1
1.2 SNARE PROTEIN FAMILY	2
1.3 SM PROTEIN FAMILY	5
1.4 MUNC18-1	6
1.4.1 MUNC18-1/SYNTAXIN-1A INTERACTION	7
1.5 MUNC18/SYNTAXIN COMPLEX REGULATION	13
1.5.1 REGULATION THROUGH A CONFORMATIONAL TRANSITION	13
1.5.2 REGULATION THROUGH PROTEIN-PROTEIN INTERACTIONS	14
1.5.3 REGULATION BY POST-TRANSLATIONAL MODIFICATIONS	15
2. AIMS.....	17
3 MATERIALS AND METHODS	19
3.1 CHEMICALS & ENZYMES.....	19
3.2 DNA CONSTRUCTS	19
3.2.1 PROTEIN EXPRESSION AND PURIFICATION.....	21
3.3 ANALYTICAL SIZE-EXCLUSION CHROMATOGRAPHY.....	22

3.4	ANALYTICAL POLYACRYLAMIDE GEL ELECTROPHORESIS	23
3.5	INTRINSIC TRYPTOPHAN FLUORESCENCE MEASUREMENTS	23
3.6	FLUORESCENCE ANISOTROPY	24
3.6.1	FLUORESCENT PROTEIN LABELLING	24
3.6.2	FLUORESCENCE ANISOTROPY	24
3.7	HOMOLOGY MODELLING	25
4.	<u>RESULTS</u>	<u>26</u>
4.1	SYNTAXIN-1A AND MUNC18-1 MUTATIONS USED IN THE STUDY	26
4.2	MUTATIONS IN THE LINKER REGION OF SYNTAXIN-1A EASE SNARE COMPLEX FORMATION IN THE PRESENCE OF MUNC18-1.	27
4.2.1	SYNTAXIN-1A LINKER VARIANTS BIND TO MUNC18-1WT	27
4.2.2	MUNC18-1 EXERTED INHIBITION OF SNARE COMPLEX FORMATION IS OVERCOME BY SYNTAXIN-1A LINKER MUTANTS.....	28
4.3	THE INTRINSIC TRYPTOPHAN FLUORESCENCE EMISSION OF MUNC18-1_{WT} INCREASES WHEN INTERACTING WITH SYNTAXIN-1A_{WT}	32
4.3.1	TRYPTOPHAN EMITTED FLUORESCENCE INCREASE IS CAUSED BY THE INTERACTION OF MUNC18 TRYPTOPHAN ²⁸ WITH SYNTAXIN PHENYLALANINE ³⁴	32
4.3.2	THE MUNC18 TRYPTOPHAN ²⁸ – SYNTAXIN PHENYLALANINE ³⁴ PAIR CONTRIBUTES TO THE TIGHT INTERACTION OF THE TWO PROTEINS.....	34
4.4	THE LINKER BETWEEN THE N-PEPTIDE AND THE HABC DOMAIN OF SYNTAXIN-1A ALSO CONTRIBUTE TO THE TIGHT INTERACTION OF SYX AND MUNC18.	35
4.5	MUNC18-1 DOMAIN 3A REGULATES SNARE COMPLEX FORMATION	37
4.5.1	MUNC18 _{P335A} SIGNIFICANTLY AFFECTS THE INHIBITION	38
4.5.2	INHIBITION REGULATION BY DOMAIN 3A COULD BE CAUSED BY “ <i>STERIC</i> ” RESTRICTIONS.....	39
4.5.3	SNARE COMPLEX FORMATION IS PH SENSITIVE	40
4.5.4	THE A11A12 HELICAL HAIRPIN IS DISPENSABLE FOR MAINTAINING THE INHIBITION, BUT IT IS NEEDED TO KEEP THE INTERACTION.	42
4.5.5	INTERACTIONS OF BOTH DOMAIN 3A AND 1 OF MUNC18 WITH SYNTAXIN ARE NEEDED TO MAINTAIN THE TIGHT GRIP	43
4.5.6	DOMAIN 3A EXTENSION DOES NOT CLASH WITH SYNTAXIN BINDING.....	44
4.5.7	MUNC18 DOMAIN 3A TEMPLATING ROLE WAS NOT DETECTED.....	45
4.5.8	THE MUNC18 _{B10B11} HAIRPIN LOOP CONFERS INTERACTIONS NECESSARY FOR THE INHIBITION	47
4.5.9	MUTATIONS THAT DID NOT AFFECT INHIBITION.....	48

Table of contents

4.6	DISSOCIATION RATES OF THE MUNC18-1/SYNTAXIN-1A COMPLEX	51
4.6.1	SYNTAXIN LINKER MUTATIONS ACCELERATE COMPLEX DISSOCIATION	51
4.6.2	MUNC18 _{W28A} HAS THE HIGHEST DISSOCIATION RATE AMONGST THE MUNC18 MUTANTS	52
4.7	SNARE COMPLEX FORMATION OBSERVED IN THE PRESENCE OF MUNC18	53
4.8	MODELLING MUNC18 AND MUNC18/SYNTAXIN STRUCTURES IN “EXTENDED” CONFORMATION	55
4.8.1	MUNC18 AND MUNC18/SYNTAXIN MODELING BASED ON HOMOLOGOUS STRUCTURES	55
4.8.2	PREDICTED 3D STRUCTURES OF MUNC18-1 AND SYNTAXIN-1A.....	58
4.9	THE MUNC18-1/SYNTAXIN-1A COMPLEX IS PROBABLY NOT REGULATED BY NUCLEOTIDES.....	63
4.10	SNARE COMPLEX FORMS AT SIMILAR RATES ARE NOT CHANGED IN THE PRESENCE OF THE MUN DOMAIN. 65	
5.	<u>DISCUSSION</u>	<u>70</u>
6.	<u>CONCLUSION AND FUTURE DIRECTIONS</u>	<u>83</u>
7.	<u>BIBLIOGRAPHY.....</u>	<u>87</u>
APPENDIX	<u>.....</u>	<u>I</u>

List of Figures

Figure 1.1: SNARE complex assembly drives membrane fusion.	1
Figure 1.2: SNARE complex structure in cartoon with surface representation	2
Figure 1.3: Illustration of eukaryotic cell trafficking steps and indication of the SNARE subgroups involved at every step	3
Figure 1.4: Syntaxin-1a domain composition and conformations. Schematic representation of Syntaxin-1a domain composition	4
Figure 1.5: Munc18-1 in complex with Syntaxin-1a structure.	7
Figure 1.6: SM protein topology derived from eight unique crystal structures	9
Figure 1.7: Munc18 structural features: domain composition and topology.	11
Figure 1.8: Comparison of Munc18/Syntaxin complex to Vps45/Tlgg3 complex.	12
Figure 1.9: Comparison Syntaxin closed conformation to Sso1p structure.	14
Figure 3.1: Schematic representation of homology modelling process.	25
Figure 4.1: Representation of mutations in Munc18 and Syntaxin used in this study.	26
Figure 4.2: Weblogo representation of the amino-acid conservation of the Syntaxin linker region	27
Figure 4.3: Syntaxin linker mutants form a stable complex with Munc18 _{wt} shown by native gel electrophoresis.	28
Figure 4.4: Reduced inhibition of SNARE complex formation by Munc18-1 was observed for several Syntaxin-1a linker variants by fluorescence anisotropy.	29
Figure 4.5: Syx1a _{LE} (B), Syx1a _{L169A_E170A} (C), Syx1a _{ΔLinker} (D), Syx1a _{R142A_L165A} (E) and Syx1a _{E166A_F177A} (F) variants can more rapidly form a SNARE complex in the presence of Munc18-1.	30
Figure 4.6: Rate of SNARE complex formation of different syntaxin variants in complex with Munc18 _{wt} .	31
Figure 4.7: Addition of Syntaxin-1a to Munc18-1 leads to increase in tryptophan fluorescence.	32
Figure 4.8: Munc18-1 W ₂₈ interacts through pi-pi stacking with Syntaxin-1a F ₃₄ causing the increase in Tryptophan emitted fluorescence.	33
Figure 4.9: Trp ₂₈ -Phe ₃₄ interaction is important for maintaining the inhibition	34
Figure 4.10: N-terminus mutants bind to Munc18 _{wt}	36
Figure 4.11: Syx1a _{ΔN} (A), Syx1a _{3x(11-26)} (B) and Syx1a _{Δ(11-26)} (C) variants can more rapidly form a SNARE	37
Figure 4.12: Munc18 _{P335A} binds to Syntaxin _{wt} with reduced inhibitory “power”	38
Figure 4.13: Inhibition is maintained when Tyr ₃₃₇ -Asn ₁₃₅ interaction is disrupted but is affected with the introduction of negative charge	39
Figure 4.14: SNARE complex formation accelerates at acetic pH. A	41
Figure 4.15: Munc18 α ₁₁ α ₁₂ loop residues confer to inhibition.	42
Figure 4.16: SNARE complex inhibition is almost completely overcome when interactions at domain 1 and domain 3a are affected.	43
Figure 4.17 : Munc18 _x /Syntaxin mutation combinations complexes are unstable	44
Figure 4.18: Munc18 _{KEKE} behaves like Munc18 _{wt}	45
Figure 4.19: Munc18 _{D326K} and Munc18 _{L348R} .	46

Figure 4.20: Munc18 $\beta_{10}\beta_{11}$ loop residues confer to inhibition	47
Figure 4.21: Munc18 ^{Y473D} might be inhibit SC formation more than Munc18 _{wt} .	48
Figure 4.22: Munc18 ^{N261A} behaves like Munc18 _{wt} .	49
Figure 4.23: Syntaxin ^{E224A} behaves like Syntaxin _{wt}	49
Figure 4.24: Munc18 ^{R315A} inhibits like Munc18 _{wt} .	50
Figure 4.25: Dissociation rates of the Munc18 _{wt} /Syntaxin linker mutants	51
Figure 4.26 : Munc18 mutants' complexes dissociation rates.	52
Figure 4.27: Sequential addition of proteins to follow complex incorporation of labelled Syntaxin _{wt}	53
Figure 4.28: Models of Munc18 and Munc18/Syntaxin based on available homologous structures.	55
Figure 4.29: Homologous complexes' assessment using PROCHECK	57
Figure 4.30: Munc18 crystal and models' structures.	58
Figure 4.31: Comparison between domain 3a structural features of models	59
Figure 4.32: Comparison between domain 1 structural features of models	60
Figure 4.33: Munc18-1/Syntaxin-1a crystal and model structures and their superposition	61
Figure 4.34: Syntaxin N-peptide and linker region comparisons	62
Figure 4.35: SNARE complex formation in the presence of GTP or ATP.	63
Figure 4.36: SNARE complex formation in the presence of NADP (A), NADPH (B), NAD (C) and NADH(D).	64
Figure 4.37: SNARE complex inhibition is not lifted in the presence of MUN domain.	65
Figure 4.38: Munc18 ^{Δ317-333} /Syntaxin _{wt} complexes are stable also in the presence of MUN	66
Figure 4.39: MUN or Synaptobrevin gradients did not affect the Munc18/Syntaxin complex	67
Figure 4.40: SDS and Native gel electrophoreses of mixtures containing Syntaxin* ¹	68
Figure 6: Syntaxin-1a and Munc18-1 undergo a conformational transition in complex	90

List of Tables

Table 1.1: Table of PDB available Sec1/Munc18 (SM) family structures	8
Table 3.1: Munc18-1 constructs used in this study.	19
Table 3.2: Syntaxin-1a constructs used in this study.	20
Table 3.3: SNAP25, Synaptobrevin and MUN constructs used in this study.	21

1. Introduction

1.1 Presynaptic fusion machinery

One of the defining characteristics of the eukaryotic cell is the compartmentalization into membrane enclosed systems. Intracellular transport of molecules between these compartments involves membrane fusion between transport vesicles and specific compartment membranes. Soluble NSF Attachment Protein Receptor (SNARE) complex formation is the core machinery driving fusion of transport vesicles and target membranes. SNARE complex assembly is assisted by other proteins, such as tethering factors and the Sec1/Munc18 (SM) proteins, and disassembled by NSF proteins and soluble NSF attachment proteins (SNAPs). SNARE mediated fusion of the membranes is characteristic of numerous processes, including exocytosis, i.e., neuronal, pancreatic and blood cell.

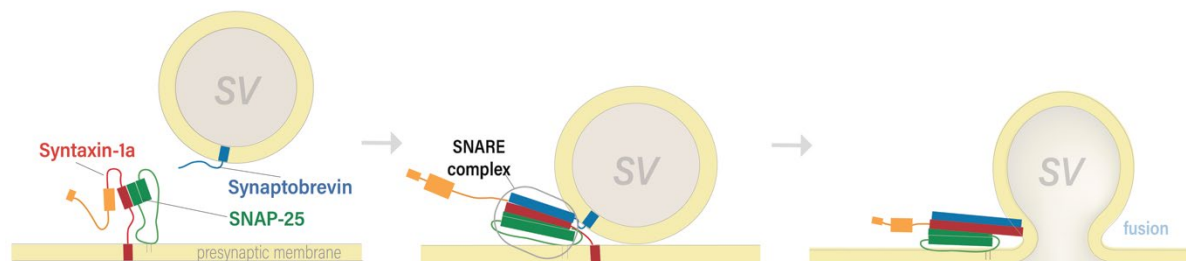


Figure 1.1: SNARE complex assembly drives membrane fusion. Assembly of the two target membrane proteins, Syntaxin and SNAP25, with the vesicle protein, Synaptobrevin, leads to the formation of a SNARE complex. This tight four-helix bundle assists the merging of the two membranes, i.e. the fusion of the vesicle with the plasma membrane.

Neuronal communication between nerve terminals is achieved by the release of neurotransmitter molecules at the synaptic cleft. Neurotransmitters are loaded to synaptic vesicles via active transport performed by proton pumps. Synaptic vesicles then translocate to the release site and cluster at the active zone where they are docked and primed (Jahn and Fasshauer, 2012, Sudhof, 2004). Action potentials arriving to the presynaptic terminals trigger Ca^{2+} -depended synaptic exocytosis, characterized by the fusion of synaptic vesicles carrying neurotransmitters with the presynaptic plasma membrane (Figure 1.1). Synaptic fusion is achieved by the zippering of the SNARE domains of Syntaxin-1a and SNAP25 (plasma membrane) with the SNARE domain of Synaptobrevin (vesicle) into a four-helical bundle, the SNARE complex (Sutton et al., 1998).

1.2 SNARE protein family

SNARE proteins are relatively small cytoplasmatic orientated membrane associated proteins, characterized by the presence of the 70-residue long SNARE motif, by which they interact forming the SNARE complex (Figure 1.2.). In isolation, they are intrinsically disordered. They interact by zippering into a four-helical bundle, a parallel coiled coil. Coiled-coil proteins are characterized by seven residue repeats, with nonpolar side chains at the first (a) and fourth (d) positions (Hodges, 1973).

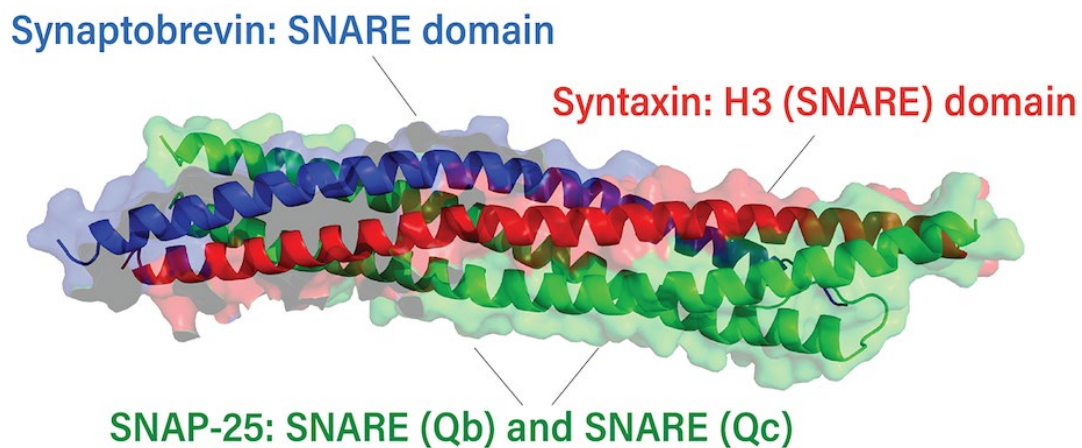


Figure 1.2: SNARE complex structure in cartoon with surface representation (PDB: 1sfc). SNARE motifs are contributed by Qa SNARE-Syntaxin (red), Qb SNARE-SNAP25-N (green), Qc SNARE-SNAP25-C (green), R- SNARE-Synaptobrevin (blue).

The structural features of the assembled SNARE complex allowed for the identification of the 16 highly conserved layers of interacting amino acid side chains in the center of the four-helix bundle (Fasshauer et al., 1998). The central layer (0 layer) is composed of three Glutamine (Q) residues and one Arginine (R) residue, each contributed by a distinct SNARE motif. The presence of these conserved residues at the center of the SNARE motif led to the classification of the SNARE protein family into Q-SNAREs and R-SNAREs, thus forming the Qa, Qb, Qc and R classes (Bock et al., 2001). They were afterwards further classified by sequence analysis into 20 basic SNARE subgroups where they cluster according to their sequence. SNARE protein subgroups categorized based on the intracellular compartment they localize: I. Endoplasmic reticulum, II. Golgi apparatus, IIIa. *trans*-Golgi network, IIIb. Endosomal compartments and IV. Secretion (Figure 1.3) (Kloepper et al., 2007).

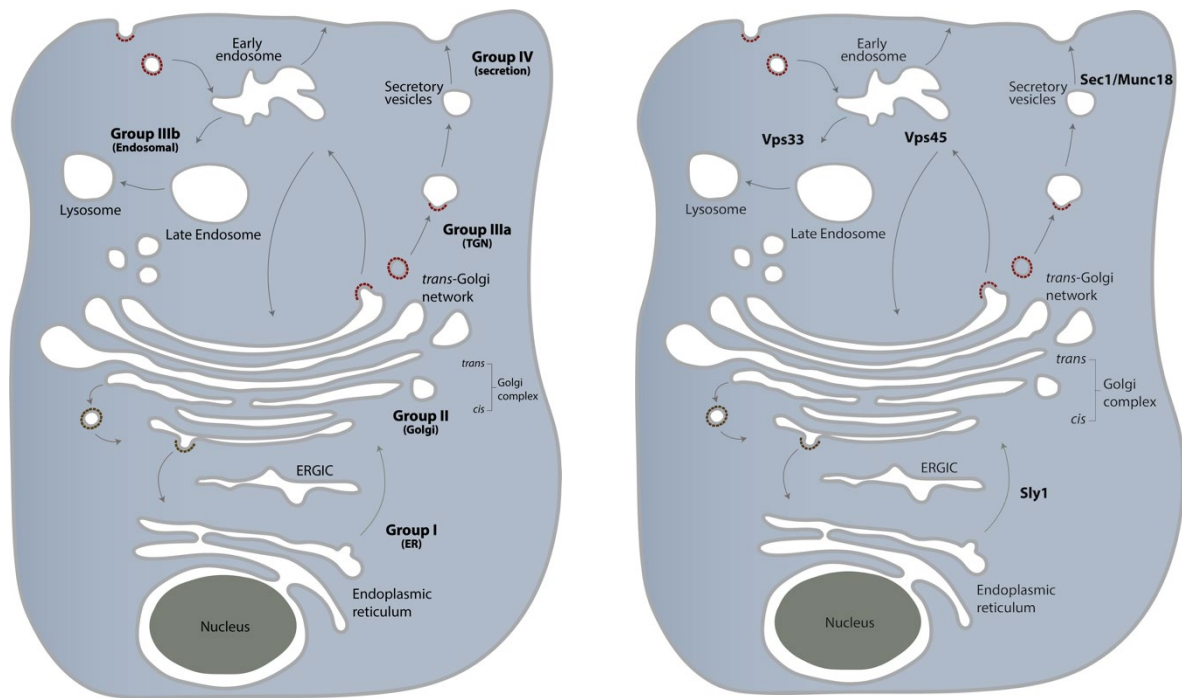


Figure 1.3: Illustration of eukaryotic cell trafficking steps and indication of the SNARE subgroups involved at every step (left) and the SM proteins involved in the respective steps (right). Adapted from (Yu and Hughson, 2010).

At the presynaptic terminal, besides with its SNARE partners, Syntaxin-1a (Qa_{IV}), also interacts with Munc18-1, an SM protein. Members of the SM family interact with their cognate Syntaxin (Qa-SNARE) and facilitate vesicle fusion, in a fashion that is not well understood yet. *In vitro*, the strong interaction of Munc18-1 with Syntaxin-1a inhibits binding of the latter to its SNARE partners, SNAP25 and Synaptobrevin (Pevsner et al., 1994c). This interaction will be further discussed later.

Syntaxin-1a possesses three larger structurally distinct regions: a SNARE motif (H3 domain), an N-terminal regulatory domain, which folds into a three-helix bundle (Habc domain), and a C-terminal transmembrane domain (TMR) (Figure 1.4). Other smaller regions, such as the very N-terminal region (the so-called N-peptide) and the region between the Habc and H3 domains, the linker region, have a regulatory function for the interaction of Syntaxin-1a with Munc18-1 (Burkhardt et al., 2008).

Mutations in these regions seem to affect the function of Syntaxin-1a, probably due to interference with its interactions with binding partners and its conformational transitions.

Syntaxin-1a assembles into SNARE complex with SNAP25 and Synaptobrevin through interactions with its H3 forming (Söllner et al., 1993, Sutton et al., 1998). Additionally, Syntaxin-1a assembles in another interacting complex. Syntaxin-1a interacts with Munc18-1, through an interaction which inhibits Syntaxin-1a from interacting with SNAP25 and Synaptobrevin (Pevsner et al., 1994a). Structurally, Syntaxin-1a is thought to exist in two conformations: Open and closed (Fig 1.4). Syntaxin is considered in open conformation when the SNARE motif (Syntaxin H3) is in SNARE complex (PDB entry: 1sfc). Within the SNARE complex, the Syntaxin H3 folds into an extended non-interrupted helix. However, in closed conformation, as determined when Syntaxin-1a interacts with Munc18-1 (PDB entry: 3c98), H3 is partially interacting with its own Habc domain, and is partially distorted and buried within the Munc18 central

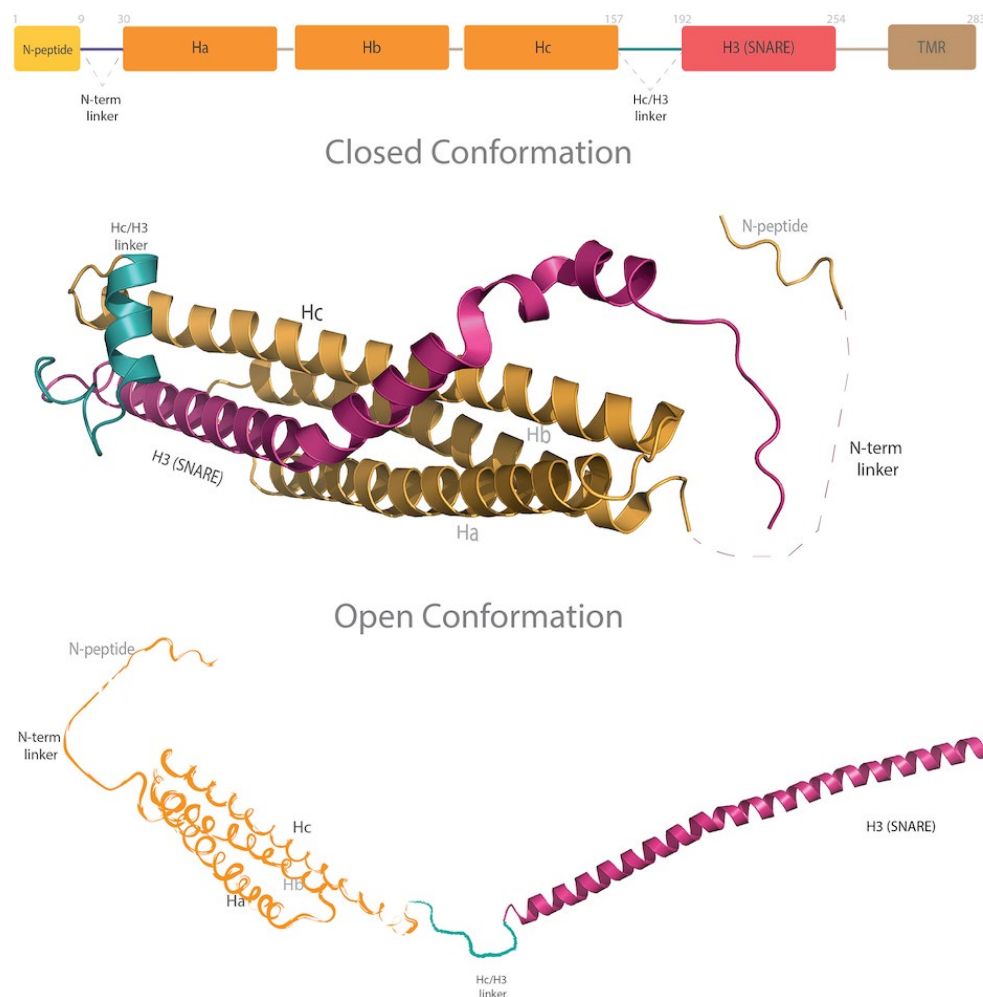


Figure 1.4: Syntaxin-1a domain composition and conformations. Schematic representation of Syntaxin-1a domain composition (top) Highlighted with light yellow the N-peptide, with orange the Habc domain, red the SNARE motif and pink the transmembrane domain (TMR). Cartoon representation of closed conformation (middle) from the Munc18/Syntaxin complex (pdb: 3c98) and drawing of a hypothetical open conformation based on the SNARE domain structure from the SNARE complex (pdb: 1sfc).

cavity. The linker between the domains Habc and H3 partially forms a small helix extending almost vertically over the end of Hc and the start of H3 helices. In this conformation, Syntaxin does not allow SNARE complex formation.

The structure of Syntaxin linker region is flexible. This means that it can fluctuate between a partially helical structure, described above for the closed conformation, to being mainly unstructured in the open conformation (Margittai et al., 2003). A well-studied mutant in the Syntaxin linker region, the so-called LE mutant, referred to hereafter as Syx1a^{LE}, also supports the importance of this region for the function of Syntaxin (Dulubova et al., 1999). Although Syx1a^{LE} is often referred to as "open Syntaxin", since it was initially thought to prevent Syntaxin to form the closed conformation and to be unable to interact with Munc18 (Dulubova et al., 1999), it was later shown that Syx1a^{LE} can still bind tightly to Munc18 but also that the mutation overcomes the inhibition of Munc18-1 observed *in vitro* and that Syx1a^{LE} proceeds to SNARE complex formation even in the presence of Munc18-1 (Burkhardt et al., 2008). In Syntaxin-1a knock out mice, expression of Syntaxin-1b^{LE}, the second Syntaxin isoform carrying the LE mutations, drastically enhances the rate of synaptic vesicle fusion (Gerber et al., 2008). In the same study, homozygous Syx1b^{LE} mice were severely ataxic with lethal epileptic seizures after that are 2 weeks old. Combined, these observations suggested an important role for the Syntaxin linker in maintaining or regulating the "opening" of Syntaxin-1a and/or its interaction with Munc18-1 and SNARE proteins. Therefore, further investigation on the effect of this region on the interaction with Munc18-1 and SNARE complex formation could shed light on how the transition of Syntaxin-1a conformations is achieved.

1.3 SM protein family

As mentioned above, the SNARE mediated fusion of vesicles is regulated also through their interaction with proteins of the SM family. Members of this family were initially discovered by genetic screening of *C. elegans* with uncoordinated behavior phenotype, unc-18, (Brenner, 1974) and of secretion mutants, Sec1, of the yeast *S. cerevisiae* (Novick and Schekman, 1979). Generally, SM proteins are cytoplasmic proteins, with a molecular weight of around 70kDa, that act at distinct vesicle trafficking steps by interacting with their cognate Syntaxin (Qa-SNARE). As outlined above, Munc18s (Munc18-1 orthologs or isoforms) are involved in exocytosis, whereas other SM proteins function in vesicle trafficking steps between compartments: Sly1s in ER-Golgi trafficking, Vps45s in the

trans-Golgi network and Vps33s in the vacuolar-lysosomal processes (Toonen and Verhage, 2003, Morey et al., 2017). However, it is not entirely understood how the vesicular transport is facilitated by SM proteins.

1.4 Munc18-1

Whereas most eukaryotes possess one SM protein involved in secretion, vertebrates possess three Munc18 isoforms with tissue specific distribution. Munc18-1 is involved mainly in neuronal exocytosis, whilst Munc18-2 and Munc18-3 are, among other things, involved in immune cells' exocytosis and glucose transporter 4 (GLUT4) exocytosis, respectively, have a more ubiquitous distribution (Toonen and Verhage, 2003).

Munc18-1 is the most extensively studied member of the SM family. Interaction of Munc18-1 with Syntaxin-1a at the presynaptic terminals is indispensable for neurotransmission, as Munc18-1 knock-out in mice leads to depletion of synaptic transmission (Verhage et al., 2000). The distribution of two known splice variants of Munc18, long (M18L, or Munc18-1a) and short (M18S, or Munc18-1b), has been characterized. M18L variant (603aa) differs from the M18S variant (594aa) by an eleven amino-acid elongation of the C-terminus. M18L variant localizes specifically in inhibitory (GABAergic) terminals of hippocampal interneurons and its reduction is suspected to contribute to cognitive decline. M18S is broadly distributed to both GABAergic as well as glutamatergic terminals (Ramos-Miguel et al., 2015). Both splice variants shown to support synaptic secretion to a similar extent, differ however in their ability to support vesicle release during short term plasticity (Meijer et al., 2015).

Variations in Munc18 quantities are responsible for several neuro and neurodevelopmental disorders. Destabilization of the Munc18-1/Syntaxin-1a balance has been linked with Schizophrenia (Gil-Pisa et al., 2012). *De novo* mutations (missense, nonsense, splice site and frameshift) in the STXBP1 gene, which codes for Munc18-1, have been identified in patients with Ohtahara, West, and Dravet syndromes, early-onset epileptic encephalopathy, non-syndromic epilepsy, intellectual disability, and autism (Stamberger et al., 2016). Synaptic strength reduction of parvalumin-expressing interneurons and decreased connectivity of somatostatin-expressing neurons in STXBP1 haploinsufficient mice was suggested to be the defying mechanism for the observed reduced cortical inhibition and the linked neurobehavioral phenotypes (Chen et al., 2020a). However, it has been also suggested that missense mutations of Munc18 can have

dominant negative effect, as they misfold and act as aggregation nuclei for Munc18 wt, resulting to even lower levels of functional proteins (Guiberson et al., 2018).

1.4.1 Munc18-1/Syntaxin-1a interaction

Munc18-1 consists of 3 structurally distinct domains that fold into an arch-shaped globular protein (Figure 1.5). This arch-shaped protein wraps around Syntaxin-1a in closed conformation through interactions of the Syntaxin Ha and Hc helices with the binding cleft of Munc18-1, the inner hydrophobic cavity formed between the domains 3a and 1 (Misura et al., 2000, Burkhardt et al., 2008). This interaction locks Syntaxin in the closed conformation and in which, *in vitro*, Syntaxin is unable to form the SNARE complex

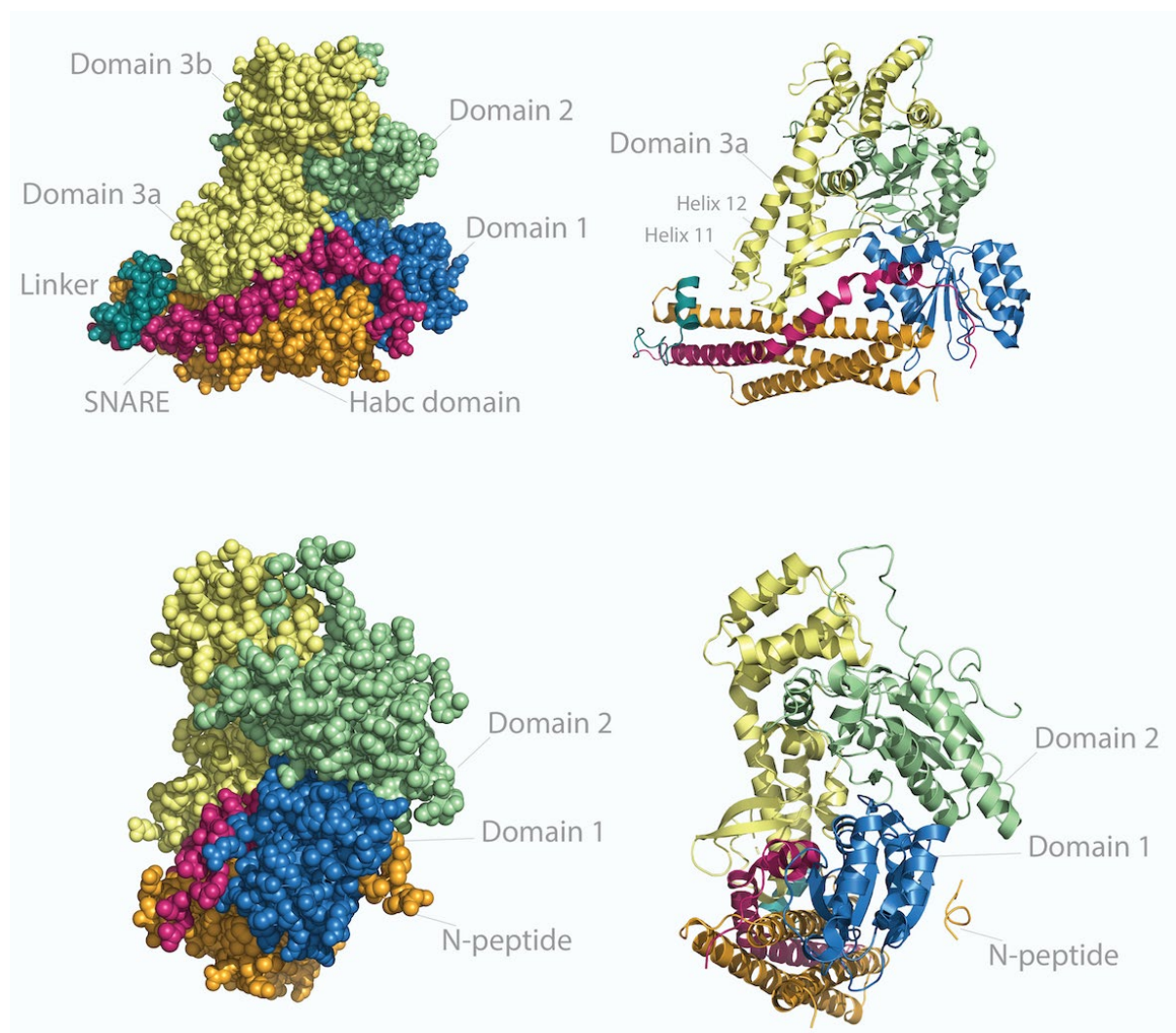


Figure 1.5: Munc18-1 in complex with Syntaxin-1a structure. Spheres (left) and cartoon representation (right) of the two proteins in complex (pdb: 3c98) in “front” (top) and “side” view (bottom). Munc18 domain 1 is coloured blue, domain 2 green and domain 3 yellow. Syntaxin Habc is coloured orange and SNARE magenta. Domains as well as important regions on both proteins (Syntaxin Linker, Munc18 domain 3a helices 11 & 12) that are mentioned in the current study are indicated.

(Dulubova et al., 1999). This tight binding mode appears to disagree with genetic observations, which rather promote a facilitating role of Munc18 in vesicle fusion. An additional binding site involves interactions at the outer surface of domain 1 of Munc18 with the Syntaxin-1a N-peptide (Burkhardt et al., 2008).

The N-peptide interaction mode is common between Munc18s (Hu et al., 2007, Christie et al., 2012, Morey et al., 2017) as well as other SM proteins, such as Vps45 (Furgason et al., 2009, Eisemann et al., 2020) and Sly1p (Demircioglu et al., 2014, Yamaguchi et al., 2002). Interestingly, some members of this family do not possess the N-peptide binding mode. In particular, Vps33A does have the necessary hydrophobic N-peptide binding pocket (Hu et al., 2007). It should be noted that Vam3, which is a cognate Qa- SNARE, does not adopt a closed conformation (Dulubova et al., 2001).

The *in vivo* role of this N-peptide interaction is elusive. In Munc18 null neurons, and Syntaxin-depleted PC12 cells, secretion is restored even if N-peptide interactions are disrupted (Meijer et al., 2012, Park et al., 2016). Additionally, PC12 secretion as well as Syntaxin plasma membrane localization are abolished when single N-peptide mutations are introduced to Syx^{LE}. These observations agree with a recent study in Syntaxin null mice, where neuronal survival and neurotransmitter release from central synapses are not impaired when N-peptide is deleted (Vardar et al., 2021). Interestingly, in the same study, neurotransmitter release was not affected when they used a Syx^{LE} mutant lacking

Entry ID	DOI	Publication Year	Structure Title
1EPU	10.1016/S0969-2126(00)00156-8	2000	X-ray crystal structure of neuronal Sec1 from squid
1FVF	10.1006/jmbi.2000.4347	2001	Crystal structure analysis of neuronal Sec1 from the squid <i>L. palei</i>
1FVH	10.1006/jmbi.2000.4347	2001	Crystal structure analysis of neuronal Sec1 from the squid <i>L. palei</i>
1HS7	10.1038/85012	2001	Vam3p N-terminal domain solution structure
1MQS	10.1093/emboj/cdf608	2002	Crystal structure of Sly1p in complex with an N-terminal peptide of Sed5p
1Y9J	10.1016/j.jmb.2004.12.004	2005	Solution structure of the rat Sly1 N-terminal domain
3C9B	10.1038/emboj.2008.37	2008	Revised structure of the munc18a-syntaxin1 complex
2XHE	10.1073/PNAS.1106189108	2011	Crystal structure of the Unc18-syntaxin 1 complex from <i>Monosiga brevicollis</i>
3PUJ	10.1073/pnas.0914906108	2011	Crystal structure of the Munc18-1 and Syntaxin-4 N-Peptide complex
3PUK	10.1073/pnas.0914906108	2011	Re-refinement of the crystal structure of Munc18-3 and Syntaxin4 N-peptide complex
4BX8	10.1073/PNAS.1307074110	2013	Human Vps33A
4BX9	10.1073/pnas.1307074110	2013	Human Vps33A in complex with a fragment of human Vps16
4CCA	10.1073/PNAS.1313474110	2013	Structure of human Munc18-2
4JCB	10.1371/journal.pone.0067409	2013	Crystal Structure of HOPS component Vps33 from <i>Chaetomium thermophilum</i>
4JEH	10.1073/pnas.1303753110	2013	Crystal Structure of Munc18a and Syntaxin1 lacking N-peptide complex
4JEU	10.1073/pnas.1303753110	2013	Crystal Structure of Munc18a and Syntaxin1 with native N-terminus complex
4KMO	10.1371/journal.pone.0067409	2013	Crystal Structure of the Vps33-Vps16 HOPS subcomplex from <i>Chaetomium thermophilum</i>
5BUZ	10.1126/science.aac7906	2015	Crystal Structure of a Complex Between the SNARE Vam3 and the HOPS Vps33-Vps16 subcomplex from <i>Chaetomium thermophilum</i>
5BV0	10.1126/science.aac7906	2015	Crystal Structure of a Complex Between the SNARE Nyv1 and the HOPS Vps33-Vps16 subcomplex from <i>Chaetomium thermophilum</i>
5BV1	10.1126/science.aac7906	2015	Crystal Structure of a Vps33-Vps16 Complex from <i>Chaetomium thermophilum</i>
6LPC	10.15252/emboj.2019103631	2020	Crystal Structure of rat Munc18-1 with K332E/K333E mutation
6XJL	10.7554/eLife.60724	2020	Structure of the SM protein Vps45
6XM1	10.7554/eLife.60724	2020	SM Protein Vps45 in Complex with Qa SNARE Tlg2
6XMD	10.7554/eLife.60724	2020	SM Protein Vps45 in Complex with Qa SNARE Tlg2 (1-310)

Table 1.1: Table of PDB available Sec1/Munc18 (SM) family structures

Introduction

the N-peptide, despite the observed reduction of docked vesicles and ultimate neuronal death.

An annotation of the available PDB structures of SM proteins is demonstrated at Table 1.1. Notably, other SM proteins fold into the same arch-shaped structure with conserved topology (Figure 1.6). As summarized by Archbold et al., 2014, all SM proteins share U-shaped architecture, where domain 3 is inserted by splitting domain 2. Domain 1 adopts a Rossmann fold and domain 2 is structurally similar, but with some difference in the connectivity to domain 1. Domain 3, whose topology is conserved in all SM crystal structures is subdivided into domain 3a and 3b (Archbold et al., 2014).

The structure of Vps33 in complex with Vam3 (Qa SNARE) and Nyv1 (R SNARE), has revealed a different binding mode where both SNARE motifs of the Qa- and R-SNAREs bind to Vps33 at two, non-overlapping, binding sites (Baker et al., 2015). Whether this binding mode is different to the one observed for Munc18 or whether it

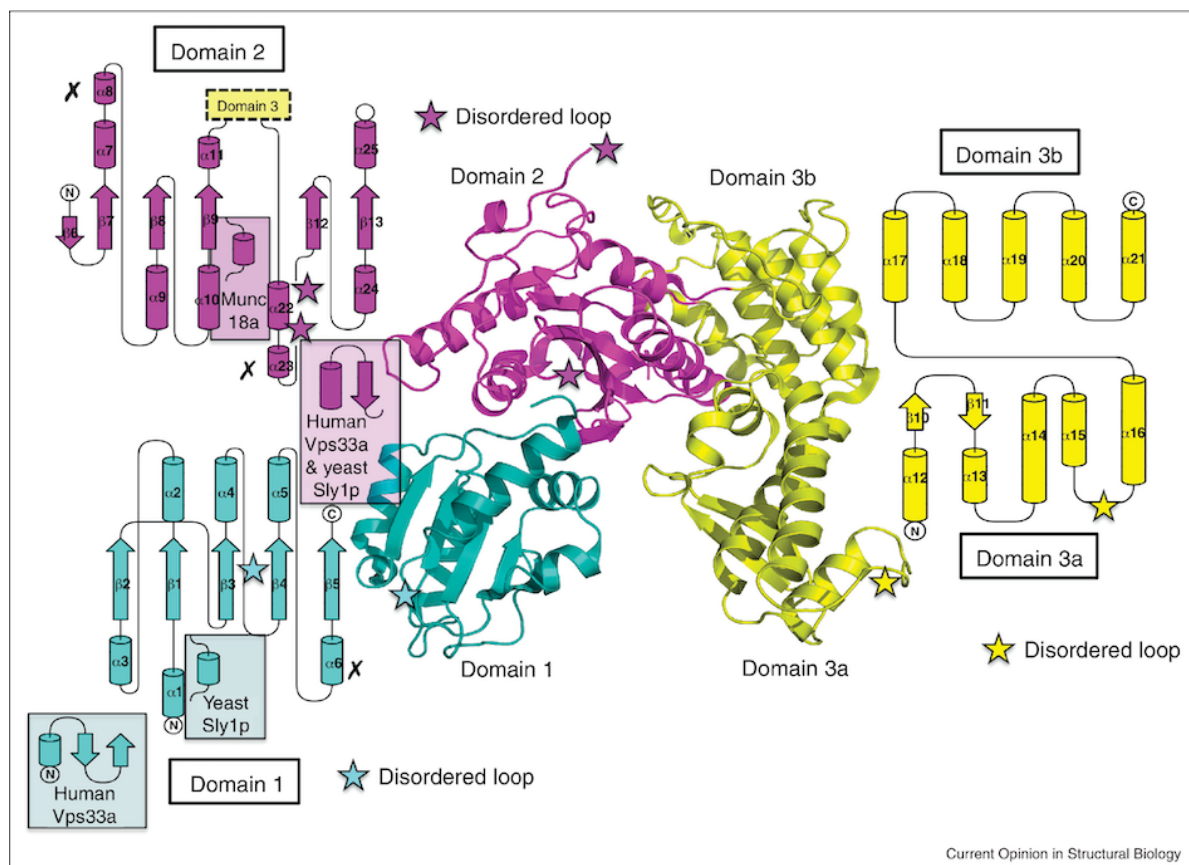


Figure 1.6: SM protein topology derived from eight unique crystal structures. *Monosiga brevicollis* Unc18-1 (pdb: 2xhe) in cartoon representation in the central panel. SM proteins fold into the arch shape of three structurally distinct domains: domain 1 (blue), domain 2 (magenta) and domain 3 (yellow). The disordered regions are indicated with stars. Adopted from (Archbold et al., 2014).

could be a snapshot of a later step in the assembly cascade, at which the SM protein arranges SNARE proteins for final zippering is unclear yet.

Of specific importance is the loop between the helices 11 and 12 of domain 3a (residues 317-333). In the Munc18-1/Syntaxin-1a structure (PDB Entry: 3C98), this loop is partly disordered (Figure 1.7). The rest folds back towards Munc18, whilst in the structure of Munc18-1 and of Munc18-3 in complex with the Syntaxin-4 N-peptide (PDB Entries: 3PUJ, 3PUK) or the Munc18-2 alone (PDB Entry: 4CCA) this region adopts a helical fold which leads to an extension of helix 12.

Several residues of domain 3 loop have been studied for their contribution to the interaction Munc18-1/Syntaxin-1a. For instance, mutations clustering at tip of *sec1* (yeast Munc18-1 homologue) domain 3a were found to have dominant negative effect on invertase secretion. Their corresponding mutations on Munc18-1 caused inhibition of exocytosis when tested in bovine chromaffin cells (Boyd et al., 2008a). Munc18-1 domain 3a is thought to interact with Synaptobrevin. Mutations such as D326K and L348R were introduced into Munc18-1 to study the effect on Synaptobrevin binding. The effect of these mutations, promotion (D326K) and inhibition (L348R) of SNARE complex formation SNARE assembly assessed through lipid mixing assays was attributed to an interference with binding of Synaptobrevin-2 to Munc18-1on (Parisotto et al., 2014, Sitarska et al., 2017).

In Munc18-1 deficient cells, neither Munc18-1 Δ 317-333 nor Munc18-1 Δ 324-339, Munc18-1 variants with truncated loop, were able to rescue fusion of secretory granules, although binding to Syntaxin-1a *in vitro* seemed indistinguishable from that of Munc18-1 wt (Martin et al., 2013, Munch et al., 2016). Munc18-1 Δ 317-333 has reduced mobility, to Munc18-1_{wt} when probed by single molecule analysis (Kasula et al., 2016).

Also, the presence of a Proline residue (P335) at the tip of helix 12, which can act as a hinge residue for regulation of the loop, supports the idea of a conformational switch (Han et al., 2014). Substitution of P335 with an alanine residue, inserted to extend helix 12, exhibits gain-of-function effects on exocytosis, *in vivo* and *in vitro* (Han et al., 2014; Parisotto et al., 2014; Munch et al., 2016; Park et al., 2017). The marked conservation of proline 335 and the pathogenic phenotype of individuals carrying mutations at this position (P335S and P335L) point towards a key role of this helix breaking proline for Munc18-1 function (Hu et al., 2011, Stamberger et al., 2016).

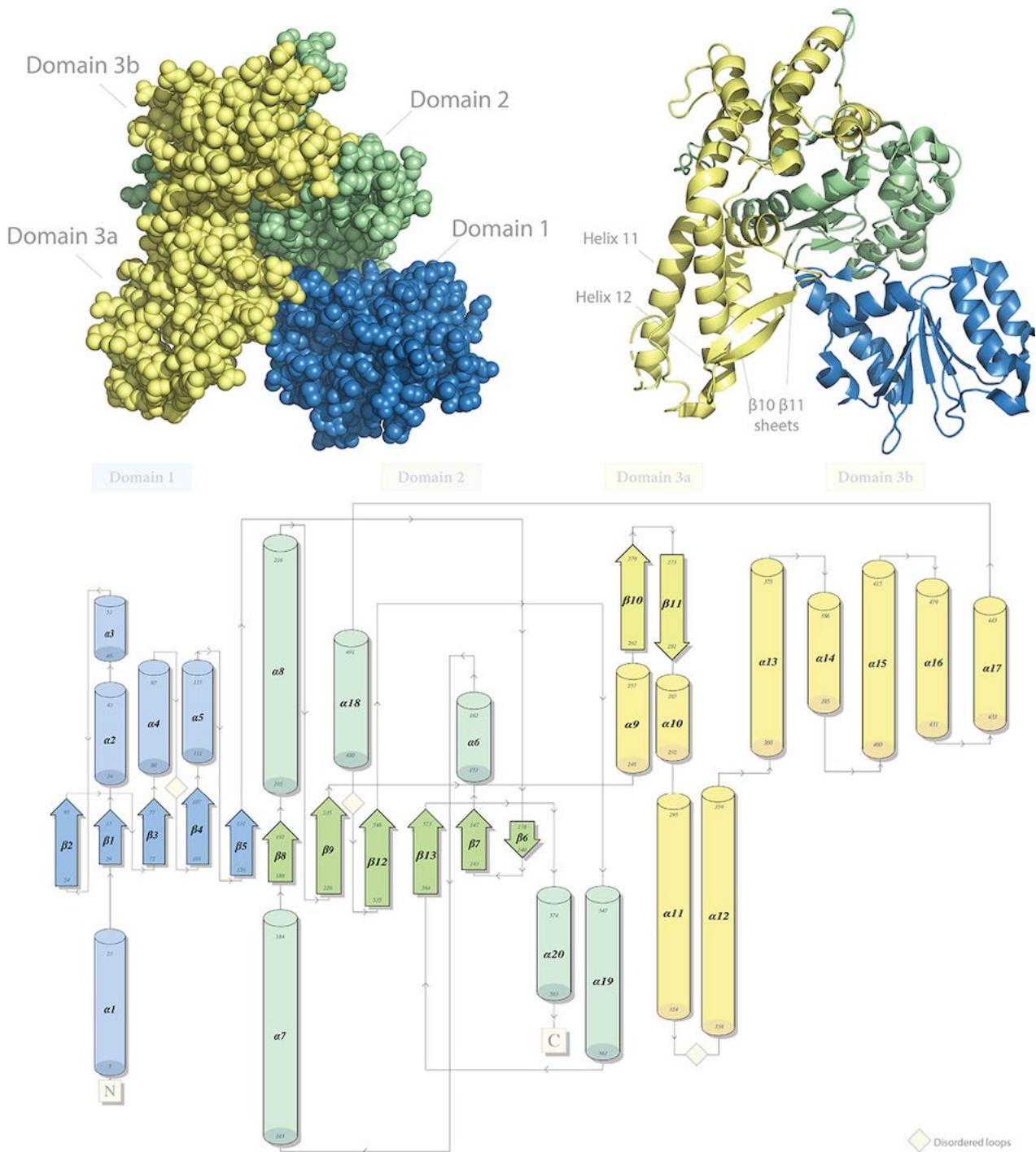


Figure 1.7: Munc18 structural features: domain composition and topology. Munc18 from [pdb:3c98](#) structure in spheres (left), cartoon representation (right) and structural topology (bottom). Domain 1 is coloured blue, domain 2 green and domain 3 yellow. Important loops that are mentioned in the current study are indicated (Helices 11& 12, $\beta 10\beta 11$ loop). Disordered loops from the complex' structure are noted with square.

In agreement with this idea, the recently resolved structure of another SM, Vps45, in complex with its cognate Qa- SNARE, Tlg2, has finally shed more light to the SM/Qa SNARE interaction (Eisemann et al., 2020). The structure of this complex has revealed

another binding mode for the complex. Vps45 bound to a not so closed Tlg2. Vps45 domain 3a helices 11 and 12 adopt an unfurled, helical extended conformation while Tlg2 is bound, through N-peptide, Habc domain and H3 domain (Figure 1.8). Notably, Tlg2 adopts a new conformation, neither closed nor open, where the H3 is shaping into a less interrupted, as compared to the one observed at the Munc18/Syntaxin, helix.

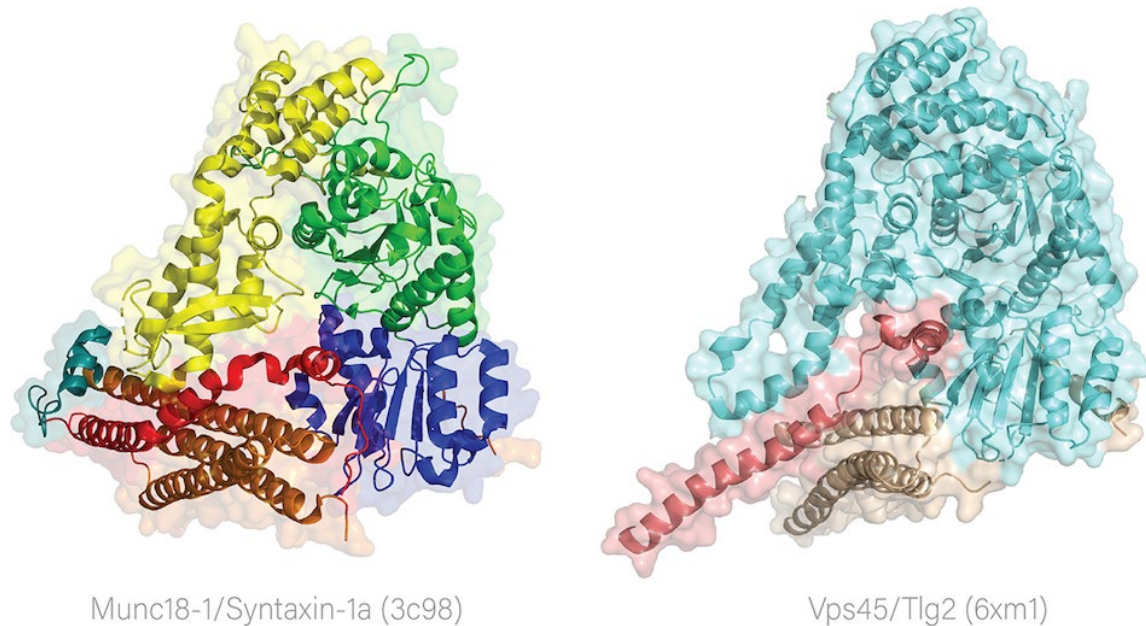


Figure 1.8: Comparison of Munc18/Syntaxin complex to Vps45/Tlgg3 complex. Cartoon and surface representations of the Munc18/Syntaxin (pdb:3c98) complex (left) and Vps45/Tlg2 (6xm1). Munc18 domains are colored as previously described (Fig 1.5). Vps45 (colored light blue), also arch shaped, with helices 11 and 12 helically structured (extended). Tlg2 Habc domain (light brown) is buried inside the cavity formed Vps45 while Tlg2 H3 domain (light red) is adopting an extended helix conformation that protrudes the complex' structure. Tlg2's linker structure has not been resolved.

The extension of Munc18 domain 3a helices 11 and 12 has been recently observed. The structure of Munc18-1 bearing two sequential mutations (K332E, K333E) at the hinge of helix 11 (Munc18^{KEKE}) has been solved (Wang et al., 2020) confirming the notion that Munc18-1 can also undergo conformational change at domain 3a as the other SM homologues. It is, therefore, becoming more and more probable that Munc18 domain 3a regulates the Munc18/Syntaxin, and SNARE, complexes' interactions in a manner involving a conformational change of the helices' 11 and 12 hinge loop.

But how is this regulation exerted?

1.5 Munc18/Syntaxin complex regulation

1.5.1 Regulation through a conformational transition

As mentioned above, Syntaxin can fold into two conformations, at least. A closed (Munc18-1 bound) and an open (in SNARE complex). So far, mutations at two Syntaxin regions, linker, and N-peptide, have indicated a possibility for additional Syntaxin conformation. *In vitro*, disruption of the N-peptide interactions impairs the Munc18 exerted inhibition of SNARE complex formation (Burkhardt et al., 2008), comparable to the Syx1a^{LE} caused effects. The differences on the emitted Tryptophan fluorescence when these mutants interact with Munc18, in comparison to when Syntaxin_{wt} is interacting, indicate that small structural changes could be taking place. Structurally, both mutants (Syx^{LE} and Syx^{ΔN}) bind to Munc18 in close conformation (Colbert et al., 2013). The overall similar effects caused by those two mutations point towards a possible communication of these two spatially distinct regions.

Consequently, the involvement of the Syntaxin linker region is being extensively studied, as its flexibility when Syntaxin is in solution (Margittai et al., 2003) as well as its protruding position and proximity to Munc18 domain 3a (when in complex with Munc18) makes it a good candidate for a Syntaxin conformational regulator. It is possible that this inhibition could be caused not only by the interactions between the two domains (Habc and SNARE), but also by the structural features of this conformation. This means that the presence of a small linker helix over the *N*-terminal end of the H3 helix could be acting as a physical obstacle, a “lid”, which precludes the other SNARE motifs from approaching and initiating the zippering of the complex. SNARE assembly proceeds from the *N*- to the *C*-terminus of the SNARE motif (Pobbati et al., 2006). Therefore, the presence of the Syntaxin linker in such configuration around the initiation point for zippering could be serving as a handle for Munc18 (or/and other factors such as Munc13) to open Syntaxin.

This idea is also being supported by the structure of the linker of Sso1p, the yeast homologue of Syntaxin-1a (Figure 1.9). As seen by the structure of Sso1p alone (PDB: 1FIO), its linker adopts a more rigid conformation, through the formation of 2 helices that interact with the Habc, which is thought to slow down SNARE complex formation observed by this protein (Munson et al., 2000).

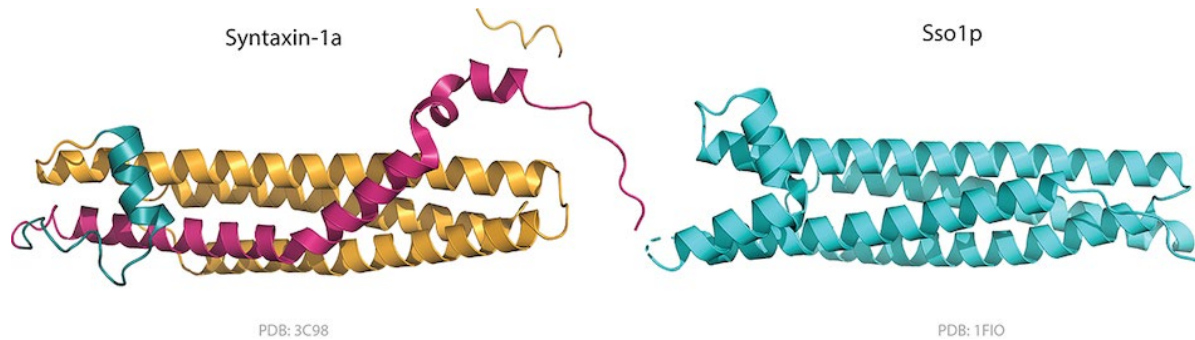


Figure 1.9: Comparison Syntaxin closed conformation to Sso1p structure. Syntaxin linker (teal) folds over Hc (orange) and H3 (magenta) into a partial helix. On the contrary, the respective region on Sso1p (right) folds into two helices that interact with the respective Hc and H3.

Similarly, Sed5p, the yeast QaI homologue, was found to interact with its cognate SM, Sly1p, in its closed conformation (Demircioglu et al., 2014), with Sly1p in this case acting as an accelerator of SNARE complex formation. Are, therefore, these two examples the extreme outliers of SM/Qa SNARE interaction or are they pieces of the same SM/Qa SNARE puzzle? Could the structure of an extended intermediate complex, like the one for Vps45/Tlg2, be a common feature for Munc18/Syntaxin in an activated form?

1.5.2 Regulation through protein-protein interactions

Several studies have proposed a templating role for domain 3a (Parisotto et al., 2014, Baker et al., 2015, Jiao et al., 2018, Wang et al., 2019, Lai et al., 2017). As mentioned above, specific mutations at domain 3a have been introduced and tested for their ability to interfere with Synaptobrevin binding, based on the Vps33/Nyv1 structure (Sitarska et al., 2017, Parisotto et al., 2014). Munc18 binding to the SNARE four helix bundle was proposed, (Xu et al., 2010, Parisotto et al., 2014) as well as the formation of a Munc18/Syntaxin/Synaptobrevin complex (Jiao et al., 2018) that acts as a template intermediate for SNAP25 Qc binding.

Munc13-1 has been suggested to act in a templating complex with Munc18/Syntaxin through interactions of its MUN domain with Munc18 domain 3a (Ma et al., 2011). At this templating complex the MUN domain is believed to promote proper Syntaxin/Synaptobrevin orientation (Lai et al., 2017). However, the exact mechanism of action of Munc13-1 is incomprehensible. *Unc-13*, discovered in the genetic studies of the worm (Brenner, 1974), is a regulator of neuronal communication. Munc13-1, the neuronal, vertebrate homologue, is crucial for spontaneous and Ca²⁺-evoked and vesicle

release from glutamatergic synapses (Augustin et al., 1999a, Varoqueaux et al., 2002). However, its action mode remains unclear.

The MUN domain belongs to the large protein family of Complex Associated with Tethering Containing Helical Rods (CATCHR) proteins. CATCHR are involved as tethering factors in different trafficking steps (Varoqueaux and Fasshauer, 2017). Munc13 domain architecture, similar to other MUN-domain proteins, is characterized by the presence of the MUN domain, C1 and C2 domains and a Ca²⁺ calmodulin and diacylglycerol binding sites. The MUN domain is a ~700 residue long autonomously folded domain (Basu et al., 2005) which folds into two stacked helical bundles (Li et al., 2011) shares structural homology with the exocyst complex type of proteins (Pei et al., 2009), the other CATCHR type of secretion tethering factors. Besides assisting the above-mentioned template complex, Munc13 is believed to catalyze SNARE complex formation through interaction of its MUN domain with the Munc18/Syntaxin complex. MUN domain is thought to catalyze SNARE complex formation through interactions at Munc18 domain 3a/Syntaxin linker region side (Wang et al., 2017, Wang et al., 2020) catalyzing this way the Syntaxin opening, although, in solution, interaction with Munc18 and/or Syntaxin is weak (~40μM).

1.5.3 Regulation by post-translational modifications

Munc18 phosphorylation by Protein Kinase C has been shown to interfere with its binding to Syntaxin (Barclay et al., 2004). PKC phosphorylates Munc18 in a calcium dependent manner at Munc18 domain 3a Ser₃₀₆ and Ser₃₁₃, which suggested a closed-cavity conformation that precludes Syntaxin from binding (Bar-On et al., 2011). Munc18 phosphorylation by Src at Tyr₄₇₃ lead to decrease in synaptic transmission in a fashion not well understood (Meijer et al., 2018). ERK1/2 phosphorylation at Ser₂₄₁, decrease in synaptic transmission through a process that ultimately leads to ubiquitination and proteasomal degradation for the ERK-phosphorylated Munc18-1 (Schmitz et al., 2016). Polyubiquitination and subsequent proteasomal degradation of Munc18 has been also reported in another study to be the causal factor for the disease phenotype of the C180Y mutation (Martin et al., 2014).

In the light of these findings, it is conceivable that the tight interaction of Munc18-1 with Syntaxin-1a in closed conformation observed by X-ray analysis is a snapshot of a low energy conformation that inhibits SNARE complex formation, while other, more loose conformations might exist as well. The interaction in closed conformation could be a safeguard for keeping Syntaxin inactive when not needed to interact with the SNAREs. But at the very moment, when the SNARE complex needs to be formed, a switch of Syntaxin to the open conformation could be assisted by a conformational switch of Munc18. But are there indications that Munc18-1 could be flexible? For starters, the presence of disordered regions in Munc18, at helices 11 and 12, which seem to adopt helical structure in homologous complexes, as well as the rotational differences between the solved structures of the SM proteins point towards structural flexibility, for Domain 3a, and Munc18 *per se*. In such a scenario, the conformational change of Syntaxin could be linked to a conformational change in Munc18, where both molecules could be changing together leading to an “activation” of Syntaxin, while still in complex with Munc18. This scenario could potentially explain the similarities in the observations arising from the Sy^{XLE} and Sy^{XΔN}.

Are, therefore, the interactions at Munc18-1 domain 3a/Syntaxin-1a linker and Munc18-1 domain 1/ Syntaxin-1a N-terminus linked? Is there an allosteric regulation taking place?

2. Aims

The interaction of Munc18-1 with Syntaxin-1a is indispensable for synaptic secretion. However, while being studied for years, the precise role of this interaction and its mechanism are still elusive. At the core of this quandary lies the apparent disagreement between genetics, which point towards a beneficial role of this interaction for vesicle fusion, and biochemistry, which rather suggests an inhibitory effect. How can this discrepancy between *in vivo* and *in vitro* observations be reconciled? Several factors have been suggested to regulate this interaction. Such factors could “open” Syntaxin-1a through a direct interaction with the Munc18-1/Syntaxin-1a complex, although no compelling evidence for such a scenario has been brought by so far. Another possible scenario is that other factors could act through post-translational modifications of Munc18-1 or syntaxin. Either way, it remains unclear how this conformational transition of Syntaxin-1a while in complex with Munc18 is taking place. Therefore, a better understanding of the intrinsic conformational flexibility of the Munc18-1/Syntaxin-1a complex is indispensable to appreciate how other factors influence this interaction.

With this study, I aimed to shed light on a putative conformational flexibility of the Munc18-1/Syntaxin-1a complex by which Munc18-1 may render Syntaxin-1a ready for SNARE complex formation. To probe this I wanted to introduce point mutations at key interaction points of the complex, based on the already available crystal structure (Burkhardt et al., 2008, Misura et al., 2000) and previous conservation studies at the lab (unpublished observations and (Morey et al., 2017)). In addition, I mutated residues in both interacting partners that could be involved in a conformational transition were targeted (Colbert et al., 2013). I planned to investigate the effect of these mutations on the interaction by a variety of biochemical and biophysical approaches

Additionally, the target was to investigate and characterize the Munc18-1/Syntaxin-1a interactions using the aforementioned mutants and to evaluate their ability to form the Munc18-1/Syntaxin-1a complex. Additionally, it was required to assess the possibility of Munc18-1a to block Syntaxin-1a from assembling into SNARE complex and to investigate the impact of the mutations on the physicochemical properties of the Munc18-1/Syntaxin-1a complex.

Furthermore, to complement my research, the putative protein-protein interactions of the Munc18-1/Syntaxin-1a complex with Munc13-1 MUN-domain (Yang

et al., 2015, Wang et al., 2017) and Synaptobrevin (Sitarska et al., 2017, Park et al., 2017, Jiao et al., 2018) were explored.

Last of all, I had the intention to inspect the structural details of the conformational transition of Munc18-1/Syntaxin-1 using homology modelling to support the hypothesis I established from this research.

3 Materials and Methods

3.1 Chemicals & enzymes

All chemicals and enzymes used in this study were purchased from Roth, Sigma, Thermo-Fisher Scientific. Bacterial media were purchased from Formedium.

3.2 DNA constructs

The protein constructs used in this study are given in tables (Table 3.1, Table 3.2 and Table 3.3). All Syntaxin-1a and Munc18-1 constructs were derived from rat (*Rattus norvegicus*). All Syntaxin-1a, Munc18-1 and MUN variants, and MUNwt were cloned in pET28a vector ordered from Genscript.

Name	Gene	Fragment	Mutation	Organism	Vector
Munc18 wt	Munc18-1	1 - 586		<i>Rattus norvegicus</i>	pET-28a
Munc18 W28A	Munc18-1	1 - 586	W28A	<i>Rattus norvegicus</i>	pET-28a
Munc18 N261A	Munc18-1	1 - 586	N261A	<i>Rattus norvegicus</i>	pET-28a
Munc18 Δ269-275	Munc18-1	1 - 268, 276 - 586	Δ269 - 275	<i>Rattus norvegicus</i>	pET-28a
Munc18 R315A	Munc18-1	1 - 586	R315A	<i>Rattus norvegicus</i>	pET-28a
Munc18 D326K	Munc18-1	1 - 586	D326K	<i>Rattus norvegicus</i>	pET-28a
Munc18 KEKE	Munc18-1	1 - 586	K332E, K333E	<i>Rattus norvegicus</i>	pET-28a
Munc18 Δ317-333	Munc18-1	1 - 316, 334 - 586	Δ317-333	<i>Rattus norvegicus</i>	pET-28a
Munc18 P335A	Munc18-1	1 - 586	P335A	<i>Rattus norvegicus</i>	pET-28a
Munc18 Y337A	Munc18-1	1 - 586	Y337A	<i>Rattus norvegicus</i>	pET-28a
Munc18 L348R	Munc18-1	1 - 586	L348R	<i>Rattus norvegicus</i>	pET-28a
Munc18 Y473D	Munc18-1	1 - 586	Y473D	<i>Rattus norvegicus</i>	pET-28a

Table 3.1 Munc18-1 constructs used in this study

Name	Gene	Fragment	Mutation	Organism	Vector
Syntaxin wt	Syntaxin-1a	1 - 262	C145S	<i>Rattus norvegicus</i>	pET-28a
Syntaxin wt*1	Syntaxin-1a	1 - 262	M001C, C145S	<i>Rattus norvegicus</i>	pET-28a
Syntaxin wt*186	Syntaxin-1a	1 - 262	C145S, S186C	<i>Rattus norvegicus</i>	pET-28a
Syntaxin ΔN	Syntaxin-1a	25-262	Δ(2-25)	<i>Rattus norvegicus</i>	pET-28a
Syntaxin Δ(11-26)	Syntaxin-1a	2-10,27-262	M001C, C145S, Δ(11-26)	<i>Rattus norvegicus</i>	pET-28a
Syntaxin 3x(11-26)	Syntaxin-1a	2-10, 3x(11-26) 27-262	M001C, C145S, 3x(11-26)	<i>Rattus norvegicus</i>	pET-28a
Syntaxin F34A	Syntaxin-1a	1 - 262	C145S, F34A	<i>Rattus norvegicus</i>	pET-28a
Syntaxin F34Y	Syntaxin-1a	1 - 262	C145S, F34Y	<i>Rattus norvegicus</i>	pET-28a
Syntaxin N135A	Syntaxin-1a	1 - 262	C145S, N135A	<i>Rattus norvegicus</i>	pET-28a
Syntaxin N135D	Syntaxin-1a	1 - 262	C145S, N135D	<i>Rattus norvegicus</i>	pET-28a
Syntaxin N135A_F177A	Syntaxin-1a	1 - 262	C145S, N135A, F177A	<i>Rattus norvegicus</i>	pET-28a
Syntaxin R142A	Syntaxin-1a	1 - 262	C145S, R142A	<i>Rattus norvegicus</i>	pET-28a
Syntaxin K146A	Syntaxin-1a	1 - 262	C145S, K146A	<i>Rattus norvegicus</i>	pET-28a
Syntaxin RI	Syntaxin-1a	1 - 262	C145S, R151A, I155A	<i>Rattus norvegicus</i>	pET-28a
Syntaxin L165A	Syntaxin-1a	1 - 262	C145S, L165A	<i>Rattus norvegicus</i>	pET-28a
Syntaxin E166A	Syntaxin-1a	1 - 262	C145S, E166A	<i>Rattus norvegicus</i>	pET-28a
Syntaxin LE	Syntaxin-1a	1 - 262	C145S, L165A, E166A	<i>Rattus norvegicus</i>	pET-28a
Syntaxin LE*186	Syntaxin-1a	1 - 262	C145S, S186C	<i>Rattus norvegicus</i>	pET-28a
Syntaxin RL	Syntaxin-1a	1 - 262	C145S, R142A, L165A	<i>Rattus norvegicus</i>	pET-28a
Syntaxin E166A_F177A	Syntaxin-1a	1 - 262	C145S, E166A, F177A	<i>Rattus norvegicus</i>	pET-28a
Syntaxin M168A	Syntaxin-1a	1 - 262	C145S, M168A	<i>Rattus norvegicus</i>	pET-28a
Syntaxin nLE	Syntaxin-1a	1 - 262	C145S, L169A, E170A	<i>Rattus norvegicus</i>	pET-28a
Syntaxin F177A	Syntaxin-1a	1 - 262	C145S, F177A	<i>Rattus norvegicus</i>	pET-28a
Syntaxin ΔLinker	Syntaxin-1a	1 - 160, 183- 262	C145S, Δ (161-182)	<i>Rattus norvegicus</i>	pET-28a
Syntaxin ΔLinker*1	Syntaxin-1a	1 - 160, 183- 262	M001C, C145S, Δ(161-182)	<i>Rattus norvegicus</i>	pET-28a
Syntaxin ΔLinker*186	Syntaxin-1a	1 - 160, 183- 262	C145S, Δ (161-182), S186C	<i>Rattus norvegicus</i>	pET-28a
Syntaxin H213A	Syntaxin-1a	1 - 262	C145S, H213A	<i>Rattus norvegicus</i>	pET-28a
Syntaxin E224A	Syntaxin-1a	1 - 262	C145S, E224A	<i>Rattus norvegicus</i>	pET-28a
Syntaxin E234A	Syntaxin-1a	1 - 262	C145S, E234A	<i>Rattus norvegicus</i>	pET-28a
Syntaxin Habc*59	Syntaxin-1a	1 - 150	C145S, S59C	<i>Rattus norvegicus</i>	pET-28a
Syntaxin H3*186	Syntaxin-1a	183 - 262	S186C	<i>Rattus norvegicus</i>	pET-28a

Table 3.2 Syntaxin-1a constructs used in this study

Name	Gene	Fragment	Mutation	Organism	Vector
SNAP25 wt	SNAP25	1 - 206		<i>Rattus norvegicus</i>	pET-28a
SN1	SNAP25	1-83		<i>Rattus norvegicus</i>	pET-28a
SN2	SNAP25	120 - 206		<i>Rattus norvegicus</i>	pET-28a
SN25 noTrp	SNAP25	1 - 206		<i>Rattus norvegicus</i>	pET-28a
Synaptobrevin wt	Synaptobrevin	1-96		<i>Rattus norvegicus</i>	pET-28a
Synaptobrevin 1-87	Synaptobrevin	1-87		<i>Rattus norvegicus</i>	pET-28a
Synaptobrevin 30-89	Synaptobrevin	30-89	Δ1-29	<i>Rattus norvegicus</i>	pET-28a
Synaptobrevin*28	Synaptobrevin	1-96	S28C	<i>Rattus norvegicus</i>	pET-28a
Synaptobrevin WW89.90SS	Synaptobrevin	1-96	W89S, W90S	<i>Rattus norvegicus</i>	pET-28a
MUN 933	Munc13-1	933-1407, EF, 1453-1531		<i>Rattus norvegicus</i>	pET-28a
MUN 933 NF	Munc13-1	933-1407, EF, 1453-1532	N1128A & F1131A	<i>Rattus norvegicus</i>	pET-28a

Table 3.3 SNAP25, Synaptobrevin and MUN constructs used in this study

3.2.1 Protein Expression and Purification

E. coli BL21 competent cells (50 µL) were transformed with the 1-2 µL of pET28a vectors carrying the sequence corresponding to the proteins of interest with the required mutations (Fig.4.1.A), by heat-shock at 42° C for 90 s. Transformed cells were selected by overnight incubation at 37° C on Luria Bertani (LB)-agar plates containing Kanamycin (50 µg/ml).

Single colonies were picked and grown overnight at 37°C with agitation in LB containing Kanamycin (50 µg/ml), which was then used for the inoculation of 500 mL of LB with Kanamycin (50 µg/ml). For Munc18-1 wt and Munc13 wt, *E. coli* cells were grown in Terrific Broth (1.2 % w/v tryptone, 2.4 %w/v yeast extract, 0.4%w/v glycerol) medium with 10%v/v TB salt (0.17 M KH₂PO₄, 0.72 M K₂HPO₄) and Kanamycin (50 µg/ml). Induction of protein expression was achieved by addition of 1 mM IPTG (or 0.25 mM for Munc18 variants) when OD_{600nm}≈0.4-0.6 for cultures in LB, or OD_{600nm}≈0.8-1.2 for cultures in TB, and incubation for 4 h at 37° C (LB) or overnight at 23° C (TB) with agitation. The bacterial pellet was collected after centrifugation at 2250 rcf for 30 min at 4° C, resuspended in Binding Buffer (500 nM NaCl, 8 mM or 15 mM Imidazole, 200 nM Tris pH 8.0) and stored at -20° C.

For purification, the resuspended bacterial pellet was thawed, and cell lysis was achieved by addition of lysis buffer (1 mM MgCl₂, 0.5% (v/v) Triton-X 100, 1 mM PMSF, 0.25 mg/ml lysozyme and 10 µg/mL DNase A). To increase the yield of purification 6M Urea was added to SNARE proteins. Following an incubation of 10min with the lysis reagents, the bacterial lysate was subjected to 4x30s rounds of sonication (Branson Ultrasonics) with 1-minute intervals on ice and then centrifuged at 9685rcf for 1 hour at 4°C. The supernatant was mixed with Ni²⁺ charged resin beads and incubated for 2h at 4°C with agitation. The supernatant-beads mixture was transferred to glass chromatography column (BioRad) and the unbound contents are collected at the flow-through fraction. The remaining unbound fraction was washed with 20x column volumes of Binding Buffer (500 nM NaCl, 8 mM or 15 mM Imidazole, 200 nM Tris pH 8.0). Then, elution of the desired proteins was achieved by 3 washes of the column with 3x column volume of Elution Buffer (500 nM NaCl, 400 mM or 500 mM Imidazole, 200 nM Tris pH 8.0). The eluates containing the protein of interest were pooled and dialyzed overnight in 2L Buffer A (100 mM NaCl, 20 mM Tris pH 7.4, 1 mM EDTA, 1 mM DTT) at 4°C.

To increase the purity of the proteins, the pooled eluates were subjected to Ion Exchange Chromatography. There, proteins of interest are bound to Mono Q 10/100 GL or Mono S 10/100 GL (Pharmacia Biotech) columns based on their pI using the AKTA purifier system and eluted with a gradient of NaCl from Buffer A (100 mM NaCl, 20 mM Tris pH 7.4, 1 mM EDTA, 1 mM DTT) to Buffer B (1M NaCl, 20 mM Tris pH 7.4, 1 mM EDTA, 1 mM DTT). Elution fractions with sufficient ratio of protein amount and purity were pooled, aliquoted and either stored at -80° C (only the SNARE proteins) or used directly in experiments. Pure Munc18-1 wt and variants, as well as MUN, were always used without prior freezing.

3.3 Analytical Size-Exclusion Chromatography

Analytical Size-Exclusion chromatography was used to get an estimation of the population composition (monomeric, oligomeric) of purified proteins. For that reason, 500µL or protein prep was loaded on a Superdex 200 10/300 GL (Pharmacia Biotech) column equilibrated with Gel Filtration Buffer (150 mM NaCl, 20 mM Tris pH 7.4, 1 mM DTT) using the AKTA explorer system, followed by wash of the column with 1x column volume of Gel Filtration Buffer. The elution volumes of the protein samples were compared to the ones of the standards for the estimation of their MW. Also, analytical

size-exclusion chromatography was used for the identification of protein-protein interactions. Equimolar concentrations of Syntaxin-1a and Munc18-1 variants were mixed and let to interact overnight at 4° C. Then, 500µL of the mixture were loaded on the column and purified as described above. The elution volume of the mixture was compared to the ones of the single proteins and any shifts to smaller elution volumes were attributed to complex formation.

3.4 Analytical Polyacrylamide Gel Electrophoresis

Besides the application of SDS Polyacrylamide gel electrophoresis (PAGE) for the evaluation of the purity of the protein preparations, PAGE was used for the identification of complex formation. With the neuronal SNARE complex being SDS resistant (Hayashi et al., 1994), SNARE complex formation can be evaluated using two types of PAGE: Native (non-denaturing) and SDS PAGE. For native gels, the concentrations and incubation times varied depending on the interaction tested. For the SNARE complex formation/inhibition tests, excess of Munc18-1 wt was premixed and incubated for 10min at RT with Syntaxin-1a mutants. Then, excess of SNAP25 wt was added to the mixture and the SNARE complex formation reactions were initiated by the addition of excess of Synaptobrevin-2 (1-96). The reactions were terminated at specific time points (0', 5', 10', 15' and 30min) by the addition of SDS loading buffer and the samples were loaded onto 10 % and 15 % SDS-PAGE and electrophoresed. All gels were stained by Coomassie.

3.5 Intrinsic Tryptophan Fluorescence Measurements

Tryptophan residues on folded proteins can be used to observe conformational changes, as their photophysical properties are highly sensitive to their local environment. With Munc18-1 carrying five Trp residues and Syntaxin-1a having none, any changes on the measured emission ($\lambda_{\text{emm}} \approx 330\text{nm}$) when specifically exciting for Tryptophan ($\lambda_{\text{exc}} = 295\text{nm}$) can be attributed to the interaction of Munc18-1 with Syntaxin-1a. Fluorescence emission measurements and scans of Munc18-1 after addition of Syntaxin-1a were performed in 1cm quartz cuvettes (Hellma) in Phosphobuffer (150 mM NaCl, 20 mM Na₃PO₄, 1 mM DTT) using a PTI QuantaMaster Spectrometer in T-configuration. Emission spectra were measured in the range of 310-450nm.

3.6 Fluorescence Anisotropy

3.6.1 Fluorescent protein labelling

Purified preparations of single cysteine carrying variants of Syntaxin and Synaptobrevin (constructs for labelling) were dialyzed twice against Phosphate Buffer (100mM Na₃PO₄, 100mM NaCl) to remove DTT. After dialysis, protein concentration of the sample was determined and 10-20x fold molar excess of respective dye, Oregon Green 488 Maleimide or Texas Red C2 Maleimide (Invitrogen), was added to it and incubated at RT for 2h with end-to-end rotation. Reaction was terminated by addition of 5mM DTT and passed through a size exclusion chromatography column (Sephadex G-50 packed column) equilibrated with Phosphate Buffer (100mM Na₃PO₄, 100mM NaCl) containing 1mM DTT to remove the remaining free dye. Samples from the eluates were loaded on SDS gels and visualized at UV and visible light after Coomassie staining. Labelled eluates were pooled, and labelling efficiency and protein concentration were determined by absorption spectroscopy.

3.6.2 Fluorescence anisotropy

Anisotropy measurements can provide information on the shape and size of proteins in real time. This is based on the principle of photoselective excitation of fluorophores by polarized light. Therefore, the local flexibility of a fluorescently labeled residue enables the detection of changes upon complex formation in real-time. Synaptobrevin-2 (1-96) labeled at Cys28 with Oregon Green dye was used to detect SNARE complex formation with Fluorescence Anisotropy. Syntaxin-1a (500 nM), wt or mutants, preincubated, or not, with 750 nM Munc18-1, wt or mutants, was mixed with 40 nM of labelled Synaptobrevin-2 in phosphate buffer (150 mM NaCl, 20 mM Na₃PO₄, 1 mM DTT) and the reaction was initiated by the addition of 750 nM SNAP25 wt. The anisotropy (r) of the mixtures was determined as $r(t) = \frac{I(par) - G(per)}{I(par) + 2xGxI(per)}$, where $I(par)$ is the intensity of light detected with a vertical excitation polarizer and a vertical emission polarizer and $I(per)$ is the intensity of light detected with a vertical excitation polarizer and a horizontal emission polarizer. The G factor was determined through a measurement with the polarizer in horizontal orientation and was defined as: $G = \frac{I_{HV}}{I_{HH}}$. Anisotropy measurements of complex formation were performed at $\lambda_{emi}=524\text{nm}$ in 1cm

quartz cuvettes (Hellma) in a total 2.5 ml reaction volume after excitation at $\lambda_{exc}=496\text{nm}$, using a PTI QuantaMaster with polarizers in T-configuration.

3.7 Homology modelling

PDB structures for the Vps45/Tlg2 complex (6xm1) and Munc18-1 K332E_K333E (6lpc) (Eisemann et al., 2020, Wang et al., 2020) were retrieved used as templates for the acquisition of a 3D models of Munc18-1/Syntaxin-1a, and Munc18-1, respectively in extended conformations. Models were created, optimized, and evaluated using the Modeller software (Webb and Sali, 2016) as demonstrated in scheme (Figure 3.1). The scripts of the code can be found at the (Appendix Fig.1).

In general, target sequences (of the query protein/s) were aligned with the sequence of the template protein, or complex using the **align2d.py** script. Then, model was created by running the **model-single.py**, or in the case of linker refining, the **model-loop-define.py** scripts using as input the output alignment file (target-template.ali) and the template pdb file. The number of models created was customized to the needs of the experiment: less for the same protein, more for the linkers' refining. Modelling was run for defined number of times and respective number of .pdb files were created, as well as a .log file with the summary of parameters. Of these, DOPE score was used to evaluate the models. The models with the lowest DOPE score were selected as the best model and then **evaluate_model.py** script was run to determine the DOPE score for each residue and plotted.

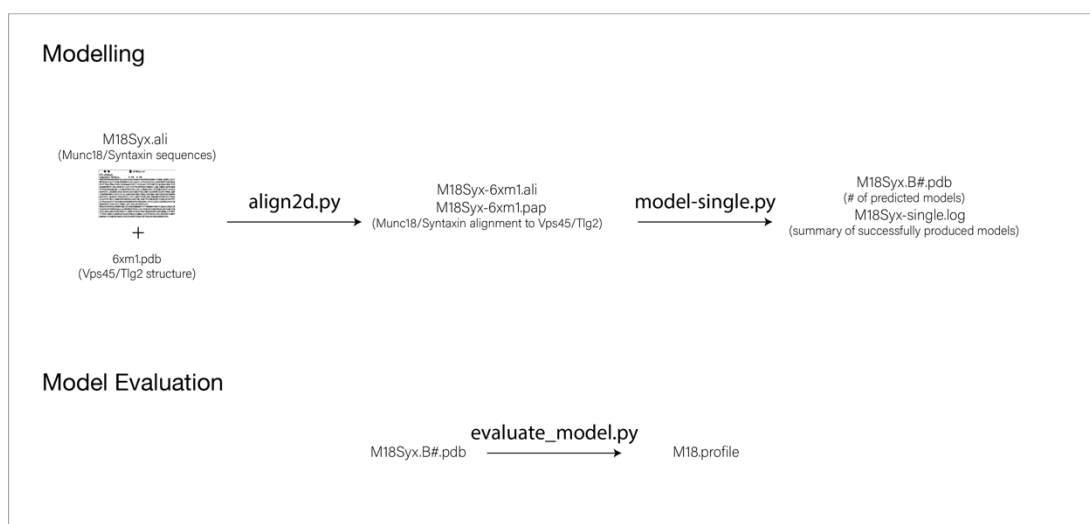


Figure 3.1 Schematic representation of homology modelling process. First structural alignment is created, followed by modeling using the alignment file as template. Then, after identification of the model with the lowest DOPE score, the energy profile for is aminoacid position is calculated using the evaluate_model.py script.

4. Results

4.1 Syntaxin-1a and Munc18-1 mutations used in the study

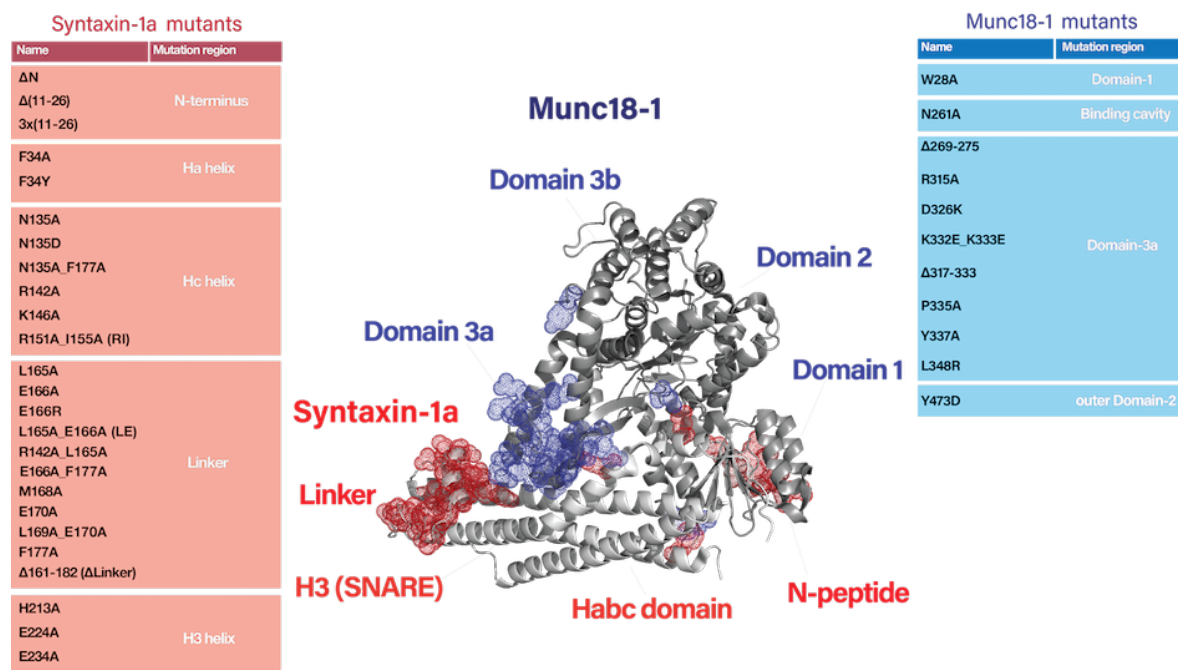


Figure 4.1 Representation of mutations in Munc18 and Syntaxin used in this study. Dot representation (center) of Munc18 (blue) and Syntaxin (red) mutated residues in the X-ray structure of the Munc18/Syntaxin complex (pdb:3c98). Table of Syntaxin (red) and Munc18-1 (blue) used in this study. The region on the molecule they localize is indicated. Throughout the study, the variants will be referred to as Syx1a or Munc18-1 with the mutations as extension as given above.

For this study, 25 different variants of Syntaxin-1a and 12 of Munc18-1 were used. Most syntaxin mutants carried single amino acid exchanges to alanine, 5 mutants carried a combination of 2 amino acid substitutions. 3 mutants were shortened variants of syntaxin and one was elongated with an insertion as described in the section 3.2. These mutations are localized at different regions of syntaxin as illustrated in Figure 4.1. Likewise, most Munc18-1 mutations were single amino acid substitutions to alanines. Two shortened variants of Munc18-1 were used as well (Figure 4.1).

4.2 Mutations in the linker region of Syntaxin-1a ease SNARE complex formation in the presence of Munc18-1.

4.2.1 Syntaxin-1a linker variants bind to Munc18-1wt

The combination of the two point mutations L165A and E166A mutation in the linker region of syntaxin 1a (Syx1a_{LE}) is known to loosen the inhibition of SNARE complex formation exerted through the tight interaction of syntaxin 1a with Munc18-1 (Dulubova et al., 1999). It was shown that Syx1a_{LE} can form SNARE complexes almost with the same speed in the absence or presence of Munc18 (Dulubova et al., 1999, Burkhardt et al., 2008). Here, we wanted to gain a deeper look into the mechanism that allows Syx1a_{LE} mutant to escape the tight grip of Munc18-1. To do so, we first inspected the conservation pattern of the Syntaxin-1a linker and how it interacts with other regions of Syntaxin 1a and with Munc18-1. The Syntaxin-1a linker is ~20 residue long region between Hc and H3 helices of Syntaxin. The conservation analysis revealed that other amino acids, e.g., M168 and F177, are even more conserved than the conspicuous L165 and E166 residues (Figure 4.2). I then substituted several residues of the Syntaxin-1a linker region to alanines. In the crystal structure, these residues are either involved in polar (R142, K146, E166) or hydrophobic (L165, M168, F177) interactions between the linker and H3 helices. Additionally, I also removed the entire linker region, i.e., residues 161 to 182 (Syx1a Δ Linker).

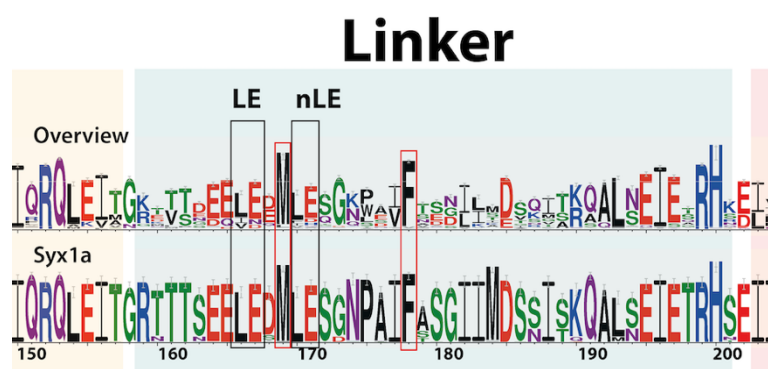


Figure 4.2: Weblogo representation of the amino-acid conservation of the Syntaxin linker region. The weblogo was generated from a multiple sequence alignment of vertebrate Syntaxin (QaIV) sequences (top) and of Syntaxin-1a sequences (bottom). Black boxes indicate the L165_E166 and L169_E166 residues, red boxes the M168 and F177 residues. The complete weblogo file (full sequence) can be found in the appendix.

To determine whether these Syntaxin-1a mutants still form a stable complex with Munc18-1_{wt}, they were mixed with Munc18-1 and ran on non-denaturing (native) gels. All linker mutants were able to bind to Munc18-1_{wt}, including Syx1a Δ Linker, the mutant in which the entire linker region had been removed (Figure 4.3). This suggests that the entire linker region of syntaxin is not essential for a tight interaction of the two proteins.

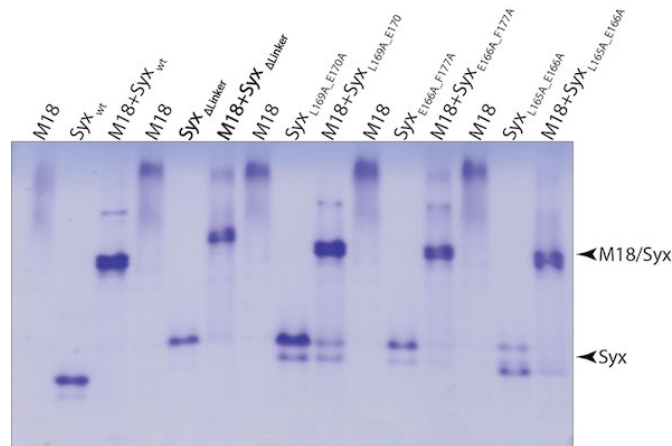


Figure 4.3 Syntaxin linker mutants form a stable complex with Munc18wt shown by native gel electrophoresis. Equimolar concentrations ($\sim 37\mu\text{mole}$ per lane) of Munc18-1 and Syntaxin mutants were loaded individually, as well as in mixtures. The Munc18-1/Syntaxin-1a complex is indicated by arrows.

4.2.2 Munc18-1 exerted inhibition of SNARE complex formation is overcome by Syntaxin-1a linker mutants

As outlined above, the LE mutant had been suggested earlier to be able to engage with its partner SNAREs SNAP-25 and synaptobrevin while in complex with Munc18-1. As the other linker variants tested here were able to form a tight complex with Munc18-1 as well, I tested next the ability of these syntaxin variants to form a SNARE complex in the presence of Munc18-1. To better compare the strength of the inhibitory effect of Munc18 on the Syntaxin variants, fluorescence anisotropy measurements using fluorescently labelled Synaptobrevin (Synaptobrevin^{*28} Oregon Green, or Syb^{*28}) were carried out. Previous studies had shown that SNARE complex (SC) formation using fluorescently labelled Synaptobrevin leads to an increase in fluorescence anisotropy (Burkhardt et al., 2008). This approach allowed me to monitor SNARE complex formation over time. When Syntaxin-1_{wt} was preincubated with wt Munc18-1, SNARE complex formation was inhibited, consistent with previous reports (Burkhardt et al., 2008) (Figure

Results

4.4). Using this assay, I was able to confirm that all Syntaxin-1a linker mutants are less inhibited than Syntaxin-1a_{wt}, as observed by the higher rate of fluorescence anisotropy increase in the presence of Munc18_{wt} as compared to the mix of Munc18_{wt} and Syntaxin-1_{wt}.

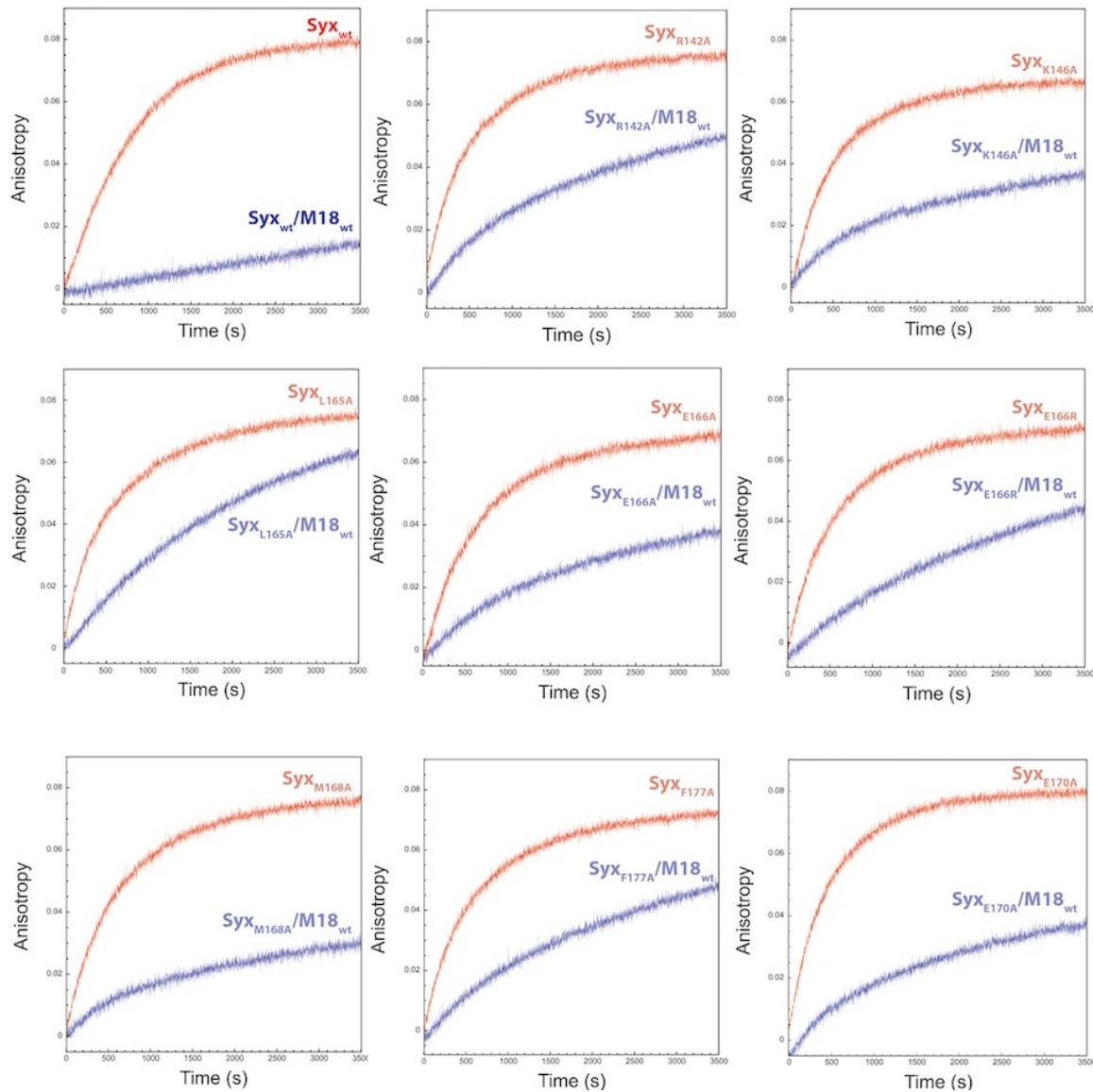


Figure 4.4: Reduced inhibition of SNARE complex formation by Munc18-1 was observed for several Syntaxin-1a linker variants by fluorescence anisotropy. 40nM of Synaptobrevin labeled with Oregon Green at Cys28 were mixed with 500nM Syntaxin-1a_{wt}, or Syntaxin-1a mutant, preincubated (blue trace) or not (red trace) with 750nM Munc18-1 wt. SNARE complex formation was followed by an increase in fluorescence anisotropy upon addition of 750nM SNAP25. Fluorescence of labeled Synaptobrevin was monitored at a wavelength of 524nm upon excitation at 496nm. When Syntaxin-1a wt is preincubated with Munc18-1 SNARE complex formation is very slow (top left). Different Syntaxin-1a linker mutants were able to more rapidly, to different extents, form a SNARE complex in the presence of Munc18-1 (rest).

Faster SNARE complex formation was observed for the mutant lacking the entire linker region, Syx1a Δ Linker. Its rate of SNARE complex formation in the presence of Munc18-1 was comparable to that of Syx1a_{LE} (Figure 4.5.B&D), corroborating earlier observations (Burkhardt et al., 2008). For both variants, the rates were comparable in the presence or absence of Munc18-1, suggesting that Munc18-1 inhibitory effect on the ability of bound syntaxin to form a SNARE complex has been removed to a great extent or even entirely.

But why and how does the linker of syntaxin play such an important role in the regulation of SNARE assembly through Munc18-1? To find out what exactly could be changing in the linker region when the two adjacent residues 165 and 166 are mutated to alanines, I re-inspected the structure of the Munc18-1/Syntaxin 1a complex. The two residues are in the centre of the small linker helix, yet, while L165 points towards a hydrophobic patch (formed by the C-terminal end of the linker and the N-terminal end of the H3-helix), the negatively charged E166 interacts with the positively charged Arg142 of the Hc-helix.

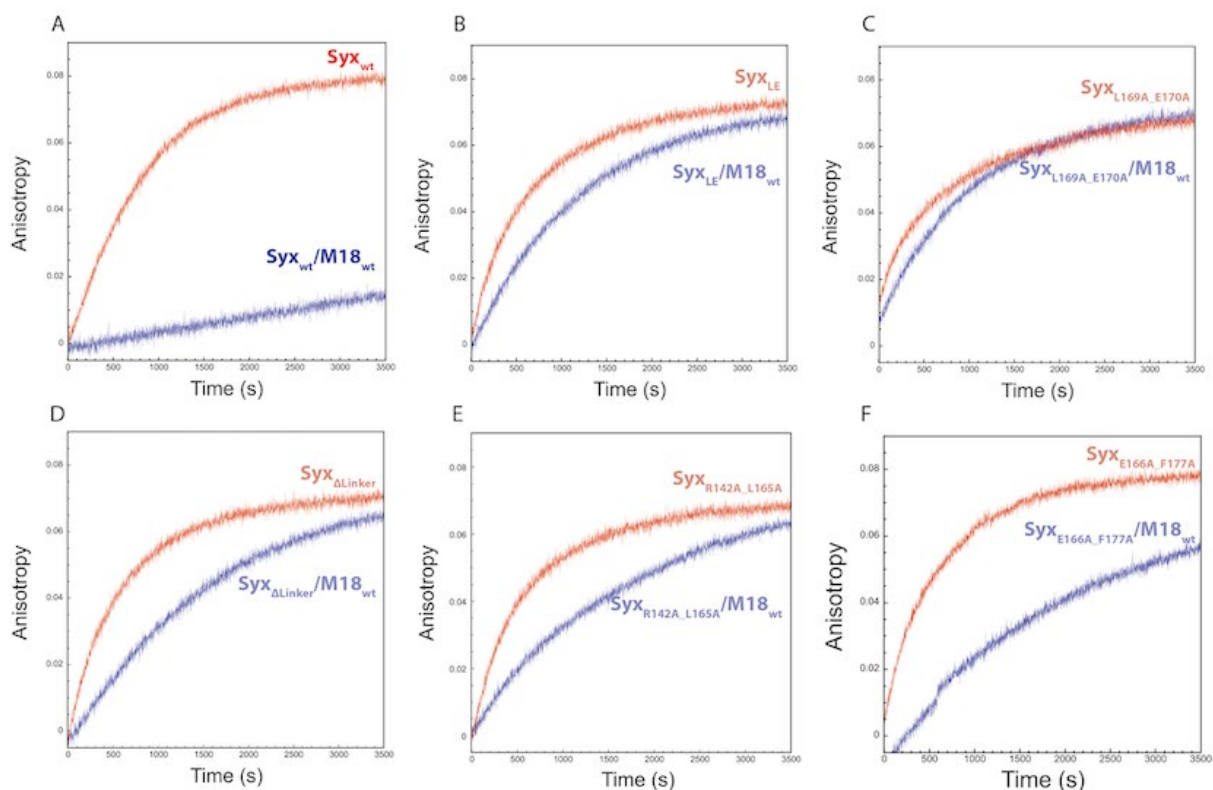


Figure 4.5: Syx1a_{LE}(B), Syx1a_{L169A, E170A} (C), Syx1a Δ Linker(D), Syx1a_{R142A, L165A}(E) and Syx1a_{E166A, F177A} (F) variants can more rapidly form a SNARE complex in the presence of Munc18-1 compared to other Syx variants tested in this study. The increase in fluorescence anisotropy was measured in the presence (blue trace) or absence (red trace) of Munc18-1.

inhibition by Munc18-1 was exerted on Syntaxin_{wt} (Figure 4.6). The least inhibited mutants were Syx_{LE} (Figure 4.6.C) and Syx_{L169A_E170A} (Figure 4.6.A).

4.3 The intrinsic Tryptophan fluorescence emission of Munc18-1_{wt} increases when interacting with Syntaxin-1a_{wt}

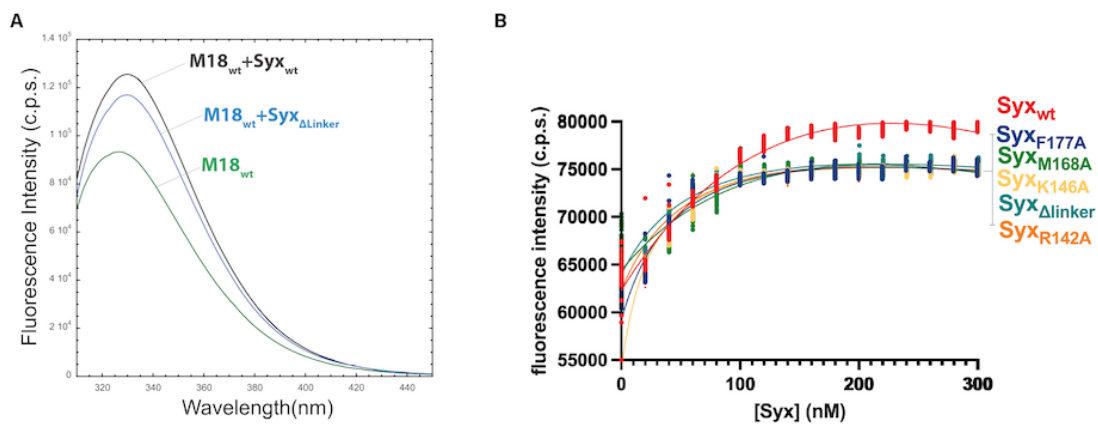


Figure 4.7: Addition of Syntaxin-1a to Munc18-1 leads to increase in tryptophan fluorescence. **A.** Tryptophan fluorescence emission spectra of individual Munc18-1 or in complex with Syntaxin-1a_{wt} or Syntaxin-1a_{ΔLinker} were recorded upon excitation at 295 nm. Addition of an excess of Syntaxin-1a_{wt} (340 nM) to 200 nM Munc18-1_{wt} leads to a higher increase in emitted fluorescence than the addition of the same amount of Syntaxin-1a_{ΔLinker}. **B.** Changes in the tryptophan fluorescence measured at 332 nm upon titration of different syntaxin 1a variants into 150 nM Munc18-1. Addition of either Syx1a_{wt} or mutants to Munc18-1 led to a clear increase in fluorescence that was saturated at an equimolar ratio.

Earlier studies had shown that the intrinsic tryptophan fluorescence of Munc18-1 is increasing when it is bound to Syntaxin-1a (Burkhardt et al., 2008). When Munc18-1 was mixed with Syx1a_{ΔLinker}, the emitted fluorescence was lower than that of the mix of the two wild-type proteins. Similarly, I found a reduced increase upon mixing with Munc18-1 for all linker region mutants compared to that of the interaction with Syntaxin_{wt} (Figure 4.7). The small reduction of the dequenching effect by the linker variants of syntaxin compared to that of syntaxin wt could reflect a change in the local environment of one or several tryptophans in Munc18-1.

4.3.1 Tryptophan emitted fluorescence increase is caused by the interaction of Munc18 Tryptophan28 with Syntaxin Phenylalanine34

Results

In order to pinpoint the tryptophan(s) involved in dequenching upon complex formation, I inspected the crystal structure of the complex (pdb: 3c98). Trp₂₈₇ is located

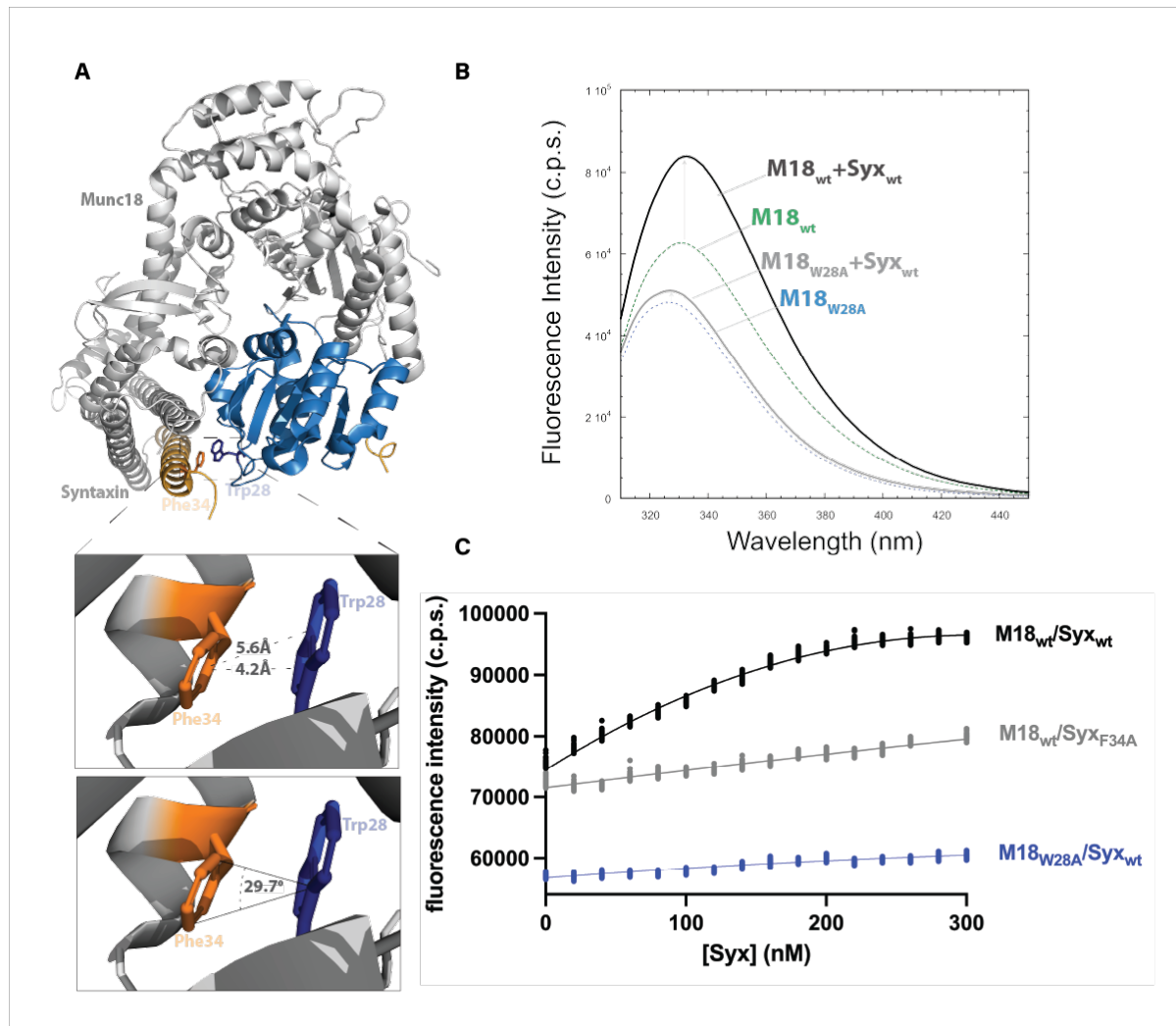


Figure 4.8: Munc18-1 W₂₈ interacts through pi-pi stacking with Syntaxin-1a F₃₄ causing the increase in Tryptophan emitted fluorescence. **A.** When in Munc18/Syntaxin complex, the aromatic rings of Syntaxin-1a Phe₃₄ and Munc18-1 Trp₂₈ lie within ~4.2Å distance and orient creating a 29.7° angle between them as measured with Pymol using the crystal structure of the complex (pdb:3c98). **B.** Tryptophan fluorescence emission spectra of individual Munc18-1_{wt}, Munc18-1_{W28A} or in complex with Syntaxin-1a_{wt} or Syntaxin-1a_{F34A} were recorded upon excitation at 295 nm. Addition of an excess of Syntaxin-1a_{wt} (300nM) to 200nM Munc18-1_{wt} or Munc18-1_{W28A}. The expected increase in emitted fluorescence is observed when Syntaxin-1a_{wt} is added to Munc18-1_{wt}, however no such an increase is observed when Syntaxin-1a_{wt} is added to Munc18-1_{W28A}. Difference at the initial fluorescence emission spectrum of Munc18-1_{wt} and Munc18-1_{W28A} are caused by the lack of one out of the 5 Tryptophans from the later. **C.** Changes in the tryptophan fluorescence measured at 332nm upon titration of different syntaxin 1a variants into 200 nM Munc18-1_{wt} or Munc18-1_{W28A}. Addition of either Syx1a_{wt} to Munc18-1_{wt} led to a clear increase in fluorescence, while titration of Syx1a_{F34A} to Munc18-1_{wt} leads to lower increase, and titration of Syx1a_{wt} to Munc18-1_{W28A} leads to almost no increase in Trp emitted fluorescence.

in the inner cavity of Munc18-1. Trp₄₇₈, Trp₅₂₂ and Trp₅₆₃ are present at the outer surface of domain 2. They are not in direct contact with syntaxin in the complex and therefore not very likely to change upon complex formation. By contrast, Trp₂₈ on the inner surface

of domain 1 is in contact with Phe₃₄ on the Ha helix of Syntaxin-1a. The distance (~ 5 Å) between the two aromatic rings of Trp₂₈ and Phe₃₄ and the angle ($\sim 30^\circ$) formed between them qualifies them for a pi-pi stacking interaction pair (Piovesan et al., 2016) (Figure 4.8.A) and thus were plausible candidates for the observed Trp fluorescence dequenching effect observed upon complex formation between syntaxin 1a and Munc18-1.

To confirm their involvement in Trp dequenching, I used a Syx1a variant in which the highly conserved Phe₃₄ was changed to alanine (Syx1a_{F34A}). In another construct, Trp₂₈ of Munc18-1 was also substituted to alanine (M18_{W28A}). Indeed, interaction of Munc18-1_{wt} with Syx1a_{F34A} led to drastic reduction of tryptophan dequenching and almost no increase was observed when Syntaxin-1a wt was titrated to M18_{W28A} (Figure 4.8.B-C). This corroborates the initial idea that the tryptophan fluorescence dequenching upon complex formation is largely caused by the close proximity of tryptophan 28 of Munc18-1 and phenylalanine 34 of Syntaxin.

4.3.2 The Munc18 Tryptophan28 – Syntaxin Phenylalanine34 pair contributes to the tight interaction of the two proteins

The proximity of Trp₂₈ to Phe₃₄ suggests that these residues also contribute to the tight interaction of the two proteins. Phe₃₄ is at N-terminal tip of the Ha helix of Syntaxin-1a which interacts with the inner cavity of domain 1. Previous observations highlighted

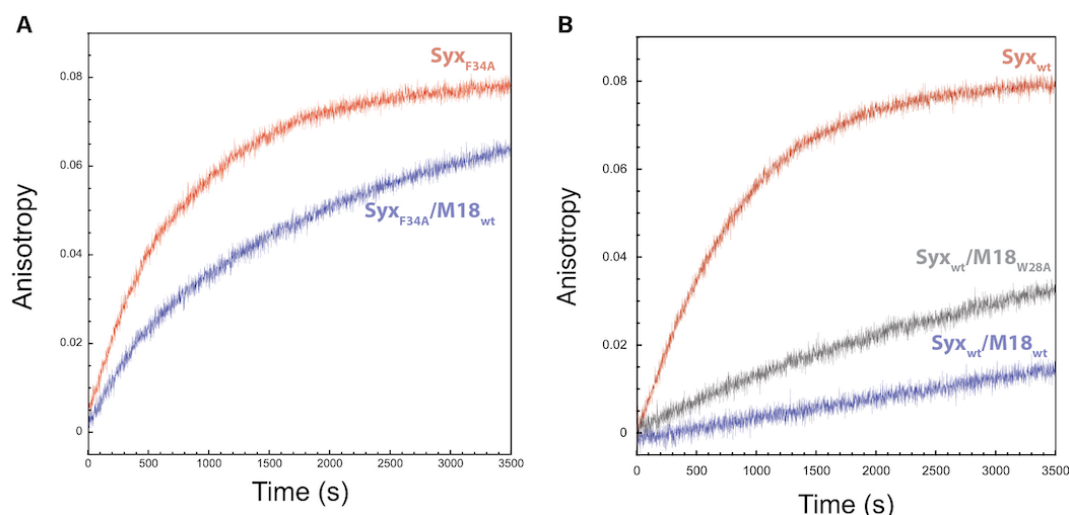


Figure 4.9: Trp₂₈-Phe₃₄ interaction is important for maintaining the inhibition. **A.** Syx1a_{F34A} variant can more rapidly form a SNARE complex in the presence of Munc18-1 compared to other Syx_{wt}. The increase in fluorescence anisotropy was measured in the presence (blue trace) or absence (red trace) of Munc18-1. **B.** SNARE complex forms more rapidly when Syx_{wt} is preincubated with Munc18-1_{W28A} (grey), as compared to when preincubated with Munc18-1_{wt} (blue).

the importance of the Syntaxin-1a N-peptide interaction with the outer surface of Munc18-1 domain 1 (Burkhardt et al., 2008, Colbert et al., 2013). I wondered whether the inner surface of domain 1 of Munc18-1 is an equally important interaction contributor to the interaction with syntaxin. To explore this, I tested the effect of the two mutations on the inhibitory effect of Munc18 on SNARE complex formation. I found that the substitution of Phe₃₄ with a tyrosine led to a partial loss of inhibition (data not shown). A much stronger loss of inhibition was observed when Phe₃₄ was changed to an alanine (Figure 4.9.A).

This effect was comparable to the one caused by double mutations in the linker of Syntaxin-1a as described above (Figure 4.5). Similarly, when I tested the effect of the W28A substitution, I found a reduction, yet smaller than for Syx_{F34A}, on the inhibition of SNARE complex formation (Figure 4.9.B). The effects caused by F34A and W28A are very interesting, because they suggest that this region, which is far away from the linker region of Syntaxin, is also involved in maintaining the tight grip of Syntaxin by Munc18.

4.4 The linker between the N-peptide and the Habc domain of Syntaxin-1a also contribute to the tight interaction of syx and Munc18

As detailed in Introduction, in the crystal structure of the Munc18a/Syntaxin 1a complex, Syntaxin adopts a closed conformation, in which the SNARE motif is bound to the Habc-domain. The closed conformation of Syntaxin is held by the concave surface between domains 1 and 3 of the arch-shaped Munc18-1. While the inner surface of domain 1 is interacting mainly with the SNARE motif of Syntaxin, the outer surface of domain 1 binds to the very N-terminal region of Syntaxin 1a, the so-called N-peptide. The two bindings sites are spatially separated, yet mutations on both sites (Syntaxin_{LE}, Syntaxin_{ΔLinker} and Syntaxin_{ΔN}, Syntaxin_{F34A}) lead to comparable effects as shown in previous studies (Colbert et al., 2013, Burkhardt et al., 2008) and here. This is puzzling as no obvious molecular communication can be gleaned from the crystal structure. I noticed that the N-peptide of Syntaxin is connected to the Ha-helix by a short stretch, which has not received a lot of attention in mutational studies so far. What role does the short linker stretch play for the interaction of Syntaxin with Munc18? When I took a closer look at the conservation of the short linker between N-peptide and Ha-helix (Appendix Fig. 2), I

noticed that this stretch is also conserved, not only in sequence composition but also in length. We thus discussed in our research group, whether the length conservation might indicate that the given length of the connection of the N-peptide (bound to the outer surface of domain 1) to the closed conformation (bound to the inner surface of domain 1) could be important to hold domain 1 of Munc18-1 at a defined distance or to restrict its movements. In this regard note that the domain 1 was found to be slightly rotated in different crystal structures (Archbold et al., 2014). Henceforth, we decided to test this idea by removing the linker ($\text{SyX}_{\Delta 11-26}$), which should make it impossible for the N-peptide to reach its binding site, or by extending the length of the linker region, which should remove the firm grip on the position of domain 1 of Munc18-1. To extend the linker, we decided to add two times the linker sequence between position 11 and 26 ($\text{SyX}_{3 \times (11-26)}$).

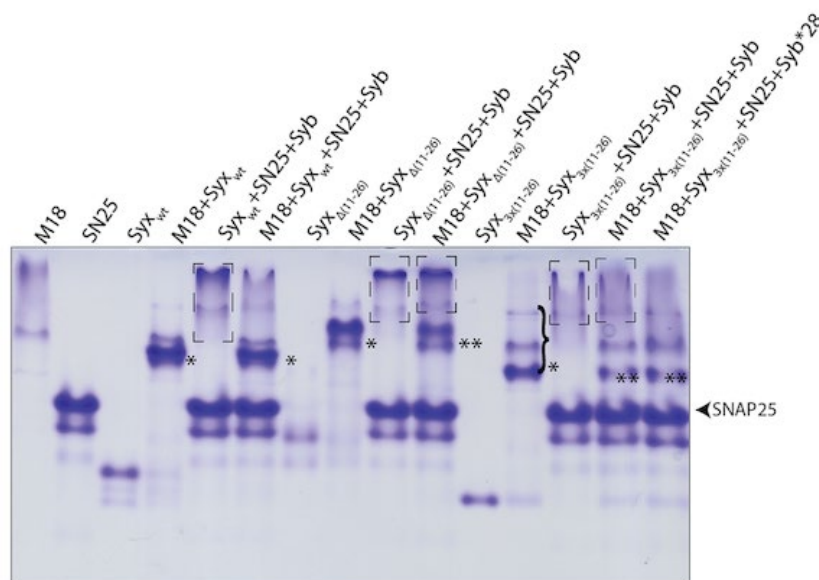


Figure 4.10: N-terminus mutants bind to Munc18_{wt}. 55 μM of Munc18_{wt}, 34 μM SyX_{wt}, SyX $\Delta(11-26)$ & SyX $3 \times (11-26)$ were loaded per lane alone, as mixtures. 82 μM SNAP25 and 82 μM Synaptobrevin (Syb) were also mixed with the syntaxin variants in the presence and absence of Munc18_{wt}. Dashed boxes indicate the smear corresponding to the SNARE complex, single asterisk the Munc18/Syntaxin complexes and double asterisks the “unstable” Munc18/Syntaxin complexes.

I found that both mutants ($\text{SyX}_{\Delta 11-26}$ & $\text{SyX}_{3 \times (11-26)}$) are able to form a stable complex with Munc18_{wt}, as seen by native gel electrophoresis (Figure 4.10). When SNAP-25 and synaptobrevin were added to the mix, SNARE complexes started to appear (Figure 4.10). This indicated that the linker variants could be more prone to escape the tight grip of Munc18-1 than wt syntaxin. To analyze this more precisely I used the fluorescence anisotropy assay for SNARE complex assembly yet again.

Results

As shown in Figure 4.10, the rate of SNARE complex formation of Syx_{3x(11-26)} in the presence of Munc18-1 was comparable to a syntaxin without N-peptide (Syx_{ΔN}). Interestingly, Syx_{Δ(11-26)} (Figure 4.11.C) assembled even somewhat faster into a SNARE complex in the presence of Munc18-1. This suggests that the 11-26 region is indeed important for the interaction of Munc18 and syntaxin and that it might play a role in the allosteric coupling of the two spatially separated interaction surfaces.

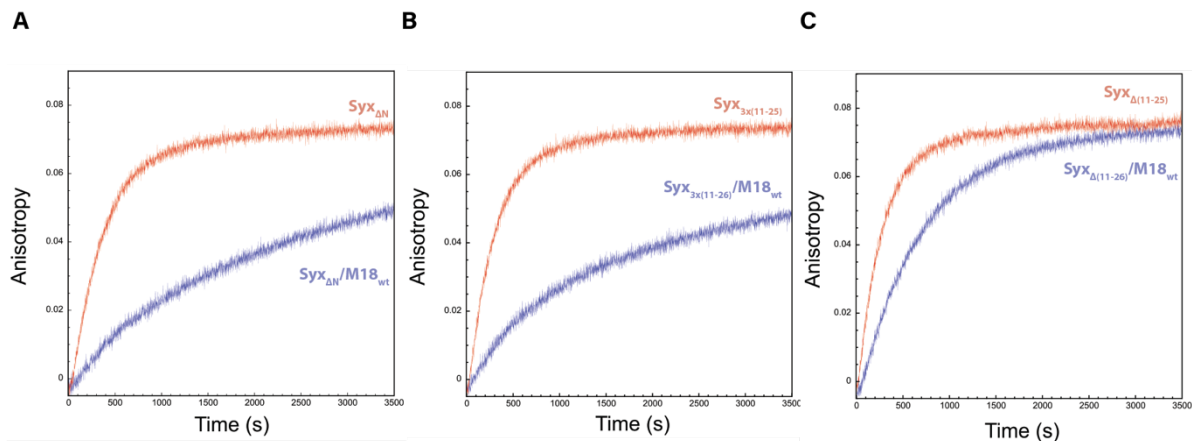


Figure 4.11: Syx1a_{ΔN}(A), Syx1a_{3x(11-26)}(B) and Syx1a_{Δ(11-26)}(C) variants can more rapidly form a SNARE complex in the presence of Munc18-1 as compared to other Syx variants tested in this study. The increase in fluorescence anisotropy was measured in the presence (blue trace) or absence (red trace) of Munc18-1_{wt}.

4.5 Munc18-1 domain 3a regulates SNARE complex formation

As outlined in the Introduction, Munc18 and other SM proteins share an overall conserved topology and structure. However, several slightly different conformations were described for the different crystal structures of this protein family. One structural difference was observed for the position of domain 1 as discussed above. Another major structural change was noticed for the so-called “helical hairpin” at the tip of domain 3a. In the absence of bound syntaxin, the “helical hairpin” usually adopts an extended conformation, whereas it is in a so-called furled conformation in the Munc18-1/syntaxin complex. It is plausible that when Syntaxin-1a is bound to Munc18-1, the extension of helix 12 is clashing the H3 helix of Syntaxin-1a in closed conformation.

Several point, deletion, and insertion mutations have been tested to understand a possible conformational change of this region upon (un-)binding to Syntaxin, but the picture remains ambiguous still. In the following sections, I have tested the effect of several Munc18 variants.

4.5.1 Munc18_{P335A} significantly affects the inhibition

A highly conserved proline is located at the hinge of $\alpha 11\alpha 12$ helices of Munc18. When mutated to alanine it was associated with gain-of-function effect as it promotes exocytosis, though the molecular mechanism by which this occurs is unclear. (Han et al., 2014, Munch et al., 2016, Martin et al., 2013). It is thought that the P335A change shifts Munc18a Munc18-1 towards the extended helix conformation that would interfere with binding of the closed syntaxin. Therefore, I wanted to get a better understanding of the involvement of this residue in the interaction of Munc18 with Syntaxin. I started by looking into the ability of Munc18_{P335A} to form a tight complex with syntaxin. For this, I used size exclusion chromatography. As it can be seen in Figure 4.12, individual Munc18_{wt} and syntaxin eluted each as single peaks from the size-exclusion column. When the two proteins were mixed, they formed a complex that eluted earlier from the column. When I ran Munc18_{P335A}, the protein eluted much earlier than Munc18_{wt}, suggesting that Munc18_{P335A} oligomerizes. Most probably, it forms a homodimer. When mixed with syntaxin, Munc18_{P335A}, a complex formed that eluted at the same volume as the Munc18_{wt}/Syntaxin-1a complex, revealing that the P335A change still allows for interaction with Syntaxin-1a (Figure 4.12.A). Munc18-1_{P335A}/Syx-1a_{wt} also migrated as a stable complex on a native gel, as seen by the appearance of a sharp band (Figure 4.17.A).

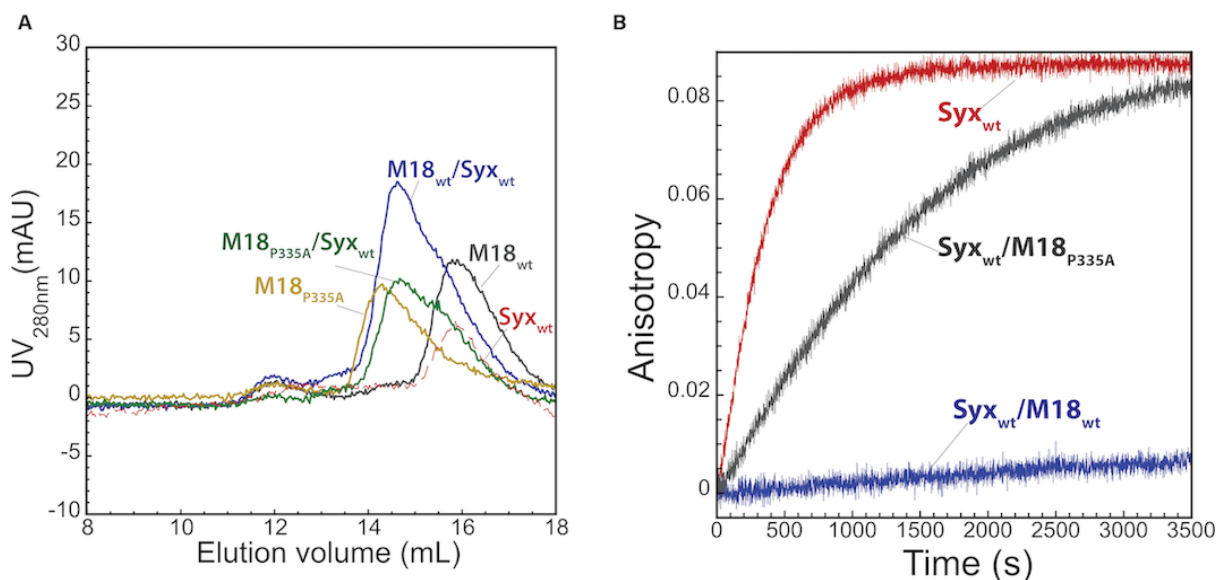


Figure 4.12: Munc18_{P335A} binds to Syntaxin_{wt} with reduced inhibitory “power”. A. Size Exclusion chromatography of $\sim 22\mu\text{M}$ individual Munc18_{P335A} (ochra), Munc18_{wt} (grey), and Syntaxin_{wt} (red dashed) alone, or in mixtures. Munc18_{P335A} alone elutes as a dimer, however, when mixed with Syntaxin, the elution peak at a value like wt complex. B. SC formation in the presence of Munc18_{P335A} (grey) is significantly faster than in the presence of Munc18_{wt}, at a level comparable to the effects seen by Syntaxin_{LE}.

Results

Next, I tested the effect of the P335A change on the block exerted on SNARE complex formation using the fluorescence anisotropy assay. As shown in Figure 4.12.B, Munc18_{P335A} slowed the transition of bound Syntaxin-1a towards the SNARE complex somewhat, but much less than Munc18_{wt}. This indicates that the P335A change might have eased the conformational change of the closed Syntaxin-1a towards a configuration that allows for SNARE complex formation. It is possible that proline 335 has a functional role to keep the loop unfurled.

4.5.2 Inhibition regulation by domain 3a could be caused by “steric” restrictions

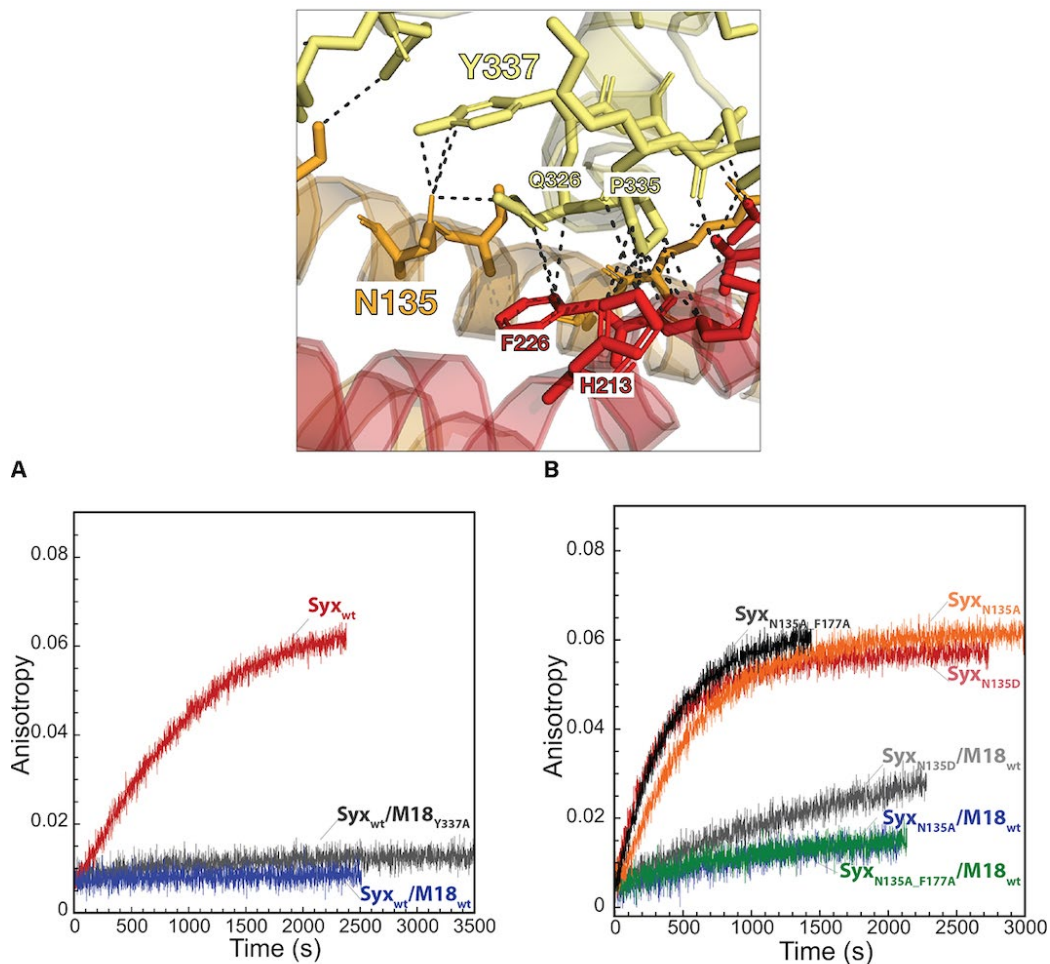


Figure 4.13: Inhibition is maintained when Tyr₃₃₇-Asn₁₃₅ interaction is disrupted but is affected with the introduction of negative charge. A. Inhibition is only mildly reduced, as seen by the small differences at SC formation when Munc18_{Y337A} is present (grey). **B.** Inhibition of SC formation is reduced when Asn₁₃₅ is substituted by an aspartate as seen by the increase in anisotropy when Syx_{N135D} is in complex with Munc18_{wt} (grey trace).

In close vicinity of Pro₃₃₅ is Tyr₃₃₇. It is on helix 12 of domain 3a and in polar contact with Asp₁₃₅ of the Hc helix of syntaxin (Figure 4.13). This residue has been previously studied in other *in vivo* studies, with unclear observations (Han et al., 2013, Boyd et al., 2008b, Han et al., 2014). Mutation of Y337 to leucine (Y337L) has been designed as the equivalent of sec1 F361L mutant. Boyd et al., 2008 discovered the F361L mutant in a random mutagenesis approach in yeast, having mutated its Munc18-1 equivalent, Y337L for further study. Munc18-1_{Y337L} was found to inhibit secretion in PC12 cells (Boyd et al., 2008b). However, Han et al. 2013 & 2014, studied the effects of the Y337L mutation in combination with other mutations at domain 3a. To study this interaction, I designed four mutants. One mutant of Munc18 where tyrosine mutated to alanine (Munc18_{Y337A}), and three mutants of Syntaxin, in which asparagine was mutated to (i) alanine (Sy_{XN135A}), (ii) aspartate (Sy_{XN135D}) and (iii) a double mutant, in which N135A was combined with the alanine mutation of the hydrophobic residue F177 in the linker helix (Sy_{XN135A_F177A}).

When measuring SNARE complex formation, I did not observe a significant difference between the inhibition on SNARE complex formation exerted by Munc18_{Y337A} and Munc18_{wt} (Figure 4.13.A). Similarly, Sy_{XN135A}, and, even the double mutant Sy_{XN135A_F177A}, to my surprise, were inhibited by Munc18_{wt} (Figure 4.13.B). However, Sy_{XN135D} showed more reduced inhibition, suggesting that the introduction of the negative charge by the aspartate affects the environment around these two interacting residues.

4.5.3 SNARE complex formation is pH sensitive

Another intriguing residue of the Munc18-1/Syntaxin-1a complex interface involved in the network of interactions is Histidine-213 of Syntaxin H3 helix. The presence of the imidazole ring of histidine side chain at the H3 helix breaking point, and, in polar interaction with Munc18 domain 3a Pro₃₃₅, made it a candidate residue for a possible conformational regulation (Figure 4.14.A). I, therefore, mutated the histidine to an alanine (Sy_{XH213A}) and monitored SNARE complex formation using the fluorescence anisotropy assay and SDS electrophoresis. Inhibition of Syntaxin_{H213A} by Munc18_{wt} was

Results

only somewhat abolished. Note that SNARE complex formation in the absence of Munc18 appeared to be somewhat slower than for wt syntaxin.

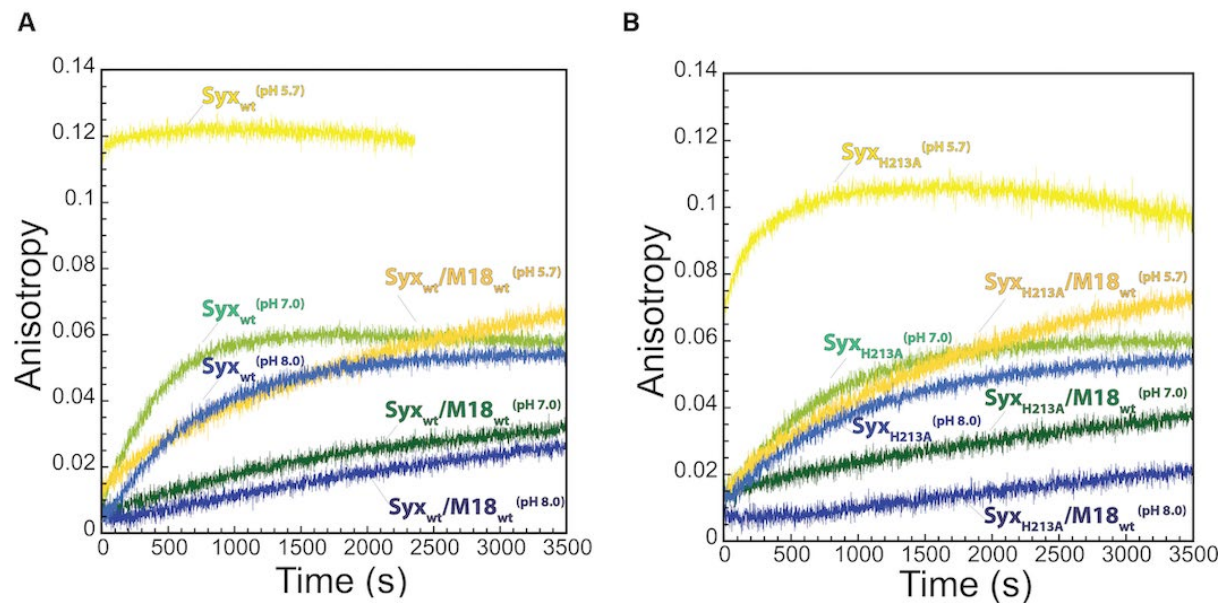


Figure 4.14: SNARE complex formation accelerates at acetic pH. **A.** SC formation at pH 5.7 (yellow traces) is very fast as observed by the immediate increase in Syb*²⁸ anisotropy. In more alkaline pH (pH 8.0) SC formation proceeds slower (blue traces). Pre-incubation of Syntaxin_{wt} with Munc18_{wt} affects the rate of anisotropy increase. **B.** As for Syntaxin_{wt}, SC formation using Syntaxin_{H213A} proceeds faster at acetic (yellow) and slower at alkaline (blue) pH. However, they rate of increase of anisotropy seems to be lower than of Syntaxin_{wt}. Interaction with Munc18_{wt} affects the rate SC formation also for Syntaxin_{H213A}.

Given the sensitivity of the imidazole ring to protonation (Schönichen et al., 2013), I sought to investigate whether Munc18/Syntaxin interaction is affected by pH changes. To study this, I measured for Syb*28 OG fluorescence anisotropy increase in three pH conditions, pH 5.7, pH 7.0 and pH 8.0. Interestingly, SNARE complex formation is accelerated drastically at acetic pH (pH 5.7) (Figure 4.14.A). Also, when Syx_{H213A} was mixed with its partner SNAREs at acetic pH, SNARE complex was accelerated, although at slower pace than with Syntaxin_{wt}, and reaches a lower saturation value (Figure 4.14.B). Nevertheless, even in acetic pH, SNARE complex formation is slowed down in the presence of Munc18_{wt}. In general, Syntaxin_{H213A} assembles more slowly into a SNARE complex than Syntaxin_{wt} at all three pH conditions studied, which suggests that His₂₁₃ might be important for SNARE complex formation. This residue lies between residues of -3 and -4 layers of the SNARE helix, and is conserved, suggesting that it could play a role during SNARE complex formation.

4.5.4 The $\alpha_{11}\alpha_{12}$ helical hairpin is dispensable for maintaining the inhibition, but it is needed to keep the interaction.

I also characterized the previously described mutant, in which the $\alpha_{11}\alpha_{12}$ helical hairpin loop residues 317 – 333 are removed entirely in order to prevent an extended conformation of that stretch (Munc18 $\Delta_{317-333}$) (Martin et al., 2013). Upon native gel electrophoresis, a stable complex formed between Syx_{wt} and Munc18 $\Delta_{317-333}$ (Figure 4.15). When Munc18 $\Delta_{317-333}$ was preincubated with Syx_{wt}, SNARE complex formation was

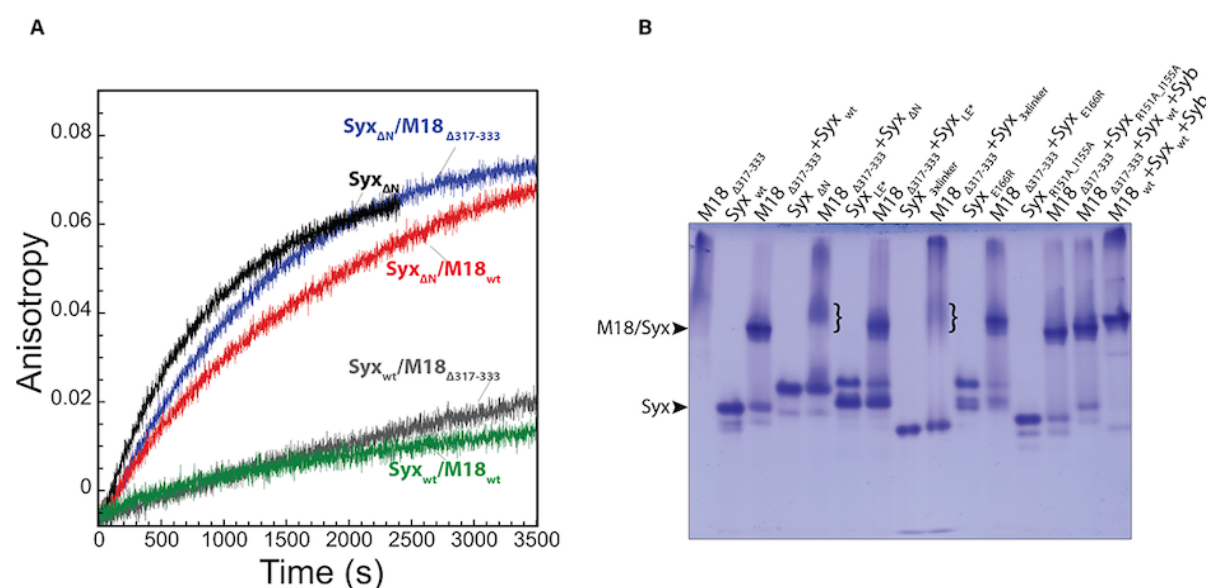


Figure 4.15: Munc18 $\alpha_{11}\alpha_{12}$ loop residues confer to inhibition. **A.** SNARE complex only slightly faster when Syntaxin_{wt} is interacting with Munc18 $\Delta_{(317-333)}$ (grey trace) than with Munc18_{wt} (green trace) as seen by the anisotropy increase of Syb*28 OG. However, when Syntaxin Δ_N is interacting with Munc18 $\Delta_{(317-333)}$ inhibition is almost completely abolished (blue trace), yet increased in comparison to then Munc18_{wt} is interacting (red). **B.** Munc18 $\Delta_{(317-333)}$ is not forming stable complex with Syntaxin Δ_N and Syntaxin_{3x(11-25)} as seen by the smear migration on the native gel electrophoresis of the respective mixtures (indicated by the brace symbol).

slightly faster compared to when Munc18_{wt} was used (Figure 4.15.A). The difference of the effects between Munc18 $\Delta_{317-333}$ and Munc18_{wt}, though, is more prominent when Munc18 $\Delta_{317-333}$ is interacting with Syx Δ_N , i.e., when the N-peptide region of syntaxin was absent. Fluorescence anisotropy was increasing at a faster rate for Munc18 $\Delta_{317-333}$ /Syx Δ_N than for the Munc18_{wt}/Syx Δ_N containing reaction, whilst still somewhat slower to when no Munc18 is present. The faster rate for Munc18 $\Delta_{317-333}$ /Syx Δ_N could have resulted by an instability of the Munc18/Syntaxin complex due to disruption of interactions at the two interacting sides. To test for this, I used native gel electrophoresis. Indeed, the Munc18 $\Delta_{(317-333)}$ /Syntaxin Δ_N mixture ran as a smear and not as a sharp band. This indicates that this complex is less stable compared to the one of Munc18 $\Delta_{317-333}$ /Syx_{wt}

(Figure 4.15.B). A similar, but even more prominent effect was observed for the combination of Munc18 $\Delta(317-333)$ and Syntaxin $_{3x(11-26)}$.

4.5.5 Interactions of both domain 3a and 1 of Munc18 with syntaxin are needed to maintain the tight grip

The experiments described above indicated that stronger effects became more noticeable when the interaction of the two molecules were perturbed at two spatially separated sites. I thus decided to explore this combinatorial approach further. In a new set of experiments, I mixed another domain 3a mutant, Munc18 $_{P335A}$, with different

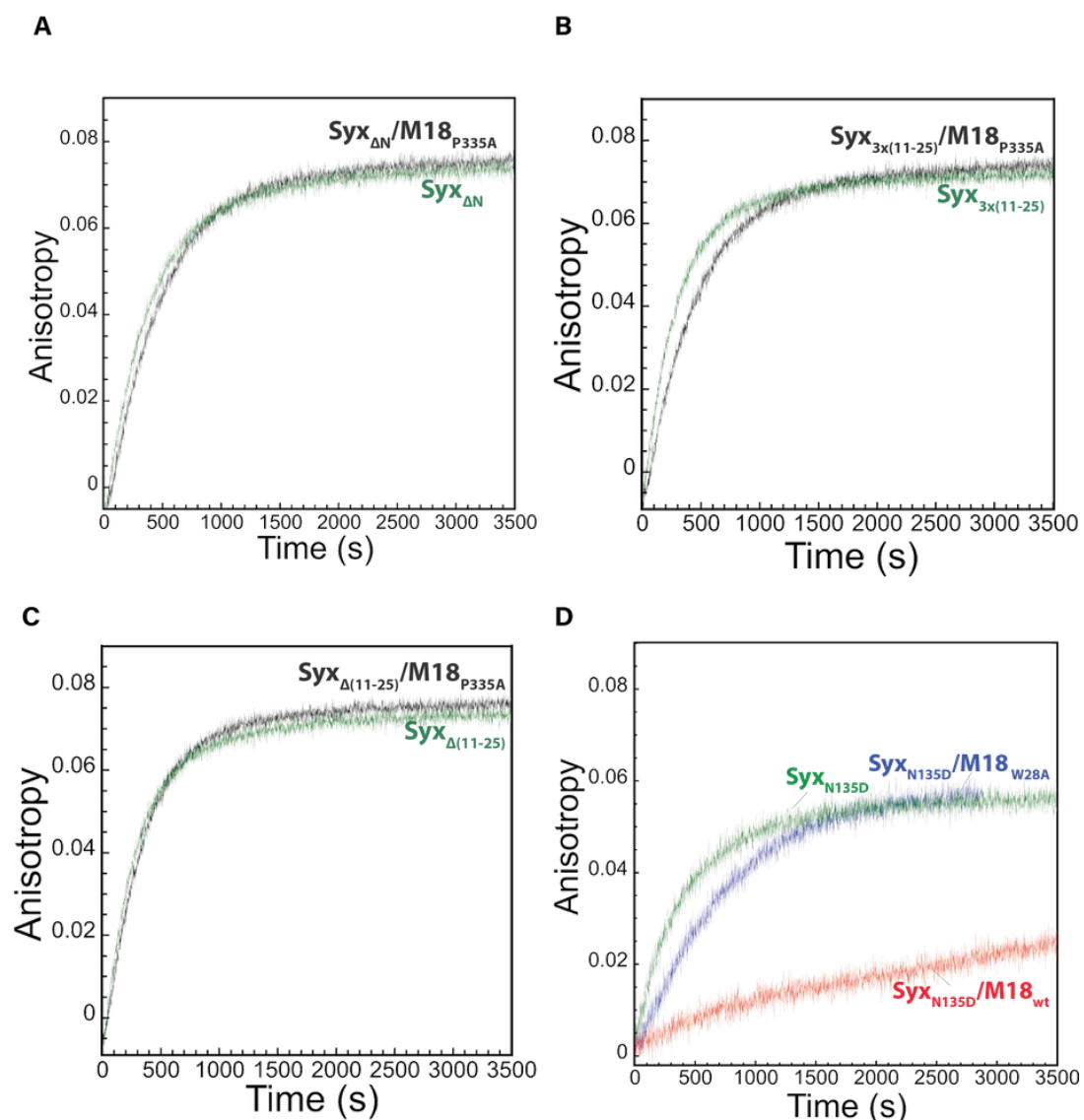


Figure 4.16: SNARE complex inhibition is almost completely overcome when interactions at domain 1 and domain 3a are affected. A-C. Munc18 $_{P335A}$ does not inhibit Syntaxin N-terminus mutants (black traces). **D.** Munc18 $_{W28A}$ does not inhibit Syntaxin $_{N135D}$ (blue), that only has a mild loss of inhibition effect when interacting with Munc18 $_{wt}$ (red trace).

Results

mediating interaction with Syntaxin-1a H3. The Munc18-1_{K332E_K333E} was first introduced by Han et al., 2013 to bear mutations at the conserved K332 and K333 lysines in order to interfere with the interactions of domain 3a with Syntaxin-1a H3. However, Munc18-1_{K332E_K333E} did not affect secretion in PC12 cells (Han et al., 2013).

Munc18-1_{KEKE} structure was solved as homodimer packed against each other through domain 3a. The structure revealed that isolated Munc18-1, like its other paralogs Munc18-2 and Munc18-3, alone can adopt a different conformation. At the Munc18_{KEKE} structure, the $\alpha_{11}\alpha_{12}$ loop is unfurled causing the extension of the helical hairpin.

To investigate how the mutations effect the interaction with syntaxin, I expressed and purified Munc18_{KEKE}. Upon size exclusion chromatography, Munc18_{KEKE} eluted as a monomer and formed a stable complex with Syntaxin_{wt} (Figure 4.18.B), corroborating the earlier study (Wang et al., 2020). Munc18_{KEKE} also inhibited SNARE complex formation to very similar degree as Munc18_{wt} (Figure 4.18.A).

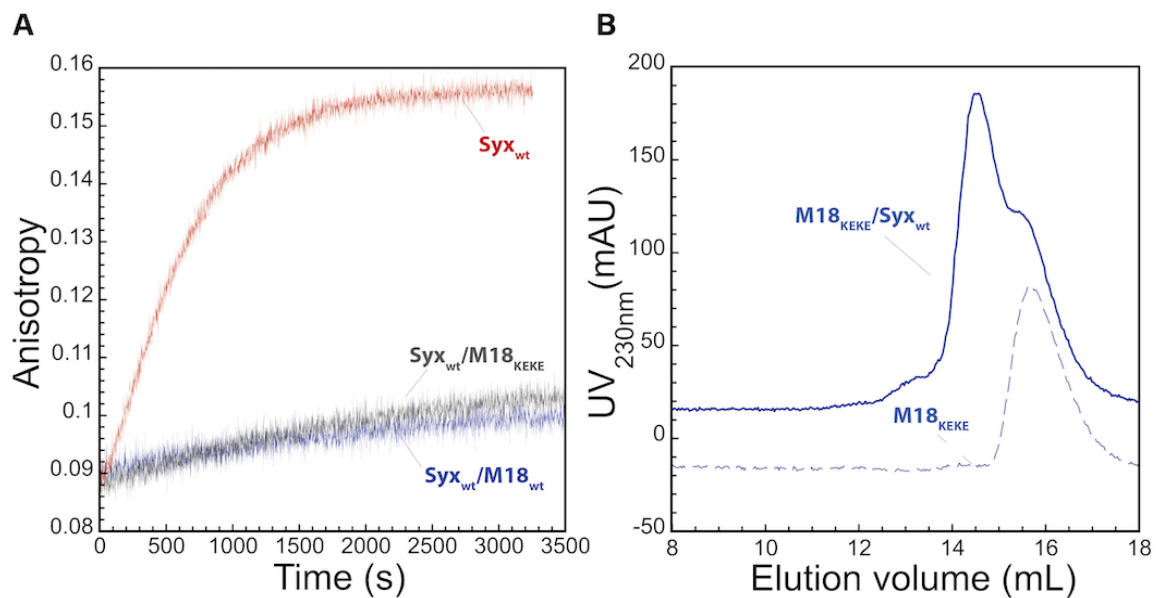


Figure 4.18: Munc18_{KEKE} behaves like Munc18_{wt}. A. SC formation is inhibited when Syntaxin_{wt} is interacting with Munc18_{KEKE} (grey trace) as when interacting with Munc18_{wt} (blue trace) as seen by the anisotropy increase of Syb*28 OG. B. Munc18_{KEKE} elutes as a monomer (dashed blue trace) and as a complex when mixed with Syntaxin_{wt} (blue solid trace).

4.5.7 Munc18 domain 3a templating role was not detected

It has been proposed that two variants of domain 3a (Munc18_{D326K} and Munc18_{L348R}) might affect SNARE complex formation through interference with a

putative Synaptobrevin binding step (Sitarska et al., 2017, Parisotto et al., 2014). Munc18_{D326K} has been suggested to promote SNARE complex formation through facilitation of Synaptobrevin binding and Munc18_{L348R} is thought to inhibit SNARE complex formation through interference with Synaptobrevin binding. I tested both variants in my assays. For both variants, SNARE complex inhibition was almost unaffected as observed by fluorescence anisotropy increase of Synaptobrevin at pH 7.4 (Figure 4.19.A&C). Bearing in mind that the potential interference with Synaptobrevin binding described for these mutants might cause problems in this experimental approach, in which only low concentrations of Synaptobrevin are used. I also checked for SNARE complex formation using the same assay at pH 5.7 for better resolution of small differences. To my surprise, SNARE complex formation was accelerated when

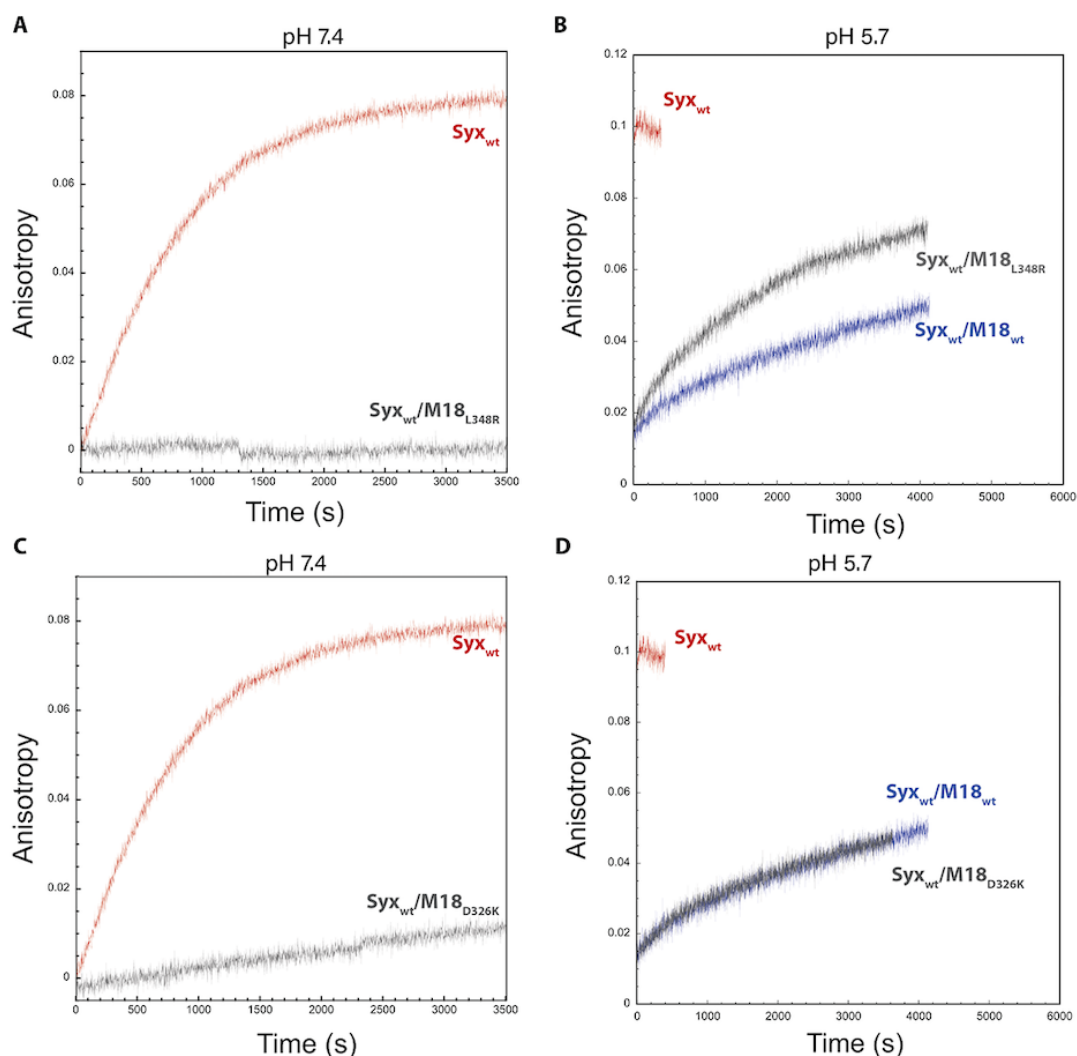


Figure 4.19: Munc18_{D326K} and Munc18_{L348R}. **A.** SC formation is inhibited when Syntaxin_{wt} is interacting with Munc18_{L348R} (grey trace) as seen by the anisotropy increase of Syb*28 OG at pH 7.4. **B.** SC formation is less inhibited when Syntaxin_{wt} is interacting with Munc18_{L348R} (grey trace) as seen by the anisotropy increase of Syb*28 OG at pH 5.7. **C.** Munc18_{D326K} inhibits SC formation at pH 7.4 and pH 5.7 (**D**).

Results

Munc18_{L348R} is present in comparison to Munc18_{wt} and Munc18_{D326K}, which were indistinguishable (Figure 4.19.B&D).

I also used gel electrophoresis. Again, I did not detect any differences between Munc18_{L348R} and Munc18_{wt} (data not shown). It is worth mentioning though that Munc18_{L348R} had an increased propensity of precipitation in comparison to other Munc18 variants.

4.5.8 The Munc18 $\beta_{10}\beta_{11}$ hairpin loop confers interactions necessary for the inhibition

A previous study of SM proteins in our laboratory revealed that $\beta_{10}\beta_{11}$ hairpin loop (residues 269-275) is shorter in Munc18-3, the pancreatic paralogue of Munc18-1, than in Munc18-1 (Morey, 2015). This loop is involved in an extensive interaction network with the Syntaxin H3 region, as seen by the crystal structure of the Munc18/Syntaxin complex. It was therefore proposed that this region could contribute to the interactions necessary to maintain the complex in closed conformation (Morey, 2015). To study that, we created a variant where those residues were removed (Munc18 $\Delta_{269-275}$).

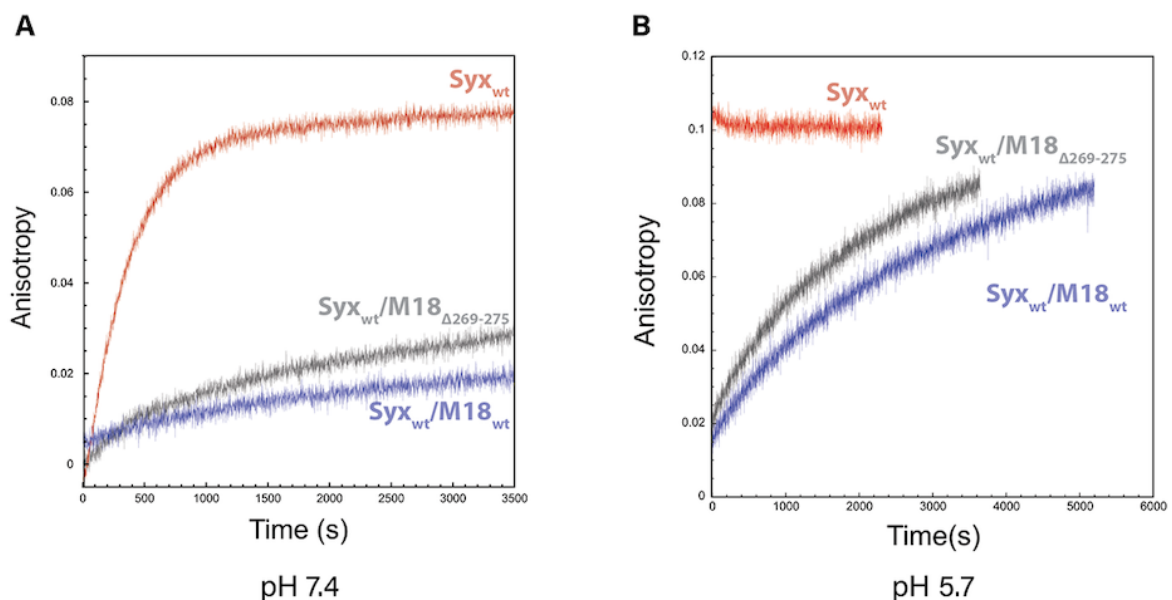


Figure 4.20: Munc18 $\beta_{10}\beta_{11}$ loop residues confer to inhibition. SNARE complex forms faster when Syntaxin_{wt} is interacting with Munc18 $\Delta_{269-275}$ (grey trace) than with Munc18_{wt} (blue trace) as seen by the anisotropy increase of Syb*28 OG in buffer at pH 7.4 (A) and pH 5.7 (B).

Using the Fluorescence Anisotropy of Syb*28 assay, SNARE complex formation was slightly faster in the presence of Munc18 $\Delta_{269-275}$ than Munc18_{wt} (Figure 4.20.A). To better address the difference arising from the removal of the $\beta_{10}\beta_{11}$ hairpin loop, I ran the same

reactions at acetic pH. Previously, I observed that SNARE complex formation proceeded faster at acetic pH and gave better resolution between small differences in reaction rate (section 4.4.3). This experiment too exhibits that SNARE complex formation proceeds at faster rate in Munc18 Δ (269-275) than with Munc18wt (Figure 4.20.B), corroborating the idea that the loop contributes to the grip of Munc18.

4.5.9 Mutations that did not affect inhibition

Few mutations designed in my study did not affect the inhibition of SNARE assembly exerted by Munc18. For example, I tested a variant that had previously described to mimic a phosphorylation site, Munc18 $_{Y473D}$, and that was reported to affect the stimulatory role of Munc18 (Meijer et al., 2018). When observing for SNARE complex formation in the presence of Munc18 $_{Y473D}$, only a minute difference in the fluorescence anisotropy increase was detected (Figure 4.21). As the change was small and not clear, I did not pursue this line further.

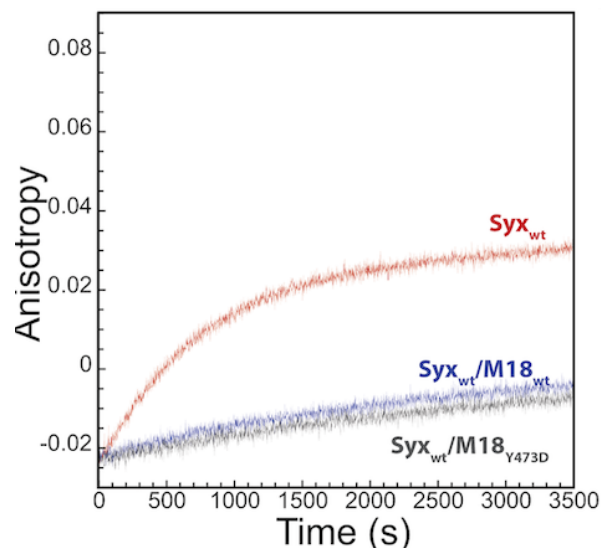


Figure 4.21: Munc18 $_{Y473D}$ might be inhibit SC formation more than Munc18 $_{wt}$. A. SC formation is inhibited when Syntaxin $_{wt}$ is interacting with Munc18 $_{Y473D}$ (grey trace) as when interacting with Munc18 $_{wt}$ (blue trace) as seen by the anisotropy increase of Syb*28 OG.

I also took a closer look to some interacting residues of the complex interface, such as the binding cleft, created by Munc18-1's inner cavity. There, Munc18 Asn $_{261}$, is involved in a network of interactions with Glu $_{324}$ and Glu $_{234}$, located on the H3 helix of Syntaxin-1a. To examine the contribution of this interaction to the inhibition, I mutated these residues to alanines. No change in SNARE complex formation was observed with either the fluorescence anisotropy or the SDS electrophoresis assays when Syntaxin $_{wt}$ was mixed with the Munc18 $_{N261A}$ mutant (Figure 4.22).

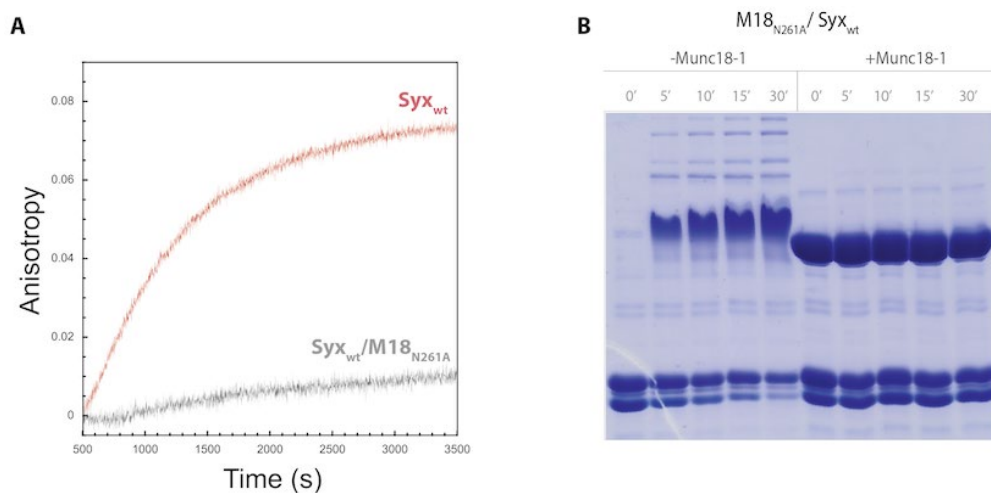


Figure 4.22: Munc18_{N261A} behaves like Munc18_{wt}. A. SC formation is inhibited when Syntaxin_{wt} is interacting with Munc18_{N261A} (grey trace) as seen by the anisotropy increase of Syb*28 OG. B. No SNARE complex was observed after SDS PAGE electrophoresis of Syntaxin, SNAP25 and Synaptobrevin mixtures, when Munc18_{N261A} was present (right panel). In the absence of Munc18, SNARE complexes formed, with the amount increasing from 0'-30' (left panel).

I also studied this interaction using Syntaxin mutants. I did not observe changes in the SNARE complex inhibition when using Syntaxin_{E224A} (Figure 4.23). The mutant seems to behave like Syntaxin_{wt}. Inhibition and binding to Munc18_{wt} is maintained, as well as tryptophan emitted fluorescence increase is similar to the one observed when Syntaxin_{wt} is titrated to Munc18_{wt} (data not shown).

The observations when using Syntaxin_{E234A}, however, were rather unexpected. Using the same assay, fluorescence anisotropy was immediately starting to increase with

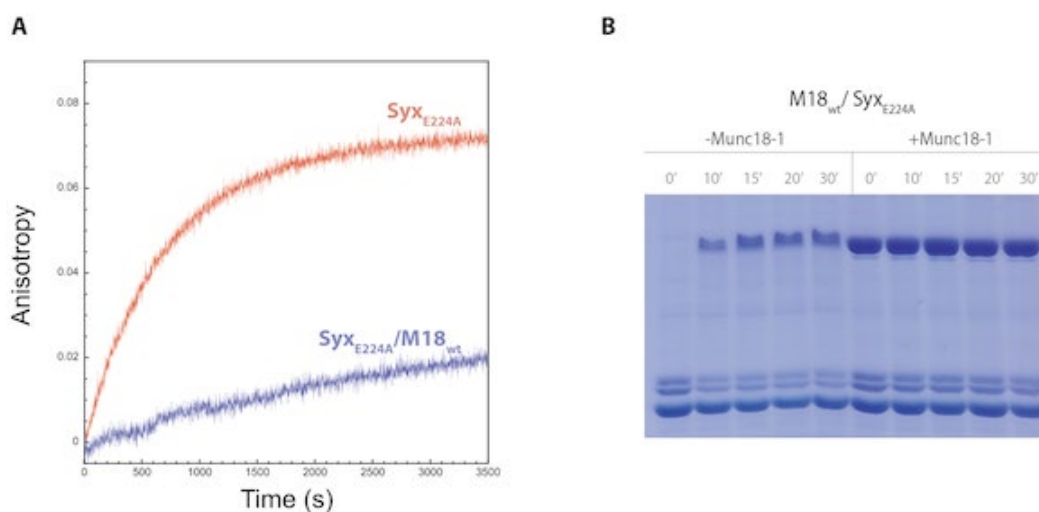


Figure 4.23: Syntaxin_{E224A} behaves like Syntaxin_{wt}. A. SC formation is inhibited when Syntaxin_{E224A} is interacting with Munc18_{E224A} (grey trace) as seen by the anisotropy increase of Syb*28 OG. B. No SNARE complex was observed after SDS PAGE electrophoresis of Syntaxin_{E224A}, SNAP25 and Synaptobrevin mixtures, when Munc18_{wt} was present (right panel).

the addition of only Syntaxin^{E234A} before addition of SNAP25. This mutation appears to have rendered Syntaxin able to directly bind to Synaptobrevin, which made it difficult to study using my assays (Appendix Fig. 3). Another residue of the complex interface I investigated was Munc18 Arg₃₁₅ of domain 3a. Munc18 Arg₃₁₅ is interacting with Syntaxin Arg₁₄₂ and Glu₁₆₆ (Figure 4.24.A). Substitution of the arginine with an alanine (Munc18_{R315A}) did not affect the inhibition, as no change in SNARE complex formation was observed in the presence of Munc18_{R315A} using the fluorescence anisotropy assay, at either pH7.4 or pH5.7 (Figure 4.25.B-C). Interestingly, the mutations on Syntaxin E166 and R142, that interact with Munc18 R315, both reduced the inhibition (Figure 4.4).

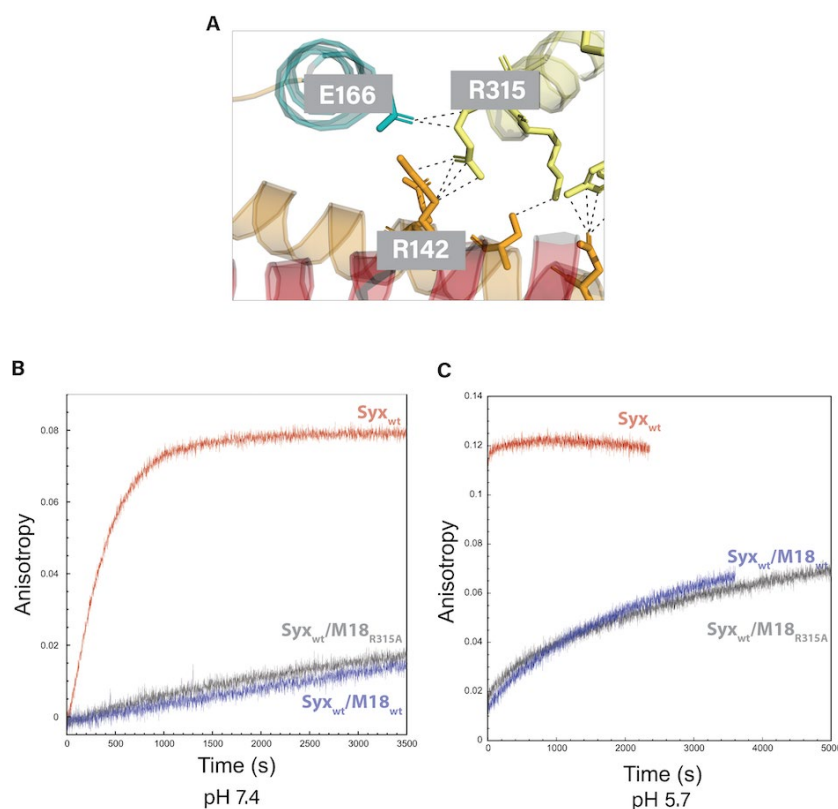


Figure 4.24: Munc18_{R315A} inhibits like Munc18_{wt}. A. Munc18 Arg₃₁₅ is in polar contacts with Glu₁₆₆ and Arg₁₄₂ of Syntaxin-1a. SNARE complex formation is inhibited when Munc18_{R315A} is in complex Syntaxin_{wt} (grey trace) at the same degree as when Munc18_{wt} is in complex Syntaxin_{wt} (blue trace) as seen by the anisotropy increase of Syb*28 OG of Syb*28 OG in buffer at pH 7.4 (B) and pH 5.7 (C).

4.6 Dissociation rates of the Munc18-1/Syntaxin-1a complex

4.6.1 Syntaxin linker mutations accelerate complex dissociation

In the previous sections, I have investigated the inhibitory effect of the Munc18-1 on Syntaxin-1a, i.e., how fast Syntaxin-1a can assemble into SNARE complex in the presence of Munc18-1. To assess the dissociation rates of the Munc18-1/Syntaxin-1a complex, I used another Fluorescence Anisotropy based assay. We created single cysteine variants of (i) Syntaxin_{wt} and Syntaxin_{Δ161-182}, at position 1 and position 186, and (ii) Syntaxin_{LE} at position 186. Each variant was labelled with Oregon Green fluorescent dye. Mixing the labeled syntaxin variant with Munc18 led to an increase in fluorescence anisotropy. I then determined the dissociation rate for each variant from the Munc18-1/Syntaxin-1a complex by measuring the anisotropy decay of the fluorescently labelled variant upon the addition of excess (200-fold) of label-free Syntaxin_{wt}. The dissociation

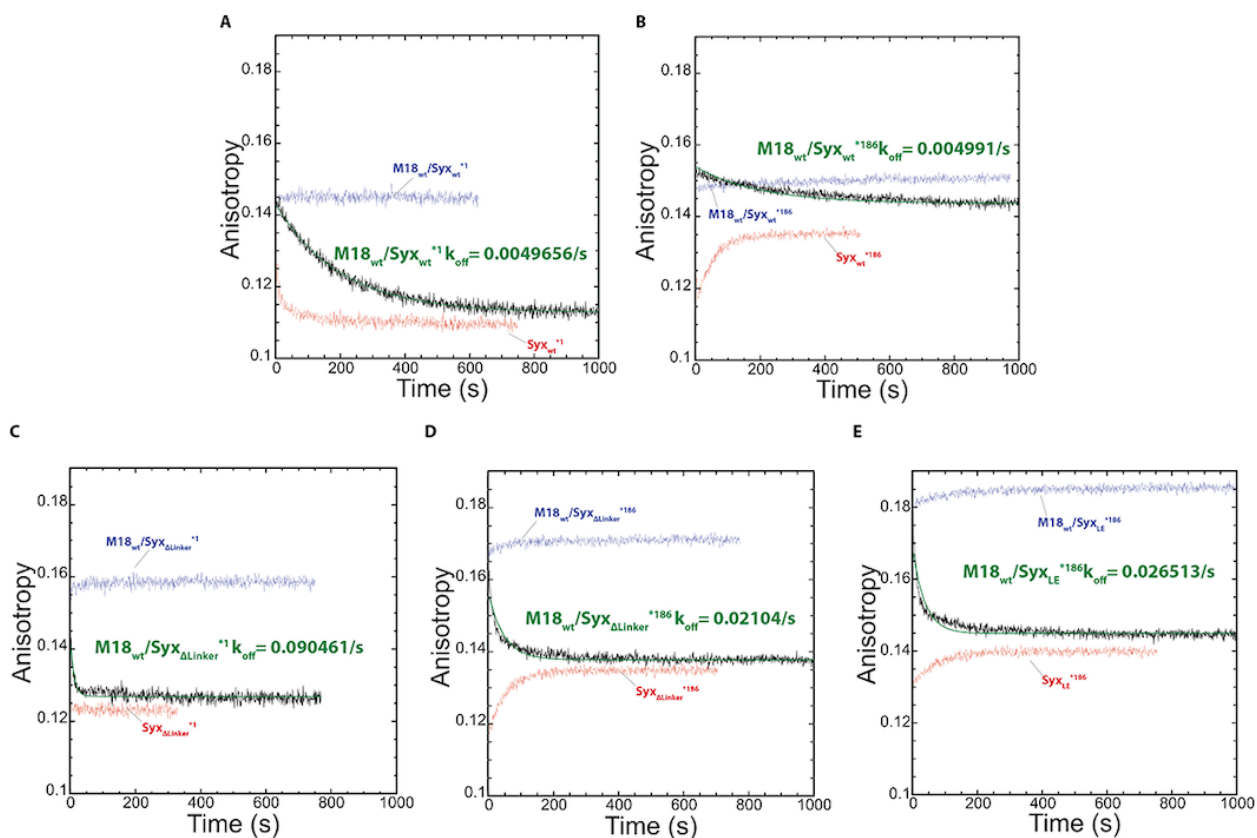


Figure 4.25: Dissociation rates of the Munc18_{wt}/Syntaxin linker mutants. A. Firstly, fluorescence anisotropy of 100nM Syntaxin_{wt}¹ is determined (red), and then after the addition of 250nM Munc18_{wt} (blue). Off rate is determined by the rate of anisotropy decay after the addition of 5μM Syntaxin_{wt}. Unless otherwise stated, all complex dissociation rates were determined likewise. B. Syntaxin_{wt} dissociation rate determined from position 186 was almost the same as when determined from position 1. C-E. Dissociation rate values for Syntaxin_{Δlinker} and Syntaxin_{LE} determined from position 186 were similar, while it was ~5x faster when determined from position 1 for Syntaxin_{Δlinker}.

rate for the Syntaxin_{wt}/Munc18_{wt} pair was comparable for both Syntaxin label positions (Syntaxin_{wt}^{*1} rate: $\approx 0.005/s$ and Syntaxin_{wt}^{*186}: $\approx 0.005/s$) (Figure 4.25.A-B). The off-rates were $\sim 5x$ faster for both Syntaxin $\Delta 161-182$ (Syx $\Delta 161-182$ ^{*186} rate: $\approx 0.021/s$) and Syntaxin_{LE} (Syx_{LE}^{*186} rate: $\approx 0.027/s$) than for Syntaxin_{wt}, when determined from position 186. Surprisingly, the off-rate for Syntaxin $\Delta 161-182$ (Syx $\Delta 161-182$ ^{*1} rate: $\approx 0.091/s$) was $\sim 18x$ faster than for Syntaxin_{wt} when determined from position 1. It is possible that the faster rate determined using Syntaxin $\Delta 161-182$ labelled at position 1 does not reflect the off-rate of the complex with Munc18-1, but rather the local flexibility of the N-peptide region.

4.6.2 Munc18_{W28A} has the highest dissociation rate amongst the Munc18 mutants

Next, I sought to determine the dissociation rate changes caused by the mutations on Munc18. To do so, I measured Fluorescence Anisotropy decay of Syx_{wt}^{*1} when in complex with different Munc18 variants. Of the mutants studied, complex dissociation was the fastest for Munc18_{W28A}. In fact, it was difficult to determine the exact value for this reaction, as the anisotropy decayed too fast for the hand-mixing approach used. Thus, the rate determined for that mutant can only be approximated (Figure 4.26.A). The

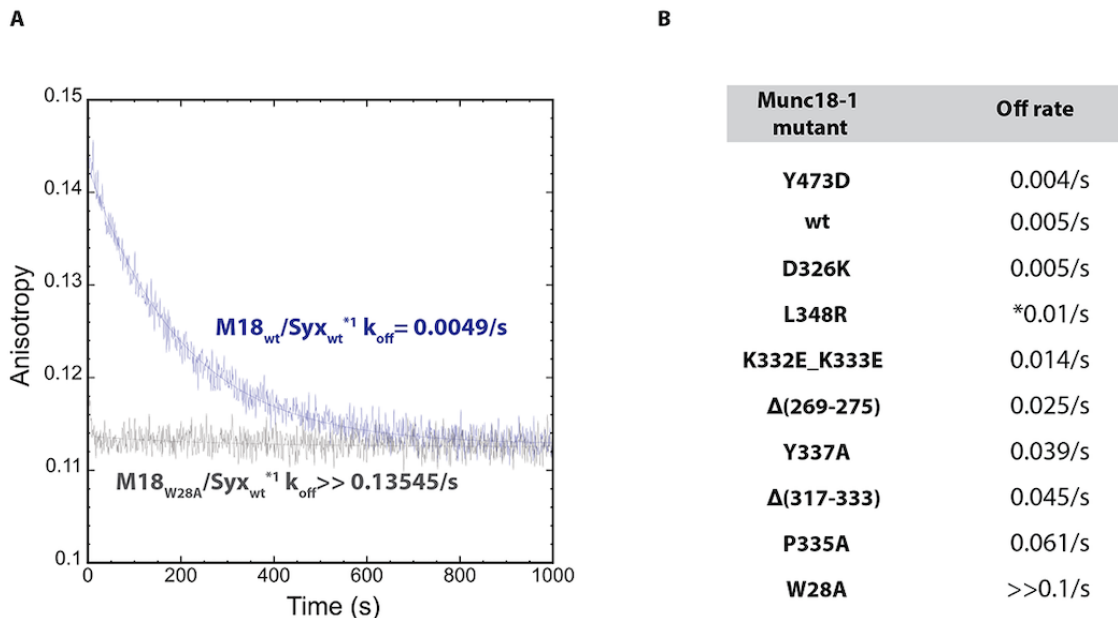


Figure 4.26: Munc18 mutants' complexes dissociation rates. Dissociation rate for all Munc18 mutants was determined by the rate of Anisotropy decay of Syntaxin_{wt}^{*1}. **A**. Dissociation rate for Munc18_{W28A} (grey) was progressing so fast that the data points could not be fit. Munc18_{W28A} dissociation rate (0.13545/s) was determined using 50nM Syntaxin_{wt}^{*1} instead for 100nM **B**. Off rates of Munc18 mutants' complexes determined from the anisotropy decay of 100nM Syntaxin_{wt}^{*1}, except for Munc18_{W28A}. The asterisk next to L348R rate is to mark that this mutant was often precipitating so the real value could be different.

dissociation rates of the other complexes were slower than for Munc18_{wt} but faster than for Munc18_{wt}, except for Munc18_{Y473D}, summarized in Figure 4.26.B.

4.7 SNARE complex formation observed in the presence of Munc18

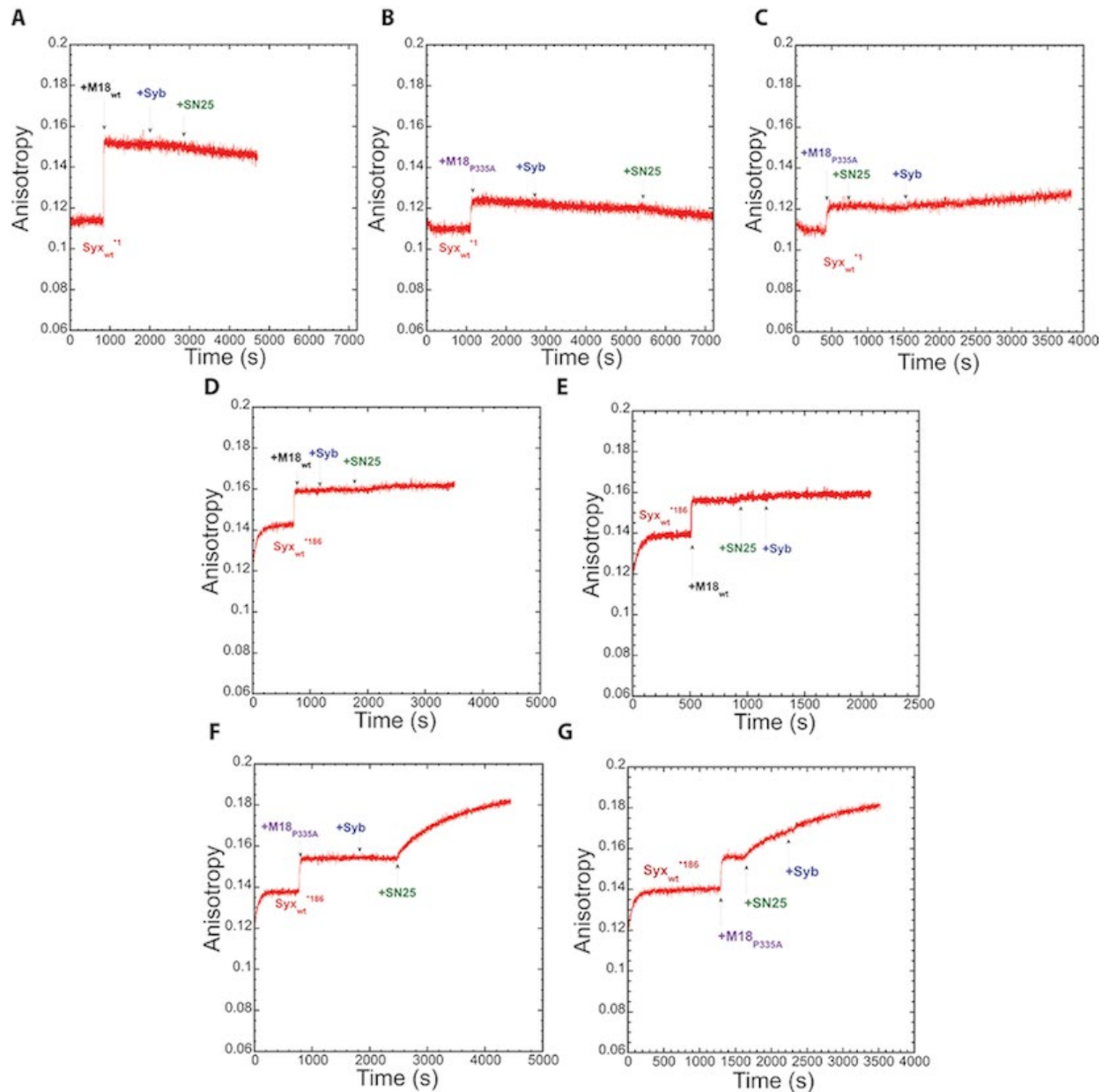


Figure 4.27: Sequential addition of proteins to follow complex incorporation of labelled Syntactin_{wt}. Fluorescence anisotropy of 50nM Syntactin^{*1} (A-C) followed by the addition of 500nM Munc18_{wt} (A) or Munc18_{P335A} (B, C), then 750nM Synaptobrevin (A, C) or SNAP25 (B) and 750nM SNAP25 (A, C) or Synaptobrevin (B). Fluorescence anisotropy of 50nM Syntactin^{*186} (D-G) followed by the addition of 500nM Munc18_{wt} (D, E) or Munc18_{P335A} (F, G), then 750nM Synaptobrevin (D, F) or SNAP25 (E, G) and 750nM SNAP25 (D,F) or Synaptobrevin (E,G).

The anisotropy measurements for off-rate determination described above indicated differences in fluorescence anisotropy between Syntactin_{wt}^{*1} and Syntactin_{wt}^{*186}.

For this reason, I decided to use this as a property to monitor local changes of the Munc18/Syntaxin complex in the presence of other SNARE proteins. In addition to the Munc18_{wt} complexes, I also tried to observe the changes caused by Munc18_{P335A}, as it is the Munc18 mutant with least inhibitory effect on SNARE complex formation.

To monitor these changes, I performed fluorescence anisotropy of labelled Syntaxins, while sequentially adding, Munc18_{wt}, or Munc18_{P335A}, Synaptobrevin and SNAP25. Addition of Munc18_{wt} led to immediate increase in fluorescence anisotropy of Syntaxin_{wt}^{*1} (Figure 4.27.A) that was higher than the one cause by the addition of Munc18_{P335A} (Figure 4.27.B). However, addition of SNAP25 to those mixtures caused a similar change (decrease) in the slope of anisotropy. A similar effect was observed despite the order in which Synaptobrevin and SNAP25 were added.

Fluorescence anisotropy profiles of Syntaxin_{wt}^{*186} differed when Munc18_{P335A} was added to the mixture when compared to Munc18_{wt}, even though the absolute anisotropy value reached was the same for both variants (Figure 4.27D-G). Addition of Synaptobrevin to the Munc18_{P335A}/ Syntaxin_{wt}^{*186} did not seem to affect the fluorescence anisotropy, however subsequent addition of SNAP25 led to substantial increase of fluorescence anisotropy, which reached a plateau after ~30min (Figure 4.27.F). Though, a similar change was observed when SNAP25 first in the solution which was followed by a slope change when Synaptobrevin was added later (Figure 4.27.G).

4.8 Modelling Munc18 and Munc18/Syntaxin structures in “extended” conformation

4.8.1 Munc18 and Munc18/Syntaxin modeling based on homologous structures

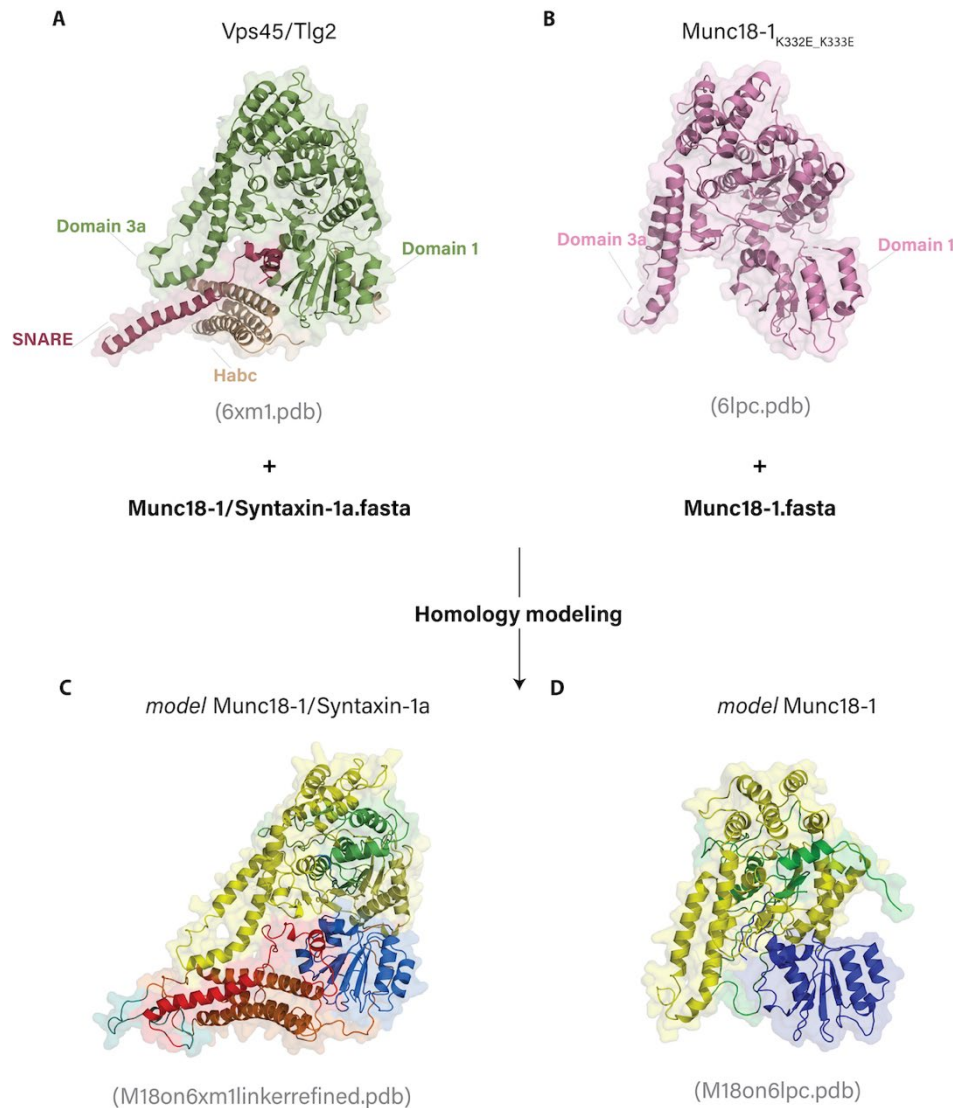


Figure 4.28: Models of Munc18 and Munc18/Syntaxin based on available homologous structures. Crystal structure of Vps45/Tlg2 homologous complex (**A**) and crystal structure of Munc18-1_{K332E_K333E} (**B**) used as templates to produce the models of Munc18-1/Syntaxin-1a (**C**) and Munc18-1a (**D**). The number of models could be further increased to increase the probability of a good model created. However, this also increases the computation time. Given the high sequence identity of Munc18-1 to Munc18-1_{K332E_K333E}, 5 models were sufficient to find a good output model, however, as Vps45/Tlg2 had 19% sequence identity to Munc18/Syntaxin, multiple initial models (1000) were generated to improve the confidence for obtaining the best model.

The experimental data presented so far, suggest that SNARE complex formation takes place in the presence of Munc18, i.e., that Munc18 serves as a SNARE assembly platform that controls the conformation of the bound syntaxin. Mutations at the interface of either Munc18-1 domain 3a/Syntaxin-1a linker or of Munc18-1 domain 1/Syntaxin-1a N-terminus led to similar outcomes: the inhibition of the Munc18-bound syntaxin to engage in interaction with its partner SNAREs was removed to different extents. In addition, somewhat reduced quenching of Trp fluorescence was observed for several spatially distant Syntaxin mutations, suggesting that a small but functionally important conformational change is taking place. However, it remains elusive what this conformational change entails.

In order to shed more light on this putative structural change of the Munc18/Syx complex, I scrutinized the available structures of SM proteins. As mentioned above, a conformational flexibility of Munc18 can be seen in the available structures of Munc18 paralogs including, (i) Munc18-1/Syntaxin-1a (pdb:3c98), (ii) Munc18-2 (pdb:4cca), (iii) Munc18-3/Syntaxin-1a N-peptide (pdb:3puk), and orthologs i.e., squid Sec1 (pdb:1fvf), (iv) *Monosiga brevicollis* Unc18/Syntaxin-1a (pdb:2xhe), etc. Of key importance for an inbuilt conformational switch are the two recently published structures of a Munc18-1 variant, Munc18-1_{K332E_K333E} (pdb:6lpc) (Wang et al., 2020) and of a homologous complex, Vps45/Tlg2 (pdb:6xm1) (Eisemann et al., 2020, Wang et al., 2020). Munc18-1_{KEKE} is in a slightly different conformation than the one observed for the Munc18-1/Syntaxin-1a complex (pdb:3c98) (citation), as its hairpin helices in domain 3a are in a somewhat “extended” conformation. The Vps45/Tlg2 structure provides a snapshot of an SM protein in complex with the Qa SNARE Tlg2, in a conformation that is not entirely closed. In contrast to the closed Syntaxin-1a in complex with Munc18, the SNARE domain of Tlg2 is extended and appears to be ready to engage with its SNARE partners. Is it possible that the Vps45/Tlg2 complex structure represents a conformational state that allows for SNARE complex formation, a state that the Munc18-1/Syntaxin-1a might go through but that is not stable enough to be isolated and characterized biochemically?

Therefore, I sought to visually observe this transition state of the Munc18-1/Syntaxin-1a complex by creating a 3D model of the *intermediate* conformation. To do so, I created homologous models using the Modeller 10.1 software (Šali and Blundell, 1993) from the Vps45/Tlg2 (Figure 4.28.A) and Munc18_{K332E_K333E} (Figure 4.28.B) structures as the templates, with the help of Justyna Iwaszkiewicz from the UniL Protein

Results

Modeling Facility (PMF). First, pairwise sequence alignment of target sequences (Munc18 or Munc18/Syntaxin) with the template sequences (Munc18_{K332E_K333E} or Vps45/Tlg2 respectively) were created. For individual Munc18-1 structure, I created 5 models with Munc18-1_{K332E_K333E} as template.

Of these, the one with the lowest DOPE score (Shen and Sali, 2006) was selected, referred to as *modelMunc18-1* in the following figure (Figure 4.28.D). DOPE score is a pairwise atomistic statistical potential which is used to distinguish "good" from "bad" models. The lower the DOPE score the better the model is. Then the model was evaluated by calculating the energy profile for each residue.

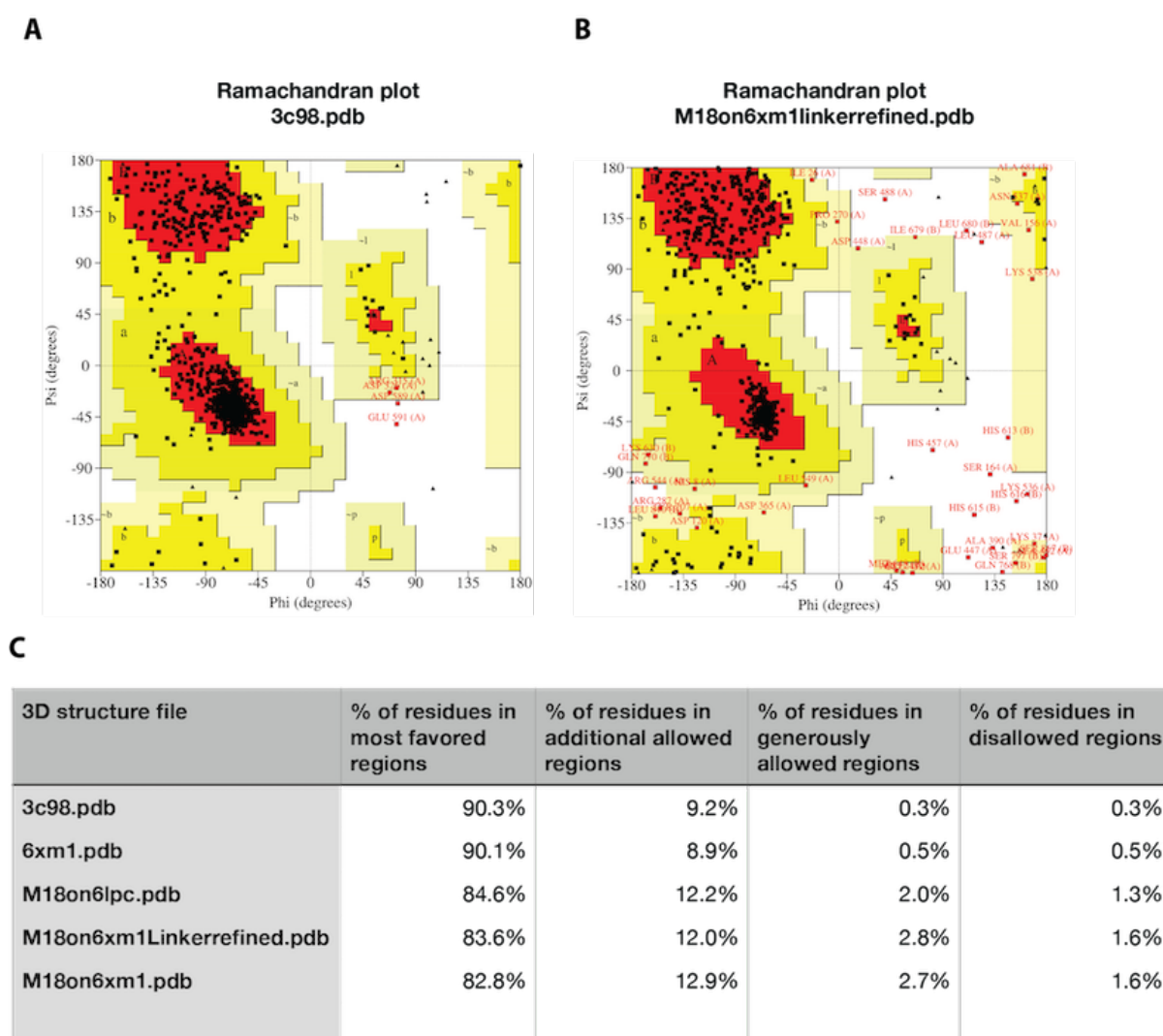


Figure 4.29: Homologous complexes' assessment using PROCHECK. Example of the Ramachandran plots of the Munc18-1/Syntaxin-1a crystal structure (A) and *modelMunc18-1*/Syntaxin-1a (B). (C) Table summary of percentages of the residue distributions of the two crystal structures and the 3 models evaluated.

The sequence identity between Munc18/Syntaxin complex and Vsp45/Tlg2 complex is only 19%. To ensure we obtain the best model despite the low sequence identity score, multiple initial models (1000) of Munc18/Syntaxin complex in the looser conformation were generated. The model with lowest DOPE SCORE was selected for further refinement of the flexible linker regions of Syntaxin (i.e., residues 1 to 20 and 151 to 161). Having selected the model with the lowest DOPE score, henceforth referred to as *modelMunc18-1/Syntaxin-1a*, I further assessed the stereochemical quality of the models using PROCHECK, a program which provides a detailed check on the stereochemistry of protein structures (Morris et al., 1992). This generated Ramachandran plots for each of the selected models, the template and the closed Munc18/Syntaxin complex structure. These plots provide information on the distribution of energetically favorable dihedral angles of the backbone (ϕ and ψ), (Ramachandran et al., 1963) (Figure 4.29.A-B). In summary, the plots indicate an overall good percentage of residues occupying the favored and allowed angle regions (Figure 4.29.C). Moreover, the validated three models only had $\sim 1.5\%$ of residues in the disallowed area (white). Post the refining process, there was an increase of only 0.6% in the presence of residues in the most favored area. However, the residues in the disallowed area did not reduce (1.6%). The optimization process was discontinued when the quality of the model complexes reached a relatively stable state.

4.8.2 Predicted 3D structures of Munc18-1 and Syntaxin-1a

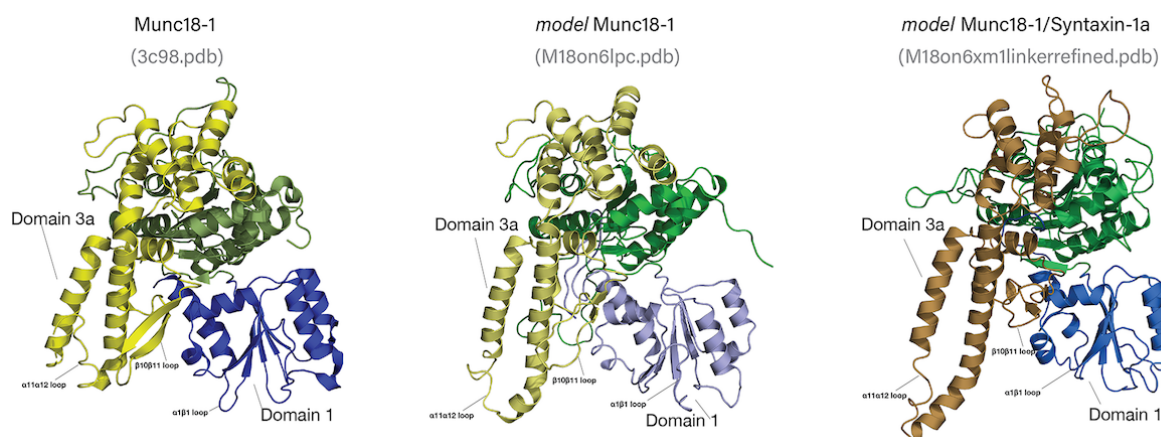


Figure 4.30: Munc18 crystal and models' structures. For all 3, domain 1 is colored in blue, domain 2 in green and domain 3 in yellow tones. Domain 1 $\alpha 1\beta 1$ and domain 3a $\alpha 11\alpha 12$ and $\beta 10\beta 11$ loops are indicated.

After the optimization process, I compared the structural features of the models with that of the crystal structure of the Munc18/Syntaxin complex (3c98.pdb). The overall structure of both Munc18 models is similar to the experimentally determined

Results

crystal structure of Munc18 (pdb: 3c98) (Figure 4.30). The most striking difference between the models and the crystal structure, is that the tip of the domain 3a helix 12 is extended in both *modelMunc18-1* and *modelMunc18-1/Syntaxin-1a*, whereas it is furled in the crystal structure. In order to check the overall integrity of Munc18-1 at domain 3a, I took a closer look to one interaction example between them, i.e., the aromatic ring interactions, as this can provide distance and orientation information. In the crystal structure, Phe310 of helix 11 is in pi-pi stacking interactions with Tyr337 and Tyr344 of helix 12 (Fig.4.31). The distances between the aromatic rings of Phe310, Tyr 337 and Tyr 340 are approximately the same in both the models as well as in the crystal structure, indicating that the interactions between the helices are not affected by the extension of helix 12.

The $\beta_{10}\beta_{11}$ hairpin loop of domain 3a seems to adopt a less structured conformation in both *modelMunc18-1* and *modelMunc18-1/Syntaxin-1a*. However, the $\beta_{10}\beta_{11}$ hairpin loop adopts a more bent conformation in the *modelMunc18-1/Syntaxin-1a* compared to the other two structures; it bends closer towards Munc18 (Figure 4.31).

Domain 3a

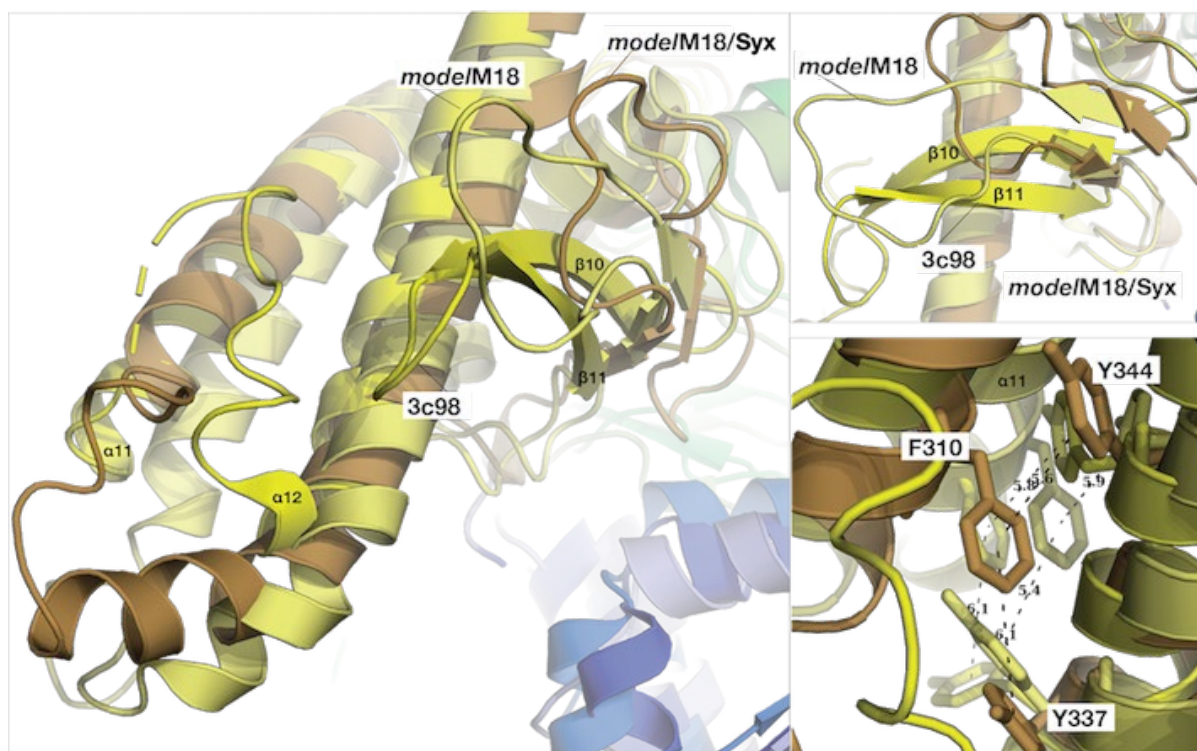


Figure 4.31: Comparison between domain 3a structural features of models. Crystal structure (yellow), *modelMunc18* (light yellow) and *modelMunc18/Syntaxin* (sand) superpositioned, with helices 11 and 12, and sheets 10 and 11 indicated on the crystal structure. Top right: close-up of the $\beta_{10}\beta_{11}$ hairpin loop. Bottom right: close-up of Phe310-Tyr337-Tyr340 side chains involved in aromatic stacking interaction.

The domain 1 backbone in the models is structurally similar to the crystal structure (Figure 4.30). However, some of the helices of the model are partially more unstructured, i.e., the loops between α helices and β sheets are longer. Also, the $\alpha_1\beta_1$ loop of the inner cavity is bent in both models and extended in the crystal structure. Trp₂₈, located at the end of this loop, was shown in the biochemical experiments to contribute to the interaction with Syntaxin.

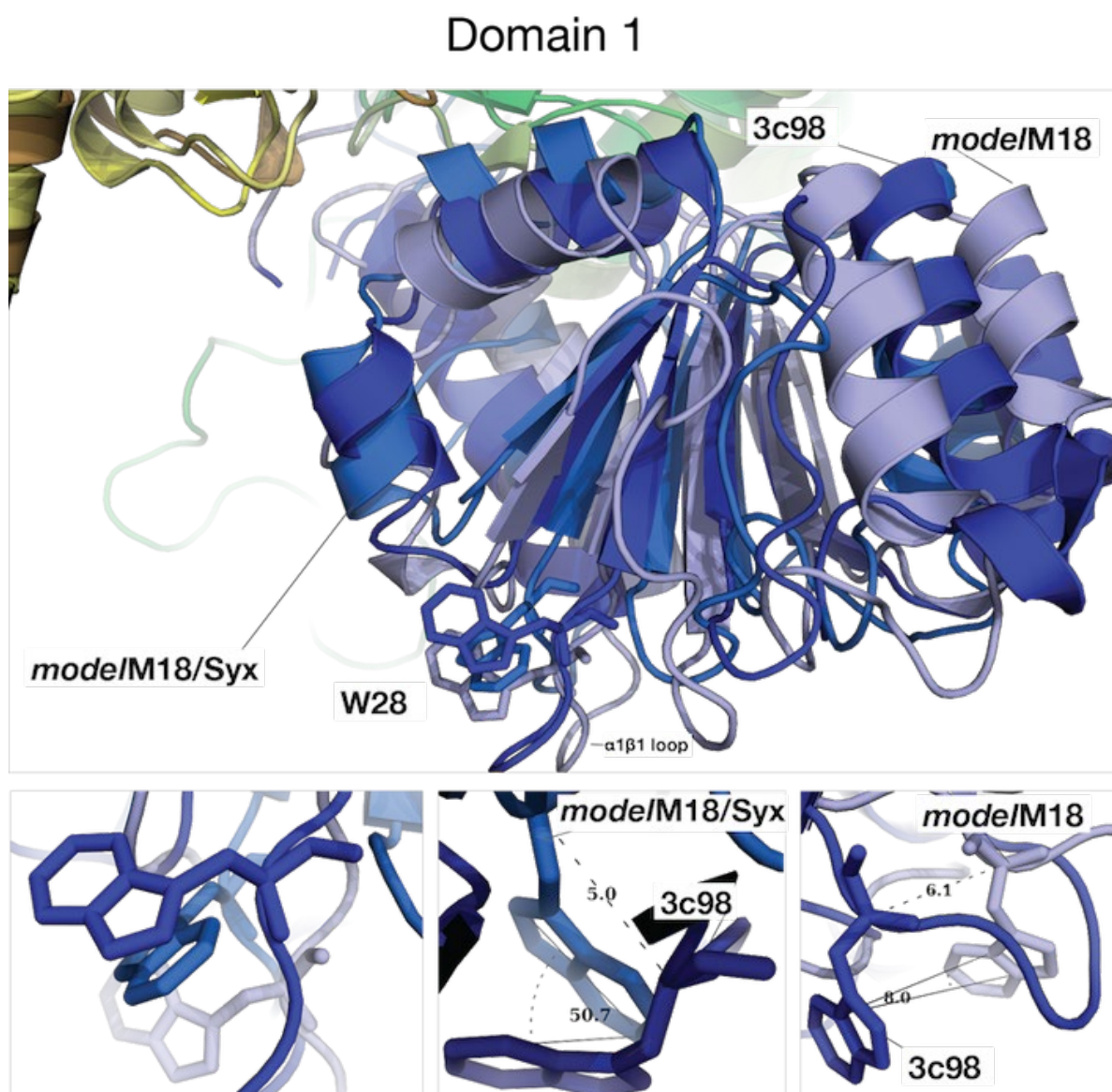


Figure 4.32: Comparison between domain 1 structural features of models. Crystal structure (blue), *modelMunc18* (violet) and *modelMunc18/Syntaxin* (light blue) superpositioned, with Trp₂₈ in sticks representation. Distances and angles between the Trp₂₈ from the crystal structure and the *modelMunc18/Syntaxin* (bottom, middle) and *modelMunc18* (bottom, right).

Results

The superposition of the three structures (Figure 4.32), indicates small conformational differences between the models and the crystal structure in domain 1. To investigate these conformational changes, I took a closer look at Trp₂₈. Domain 1 of *modelMunc18-1/Syntaxin-1a* and *modelMunc18-1* is somewhat rotated in respect to the domain 1 seen at the crystal structure. The C_α of Trp₂₈ of the *modelMunc18-1/Syntaxin-1a* is located 5Å away from the C_α of Trp₂₈ of the Munc18-1/Syntaxin-1a crystal structure, i.e., it has moved further towards the inner cavity of Munc18. While the C_α of Trp₂₈ of *modelMunc18-1* lays within ~6Å distance from C_α of Trp₂₈ of the Munc18-1/Syntaxin-1a of the crystal structure. The orientation of the *modelMunc18-1* Trp₂₈ side chain seems to be tilted towards the inside of the molecule at an angle of ~8° in comparison to the crystal

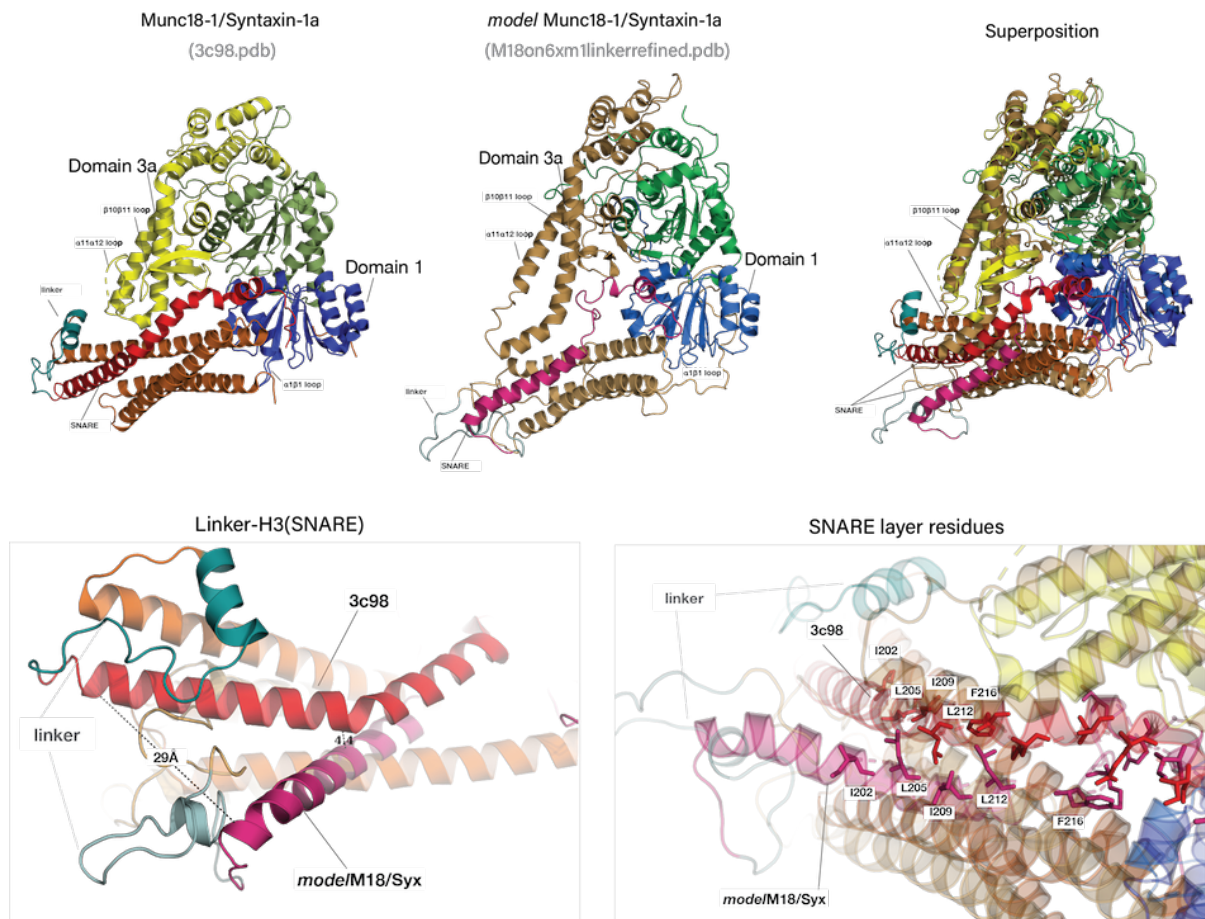


Figure 4.33: Munc18-1/Syntaxin-1a crystal and model structures and their superposition. For both, Munc18-1 domain 1 is colored in blue, domain 2 in green and domain 3 in yellow tones, and Syntaxin-1a N-peptide to Hc in orange tones and H3 (SNARE) in red tones. Bottom left: distances between H3 helices of Syntaxin-1a of the crystal and the *modelMunc18/Syntaxin* structures. Bottom right: Residues of SNARE layers in sticks representation on the crystal and model structures.

structure. Conversely, the Trp₂₈ side chain of *modelMunc18-1/Syntaxin-1a* seems to orient towards the outside, with a twist of ~130° to the Trp of the crystal

The clearest structural differences between the modeled Munc18/syx structure and the crystal structure can be seen in the linker and H3 (SNARE) region of syntaxin (Figure 4.33). The superposition of both complexes reveals that the extension of the Munc18 helical hairpin (of the model) does not support binding of a closed Syntaxin as the extended hairpin would clash with the N-terminal portion of the H3 helix. In the crystal structure, the N-terminal portion of the H3-helix interacts with a groove formed by the Hb and Hc helices of the Habc domain, whereas the remaining H3 helix bends away towards domain 3a of Munc18-1. In the modeled structure, N-terminal portion of H3 moves away from Habc following the hairpin, which is now extended. The Syntaxin H3 helix drifts ~ 30 Å outer from the complex's cavity and ~ 4.5 Å "lower" in respect to the H3 of closed Syntaxin, as determined by the distance between Gln190 on the model and the crystal structure.

This conformational change of the H3 is also accompanied by a rotational movement. Further investigations showed that the side chains of the SNARE core layer residues point towards the outer surface of the molecule, in contrast to the closed conformation which they face the Hc helix and the linker region. These residues face into the center of the four-helix bundle SNARE complex and appear to be ready to bind to other SNAREs in the modeled structure.

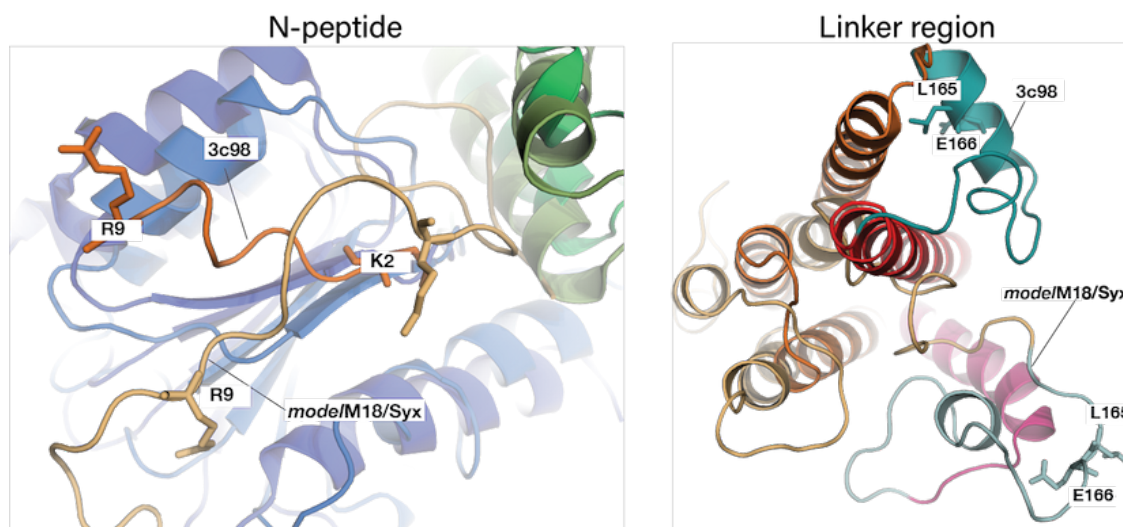


Figure 4.34: Syntaxin N-peptide and linker region comparisons. Left: Syntaxin N-peptide of the *modelMunc18-1/Syntaxin-1a* adopts a less structured conformation than the one seen at the crystal structure. Right: Syntaxin linker region at the *modelMunc18-1/Syntaxin-1a* is unstructured and the important L165 and E166 residues are facing the outer surface, rather than interacting with the H3 and H3 helices, as seen by the crystal structure.

Results

The N-peptide of syntaxin is still bound to the outer side of domain 1 in the modeled structure, but I noticed that it seems to adopt a somewhat less structured conformation (Fig.4.34). It still needs to be determined how this affects its affinity. The Syntaxin linker region of *modelMunc18-1/Syntaxin-1a* adopts a more unstructured conformation with only a very small part of its helical (Figure 4.34). The L165 and E166 residues point towards the surface and do not interact with either the H3, nor Hc or Munc18. Few additional changes seem to have occurred in the Habc domain region; they still need to be inspected in more detail.

4.9 The Munc18-1/Syntaxin-1a complex is probably not regulated by nucleotides

Munc18 domain 1 adopts a Rossmann fold, which is found in proteins that bind nucleotides (Hanukoglu, 2015). As the previous experiments revealed the importance of domain 1 in regulating the interaction of Munc18-1/Syntaxin-1a complex, I sought to determine whether its effects could physiologically be exerted through a putative

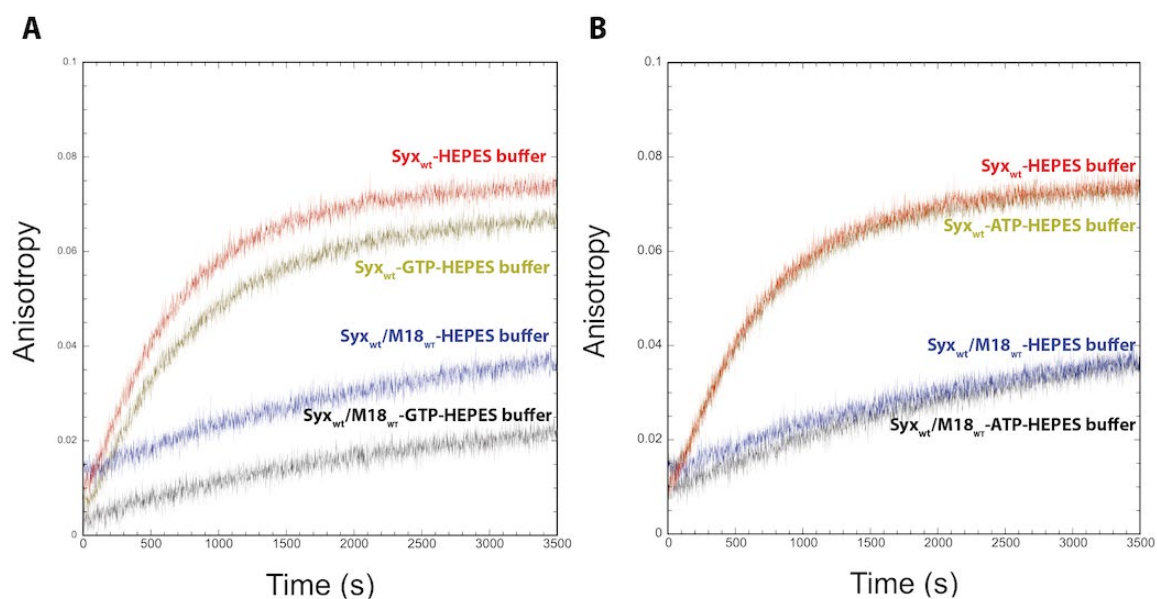


Figure 4.35: SNARE complex formation in the presence of GTP or ATP. Syb*28 fluorescence anisotropy was measured in HEPES buffer (50mM HEPES pH 7.4, 150mM NaCl, 5mM MgCl₂) in the presence of 2mM of respective nucleotide, when Syntaxin_{wt} is in complex with Munc18_{wt} (black and blue) or not (ochra and red). A. Presence of GTP in buffer seems to affect the actual amount anisotropy increase, however the rate of increase seems to follow the same trend in either the presence or absence of GTP. B. Syb*28 fluorescence anisotropy increase in ATP containing buffer was the same as no nucleotide containing buffer.

nucleotide cofactor interaction. As in the previous sections, the SNARE-regulating activity of Munc18 was measured using the Synaptobrevin*28 fluorescence anisotropy

assay in buffers containing different nucleotides (GTP, ATP, NAD, NADH, NADP, NADPH, and FAD). No significant difference in rate of SNARE complex formation (in the presence of Munc18) was observed in buffers with or without ATP or GTP (Figure 4.35).

SNARE complex formation rate seemed to be slightly affected, though, in nicotinamide (NAD, NADH, NADP and NADPH) containing buffers (Figure 4.36). However, as the maximal fluorescence anisotropy was somewhat higher, the experiments were not conclusive. Due to oxidation, FAD in solution turned yellow, which made the application Syb*28 OG fluorescence anisotropy assay not appropriate for this nucleotide (data not shown).

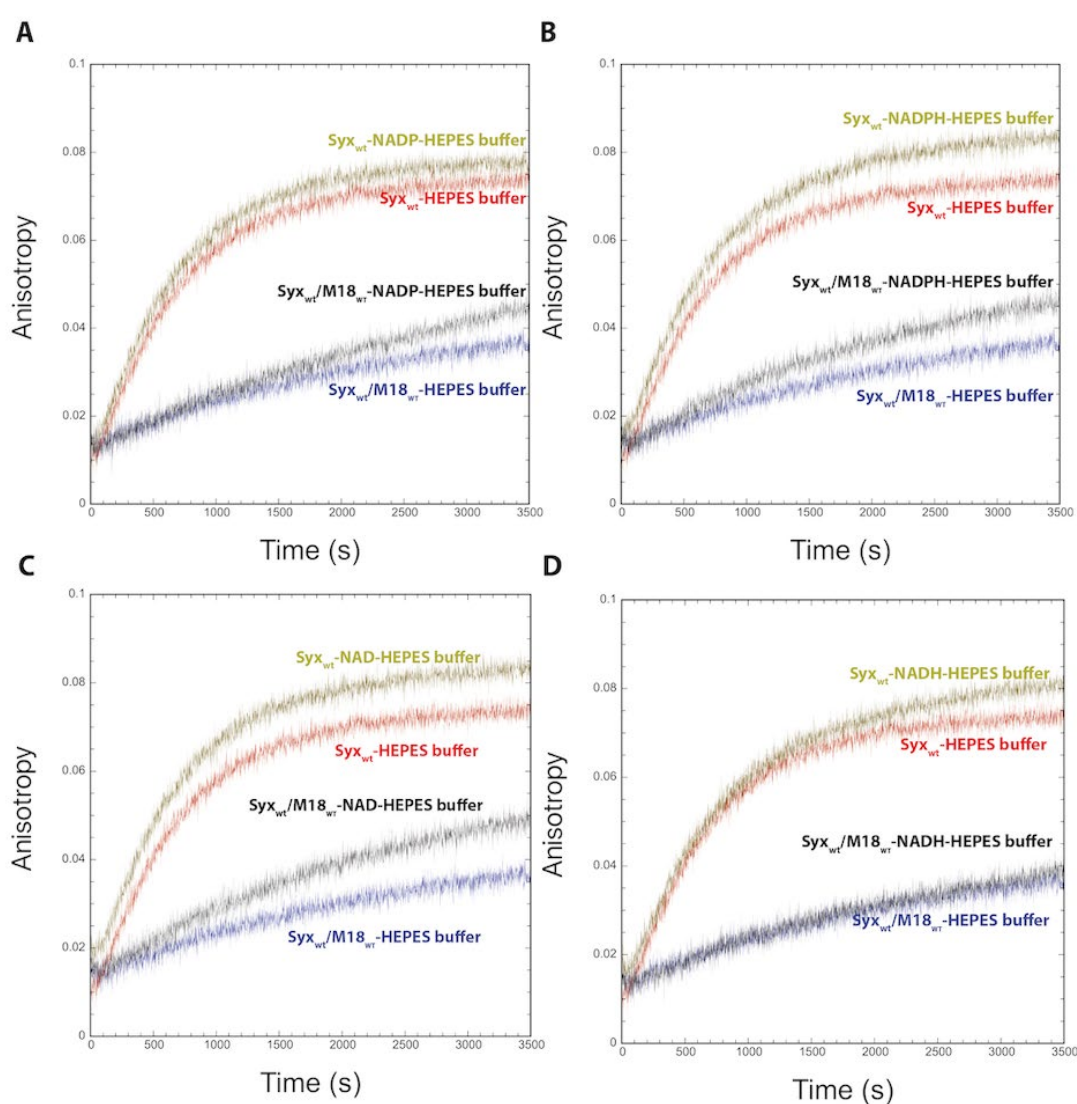


Figure 4.36: SNARE complex formation in the presence of NADP (A), NADPH (B), NAD (C) and NADH(D). Experiments were performed as described at Fig.4.29.

4.10 SNARE complex forms at similar rates are not changed in the presence of the MUN domain.

The MUN domain of Munc13-1 has been proposed to catalyze the transition of Syntaxin-1a from the Munc18-1/Syntaxin-1a to the SNARE complex (Ma et al., 2013, Yang et al., 2015). In order to characterize the effect of the MUN domain on SNARE complex formation, several approaches were followed by me. I expressed and purified MUN₉₃₃, the construct proposed to be the minimal region needed for catalytic activity (Basu et al., 2005).

I first studied SNARE complex assembly of Syntaxin-1a_{wt} in the presence of Munc18_{wt} and different concentrations of MUN₉₃₃ (Figure 4.37.A). I noticed that the fluorescence anisotropy was slightly increased in the presence of MUN₉₃₃ (20 or 40 μM). Nevertheless, the increase occurred with comparable rates as when MUN₉₃₃ was absent.

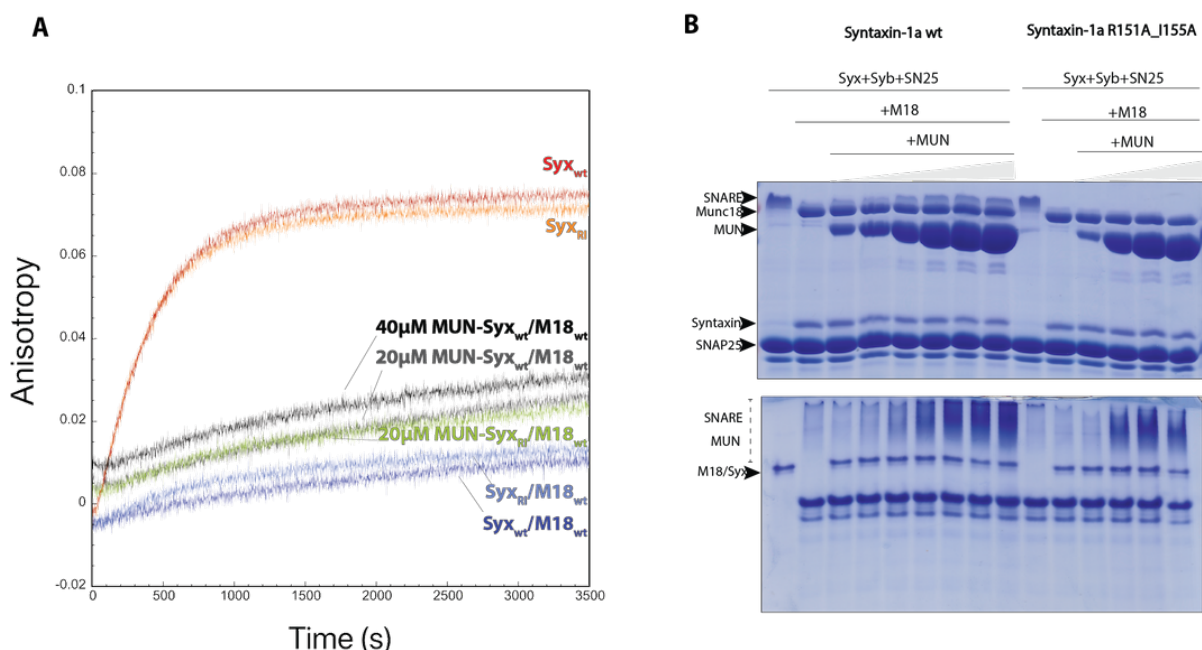


Figure 4.37: SNARE complex inhibition is not lifted in the presence of MUN domain. A. Syb*28 fluorescence anisotropy was measured for Syntaxin_{wt} (red) or Syntaxin_{R151A_I155A} (orange), also in the presence of Munc18_{wt}, and the presence of 20 μM (green or grey) or 40 μM (black) MUN domain. B. SDS glycine (top) and Native (bottom) gel electrophoreses of mixtures containing either 16 μmole per lane Syntaxin_{wt} or Syntaxin_{R151A_I155A}, SNAP25 (82 μmole per lane) and Synaptobrevin (82 μmole per lane), and, apart from one per syntaxin variant, Munc18 (72.8 μmol per lane). Mixtures also contained increasing concentrations of MUN (9 μmol, 16 μmol, 41 μmol, 65 μmol, 82 μmol, 98 μmol per lane). Bands corresponding to SDS resistant complexes overlap with the band corresponding to Munc18. The smear corresponding to the SNARE complex on the native gel overlaps with the smear corresponding to the MUN domain. The amounts of free SNAP25 are indicators of no increase in formed SNARE complex after the gradient of MUN.

The MUN domain has been proposed to bind to the Munc18-1/Syntaxin-1a complex at the Munc18-1 domain 3a/Syntaxin-linker region (Wang et al., 2017). The

binding region has been localized to the residues N1128 and F1131 on the so-called NF cavity of MUN domain and to R151 and I155 in the linker region of Syntaxin-1a (Wang et al., 2017, Yang et al., 2015). Based on that, one Syntaxin-1a mutant (Syx^{R151A_I155A}, or Syx^{RI}) and one MUN mutant (MUN^{N1128A_F1131A}, or MUN^{NF}) were suggested to interfere with MUN binding to the Munc18-1/Syntaxin-1a complex. I expressed and purified these mutants as well and studied SNARE complex assembly in the presence of Munc18^{wt}. I observed that Syx^{wt} and Syx^{RI} assembled into SNARE complexes at the same rate in the presence of Munc18 whether or not 20 μM MUN were added.

Following this, I investigated complex formation using either analytical SDS and native gel electrophoreses, as the SNARE complex is SDS resistant. It can also be detected in non-denaturing gel electrophoresis. I mixed Syntaxin-1a^{wt} or Syntaxin-1a^{R151A_I155A}, with SNAP25, Synaptobrevin and Munc18^{wt}, and added increasing amounts of MUN⁹³³. No apparent increase in SNARE complex formation was observed in the presence of increasing amounts of the MUN domain (Figure 4.37.B). Also, no apparent difference was observed for the Munc18/Syntaxin complex upon non-denaturing gel electrophoresis, for Syntaxin variants. Electrophoretic separation profiles were also indistinguishable between mixtures containing either MUN⁹³³ or MUN^{NF} (data not shown).

As the MUN domain is thought to interact with the Munc18-1/Syntaxin-1a complex at the Munc18-1 domain 3a/Syntaxin-linker region, I also used the domain 3a

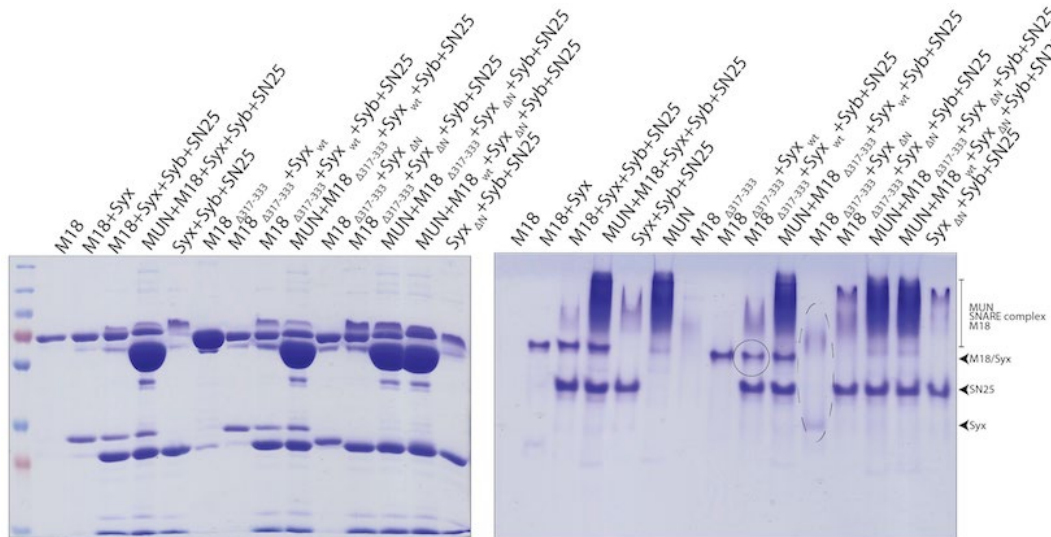


Figure 4.38: Munc18^{Δ317-333}/Syntaxin^{wt} complexes are stable also in the presence of MUN. SDS glycine (top) and Native (bottom) gel electrophoreses of mixtures containing either 16 μmol per lane Syntaxin^{wt} or Syntaxin^{ΔN}, 82 μmol per lane SNAP25 and Synaptobrevin, 16 μmol per lane Munc18^{wt} or Munc18^{Δ317-333}, and 248 μmol per lane MUN as indicated. Bands corresponding to SDS resistant complexes overlap with the band corresponding to Munc18. Munc18^{Δ317-333}/Syntaxin^{wt} is marked with a solid circle and the dashed oval the smear of the lane containing Munc18^{Δ317-333} and Syntaxin^{ΔN}.

Results

loop mutant, Munc18 Δ 317-333 as described above. Again, no apparent difference was observed (Figure 4.38). Residual amounts of uncomplexed proteins also support that no additional SNARE complex was formed.

I also monitored the effect of MUN on SNARE complex formation at low pH conditions, as applied in previous sections to better resolve between small effects. In the presence of 5 μ M MUN domain, absolute fluorescence anisotropy was again, higher, however, the rate was similar in the absence or presence of the MUN domain (Appendix Fig. 5).

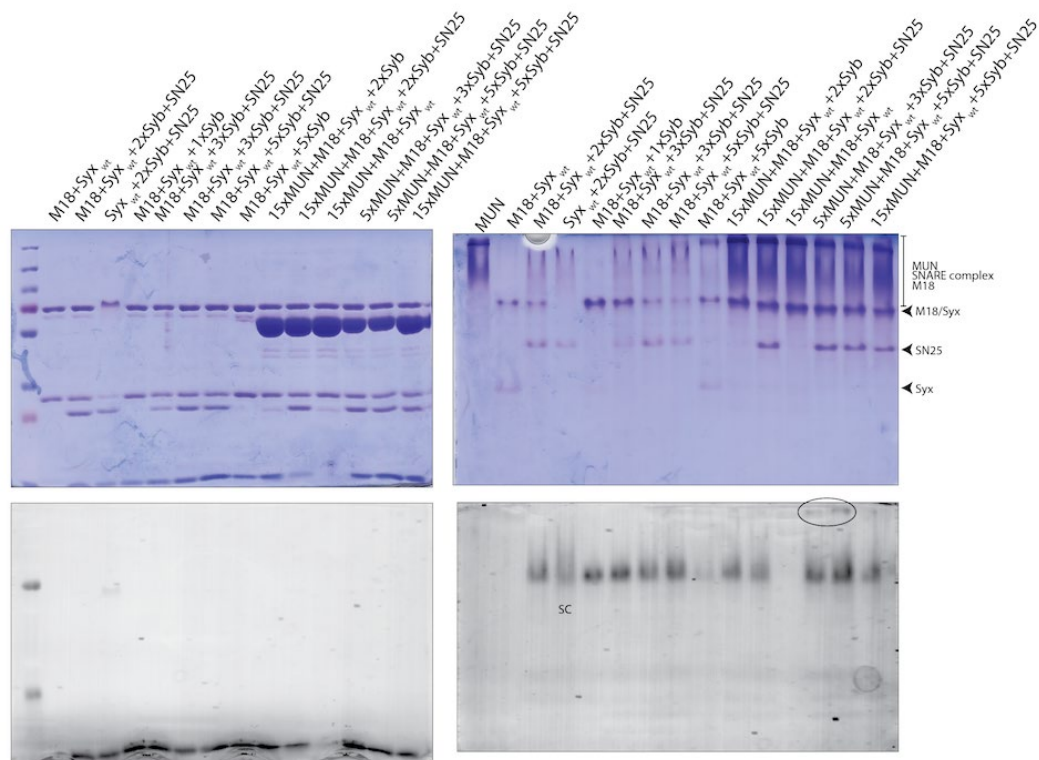


Figure 4.39: MUN or Synaptobrevin gradients did not affect the Munc18/Syntaxin complex. SDS and Native gel electrophoreses of mixtures containing 4.45 μ mol per lane Syntaxin_{wt}, 9 μ mol per lane SNAP25 and 9 μ mol per lane Munc18_{wt}, Synaptobrevin gradient (9, 13, 22 μ mol per lane) and MUN (22 or 45 μ mol per lane). After the electrophoresis, gels were exposed to UV to discriminate the bands containing the labelled Synaptobrevin (bottom) and then stained with Coomassie (top). Residual free Syntaxin on the native gel explains the appearance of SNARE complex in the presence of Munc18. Circled are the Synaptobrevin related bands that appeared at the native gels.

The fluorescence anisotropy experiments monitor SNARE complex formation by an increase of fluorescence anisotropy of labelled Synaptobrevin. Synaptobrevin is used at low concentrations. In order to look into the effect of MUN at ~equimolar ratio of SNARE proteins, I followed SNARE assembly using native gel and SDS gel electrophoresis. As the SDS-resistant SNARE complex runs at a similar size on the gel as Munc18, I added Syb^{*28} or Syntaxin_{wt}^{*1} to the reactions so that under UV exposure only the complex containing the labelled variant would be visible. Again, no apparent MUN related increase in SNARE complex formation or decrease in Munc18/Syntaxin complex were observed

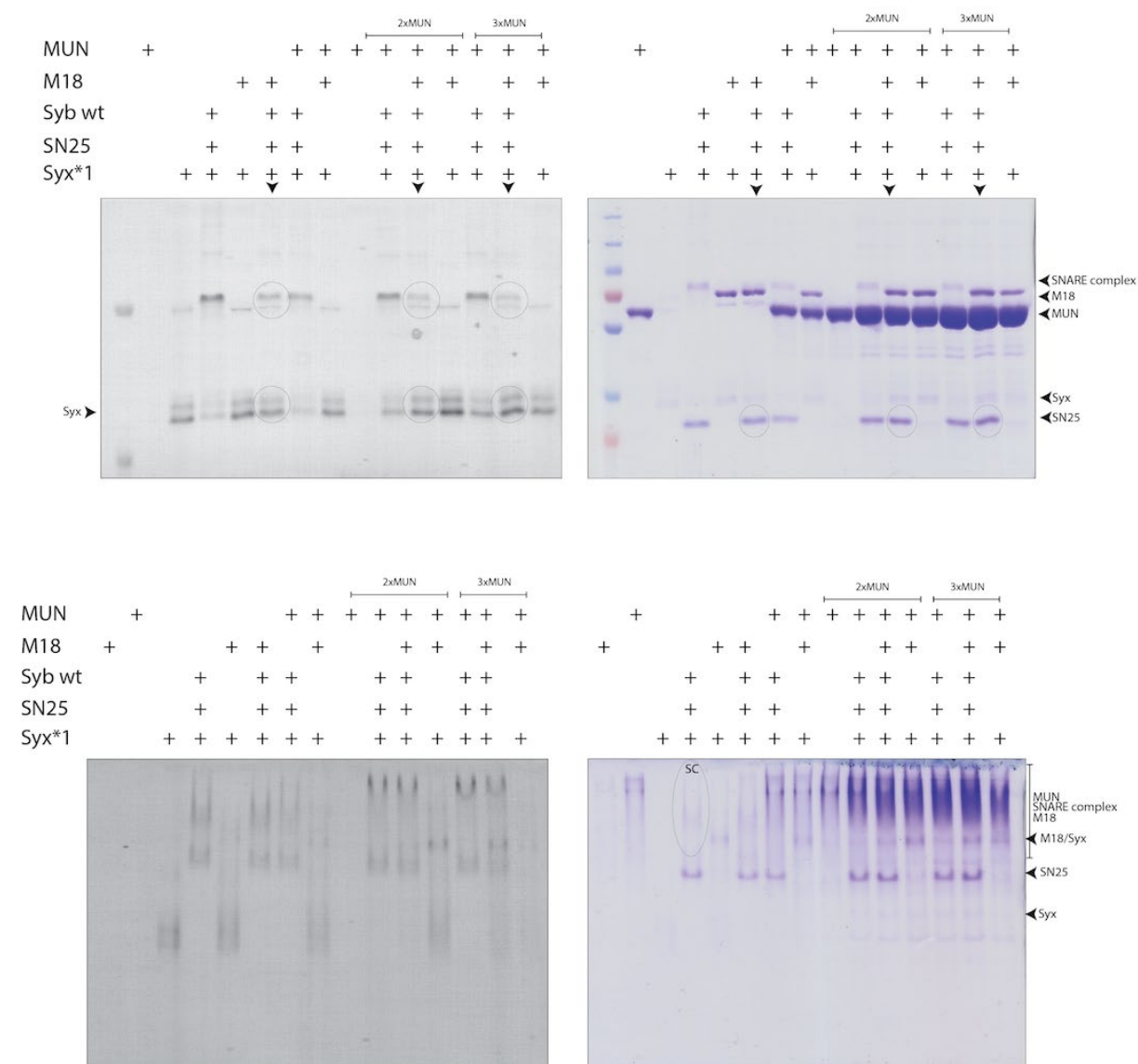


Figure 4.40: SDS and Native gel electrophoreses of mixtures containing Syntaxin*1. 4 μ mol per lane Syntaxin*1, mixed with 4 μ mol per lane Munc18_{wt}, and/or 9 μ mol per lane SNAP25 and Synaptobrevin, and/or 22 μ mol per lane MUN, or 44 μ mol per lane MUN, or 66 μ mol per lane MUN were loaded on SDS (top) and native gel. (bottom). After the electrophoresis, gels were exposed to UV (left) to visualize the bands containing Syntaxin*1 and then stained with Coomassie (right).

Results

(Figure 4.39 & Figure 4.40). The appearance of an additional Syb^{*28} band in the presence is probably caused by an interaction of a Synaptobrevin degradation product with Munc18-1 (Appendix Fig. 5).

5. Discussion

SNARE complex assembly between two membranes is the core mechanism driving fusion of transport vesicles with target membranes. SNARE complex assembly is fine-tuned by other interacting proteins, among them the SM protein family members and tethering factors. SM proteins regulate SNARE complex formation by interacting with their cognate Qa-SNARE protein. At presynaptic terminals, the interaction of Munc18-1, the neuronal SM protein, and Syntaxin-1a, the presynaptic membrane Qa-SNARE, regulates neuronal vesicle exocytosis. Their mode of interaction, though, is still controversial. *In vivo* studies had demonstrated that this interaction is essential for synaptic vesicle secretion (Verhage et al., 2000). Biochemically, the tight interaction between the two proteins prevents Syntaxin from assembling into SNARE complex, the indispensable step to drive vesicle fusion (Pevsner et al., 1994b). After many years, the question of how Syntaxin-1a can escape this tight grip has not been answered satisfactorily. Does it first have to leave Munc18-1 or is it possible that it remains bound to Munc18-1 during this process? Which structural changes are involved in the transition?

The purpose of this study was to shed more light on a putative conformational flexibility of the Munc18-1/Syntaxin-1a pair. Earlier studies had shown a mutant bearing double mutation in the linker helix of Syntaxin-1a (L165A & E166A, i.e. Syx1_{AL}E) can largely overcome the block of SNARE complex formation exerted by Munc18-1. Originally, this mutation has been thought to produce a constitutively open conformation of Syntaxin (Dulubova et al., 1999). Later experiments showed that this mutant is able to bind strongly to Munc18-1, in a similar but not identical manner as wild-type Syntaxin-1a (Burkhardt et al., 2008). The complex of Munc18-1 with Syx1_{AL}E is still tight and in a similar overall configuration, but it is possible that a small conformational change has occurred (Colbert et al., 2013). Comparable effects were observed when Syntaxin-1a lacking the N-peptide (Syx_{ΔN}) is interacting with Munc18-1. Syx_{ΔN}, like Syx1_{AL}E, binds strongly to Munc18-1, yet can escape the Munc18-1 inhibition. It seems likely that initiation of SNARE complex formation can occur when Syntaxin-1a is bound to Munc18-1, possibly in a more relaxed or loose conformation at the linker and/or the N-peptide interaction sites.

The crystal structure of the Munc18-1/Syntaxin-1a complex depicts the tight interaction between the two proteins (Misura et al., 2000). Munc18-1 binds to Syntaxin-1a through interactions of its inner cavity (formed between the inner surface of domains 1, 2 and 3a) with the Habc domain of Syntaxin-1a, as well as interactions of Syntaxin-1a N peptide with the outer surface of Munc18-1 domain 1 (Burkhardt et al., 2008). This tight interaction with Munc18-1 locks Syntaxin-1a in a closed, autoinhibitory conformation, where its SNARE motif is forming a four-helical bundle with its Habc domain. It is therefore blocked from assembling into the SNARE complex. It was thought that Syntaxin-1 needs to leave Munc18-1 in order to open and to interact with the other SNAREs. It was later shown, however, that Syntaxin-1a variants can interact with Munc18-1, while they are not blocked from assembling into a SNARE complex (Burkhardt et al., 2008, Colbert et al., 2013). It is possible that the crystal structure of the complex only represents a *snapshot* of their lowest energy conformation. Indeed, there are structures of other SM/Qa pairs that exhibit other conformations and interaction modes (Zhang and Hughson, 2021, Baker and Hughson, 2016). Do these structures provide snapshots of alternative pathways towards SNARE complex formation, specific to a different vesicle trafficking step, or can they all be integrated into a pathway shared by all SM proteins?

The SM protein Vps33 is involved in lysosomal trafficking. In contrast to Munc18-1, it seems to guide SNARE complex formation by aligning the SNARE domains of Vam3 (Qa-SNARE) and Nyv1 (R-SNARE) (Baker et al., 2015). Vam3, in contrast to Syntaxin-1a, is considered to be perpetually in the open conformation. Vam3 lacks a conserved N-peptide and the N-peptide binding pocket of Vps33 is not conserved as well. It is possible that this binding mode of an SM/Qa SNARE pair occurs after the Qa SNARE is opened, while the R-SNARE Nyv1 is aligned already for the upcoming assembly into the SNARE complex.

The structure of the Vps45/Tlg2 complex, which is involved in trans-Golgi network trafficking, shows the SM protein Vps45 interacting with a novel, more *loose* conformation of the Qa-SNARE Tlg2 (Eisemann et al., 2020). Note that Vps45/Tlg2 complex structure was published only very recently (Eisemann et al., 2020), but appears to corroborate the initial aim of my study. Tlg2 binds to Vps45 with its Habc domain to the inner cavity of Vps45 as well as the N-peptide to the outer side of domain 1. In

contrast to the tight closed conformation of Syntaxin 1a in the Munc18/Syx structure, the SNARE motif of Tlg2 is not forming a four-helix structure with its Habc domain. The SNARE motif of Tlg2 appears to bear the SNARE motif free to initiate SNARE complex assembly.

The Golgi-SNARE protein Sed5 adopts a tighter closed conformation than Syntaxin-1a, but its cognate SM protein Sly1 is able to accelerate SNARE complex formation (Demircioglu et al., 2014), possibly through opening Sed5 while still bound to Sly1. Possibly, Sed5 adopts a loose conformation similar to Tlg2 when bound to Sly1.

Another major structural difference between Vps45/Tlg2 and Munc18/Syx can be seen in the conformation of the hairpin helices of domain 3a. This region is in an extended conformation, i.e., helix 12 is extended by adopting a helical conformation of the $\alpha 11\alpha 12$ loop. The N-terminal region of the SNARE motif of Tlg2 appears to be steered away from the Habc domain by the hairpin extension. Obviously, such an extended conformation would clash with the closed binding mode found in the Munc18/Syx complex. Interestingly, extended hairpin configurations were observed in the structures of individual Munc18-2 and Munc18-3 (Hackmann et al., 2013, Hu et al., 2011). A Munc18-1 conformational switch at domain 3a that accommodates a Syntaxin-1a in a loose conformation is therefore plausible.

I sought to probe the conformational flexibility of the Munc18-1/Syx1a complex in order to understand better the presumed conformational changes taking place from a tight Munc18-1/Syx1a complex towards SNARE complex assembly. To do so, I systematically investigated the structural effects of additional mutations in the Syntaxin-1a linker region, where, as mentioned above, the LE mutations proved to have a strong effect. Mutants carrying single and double amino acid substitutions still interacted with Munc18_{wt}. Notably, even the variant, where the whole Syntaxin-1a had been taken out (Syx Δ linker), formed a stable complex with Munc18-1_{wt}. The lack of a strict requirement of the linker region for the Munc18-1/Syntaxin-1a interaction *in vitro* suggests that this region, in particular the linker helix, could mainly have a regulatory function. For instance, the linker helix could function as a physical obstacle, a "lid", precluding the binding of the SNARE partners close to the point where the SNARE complex zippering starts (Pobbati et al., 2006). A potential withdrawal of the linker helix from that point could enable access to the SNARE motif.

Discussion

I was able to observe reduced inhibition of SNARE complex assembly for all Syntaxin mutants studied. Sy^{XLE} and Sy^{XL169A_E170A} were the least inhibited amongst them. It is possible that these two mutants carry combinations of substitutions that destabilize the linker helix, allowing it to adopt a less fixed position. Strikingly, the mutant where the whole linker was removed (Sy^{XΔ161-182}) was not less inhibited than Sy^{XLE}, suggesting that the effect reached by Sy^{XLE} could be maximal.

I noted that this putative conformational switch of the linker is not independent of the rest of the protein complex. Intrinsic tryptophan fluorescence emission of Munc18-1 (Burkhardt et al., 2008) was affected when Munc18-1 was interacting with Syntaxin-1a linker mutants. I identified the primary source of increase of emitted fluorescence to be the pi-pi stacking interaction of Munc18-1 Trp28 with Syntaxin-1a Phe34, as the fluorescence increase was abolished when I mutated either Munc18-1 Trp28 or Syntaxin-1a Phe34 to alanine. Additionally, mutation of these residues to alanines also impacted the inhibition.

Munc18-1 Trp28 serving as another interaction site was an important finding. It confirmed that the spatially distinct interaction sites (Munc18-1 domain 3a/Syntaxin-1a linker and Munc18-1 domain 1/Syntaxin-1a N-peptide (Burkhardt et al., 2008, Colbert et al., 2013, Vardar et al., 2021) are connected somehow. During my experiments, Syntaxin-1a linker mutations led to a similar tryptophan emission change as observed for the Syntaxin-1a^{LE}. This suggests that each of the mutations lead to a similar structural change in the complex. The identification of the pi-pi stacking interaction of the Munc18-1 Trp28 and Syntaxin-1a Phe34 pair to be the source of the fluorescence change allowed me to localize the readout. While the entire structural change is unknown, it became evident that this region is affected and is changing slightly. As a similar effect is seen for other mutations, it is safe to assume that they all lead to a similar structural change of the complex and that this change makes SNARE complex formation for the bound Syx easier. The N-peptide of Syntaxin is connected to the Ha-helix by a short stretch, which has not been studied so far. This includes residues 11 to 26, which are conserved in residue composition and length (unpublished observations). I studied two mutants of this stretch; i. one where residues 11 to 26 were removed, Syntaxin-1a^{Δ11-26}, and ii. Syntaxin-1a^{3x(11-26)} where residues 11 to 26 were inserted two more times to extend the linker. Deletion or extension of residues 11 to 26 eased SNARE complex assembly in the presence of Munc18-1. The mutations were introduced in a region that spatially distant

from Syntaxin-1a yet lead to a similar change. How do these spatially distant regions communicate?

Colbert et al., 2013 proposed that the displacement of N-peptide binding promotes the extension of Munc18-1 domain 3a. According to this idea, these two distant sites communicate through an electrostatic network of interactions at the domain 1-domain 2 interface (at the outer surface of Munc18-1), transferring the changes from the N-peptide binding site to domain 3a. As outlined before, the available structures of SM protein isoforms and homologs indicate that the tip of domain 3a of Munc18 (the so-called helical hairpin) adopts a different, extended conformation (Hackmann et al., 2013). This region appears to undergo a conformational change upon binding and unbinding of the closed conformation, as it has been found in different conformations when bound or not bound to Syntaxin. Notably, the helical hairpin region is very close to the small linker helix of Syntaxin-1a and is involved in an extended network of interactions with Syntaxin-1a Hc, linker and H3 regions.

I extensively studied the involvement of Munc18-1 domain 3a by testing the effect of established and novel mutations in Munc18 that could interfere with either the conformational change or the binding to Syntaxin-1a. The diversity of the observed changes made it difficult to elucidate whether the observed effect was a result of conformational change, or disruption of important interactions, or both.

Broken down, I tested several point mutations on Munc18-1 domain 3a that probably affect the domain 3a interface with Syntaxin-1a. These included R315A and Y337A substitutions. Y337 is involved in polar interactions with the conserved Syntaxin N135 of Hc helix, and R315 is in polar contacts with R142 and E166 of Syntaxin Hc and linker helices. Both Munc18-1 mutants (Munc18_{R315A} and Munc18_{Y337A}) retained Syntaxin-1a inhibition. Notably, Syntaxin-1a_{N135D}, Syntaxin-1a_{R142A}, Syntaxin-1a_{E166A} and Syntaxin-1a_{E166R} exhibited reduced Munc18-1_{wt} exerted inhibition.

Deletion of the residues of Munc18-1 domain 3a helical hairpin loop (Munc18-1_{Δ317-333}) caused only a subtle reduction of inhibition. Residues 317-322 are non-resolved at the Munc18-1/Syntaxin-1a structure and residues 322-333 are folded into the unfurled loop. At the Munc18-1_{K332E_K333E} structure, residues 322-333 fold into a helix leading to an extension of helix 12. This subtle reduction of inhibition suggested that this region, in either unfurled or extended conformation, might confer mildly to the inhibition, or remove it.

Discussion

A similar subtle reduction was also observed when another domain 3a hairpin loop ($\beta 10\beta 11$) was deleted (Munc18-1 $\Delta 269-275$). Munc18-3 lacks this short loop, while the loop in Munc18-1 is involved in a network of interactions with the H3 helix of Syntaxin-1a. This subtle change probably disrupted its interactions with Syntaxin-1a.

The mutation Munc18-1 P335A exhibited the stronger effects on SNARE complex formation. Substitution of P335 with alanine is believed to induce the extension of the helical hairpin of domain 3a of Munc18-1. An extended hairpin structure would clash with the binding mode of the closed Syntaxin-1a. If the mutation extended the helix, Munc18-1 should be unable to inhibit SNARE complex formation (Han et al., 2014, Parisotto et al., 2014, Park et al., 2016, Munch et al., 2016). Indeed, corroborating previous studies, Syntaxin-1a assembled into a SNARE complex despite the presence of Munc18-1 $P335A$. The dissociation rate of the Munc18-1 $P335A$ /Syntaxin-1a complex (0.061/s), however, is $\sim 12x$ faster than that of the Munc18-1 $_{wt}$ /Syntaxin-1a complex (0.005/s). In agreement with the previous results, this finding indicated that while the mutation has some effect on the Munc18-1 affinity to Syntaxin-1a, Munc18-1 $P335A$ was still able to bind Syntaxin-1a tightly. It is possible that P335A weakens the binding of the hairpin helices to Syntaxin-1a through disruption of the extensive interaction network of Proline with the residues. It is as well possible, the weakened interaction is a result of the predicted extension of the hairpin helices that would result to binding of Syntaxin-1a in a different conformation than the closed, which in the case of extension would be sterically hindered.

Another published Munc18 variant bears mutations at the conserved lysines 332 and 333 at the tip domain 3a (Munc18-1 $K332E_K333E$). Initially designed to abolish binding to Syntaxin-1a, it was shown to act much like Munc18-1 $_{wt}$ *in vivo* (Han et al., 2013, Han et al., 2014). Biochemically, Munc18-1 $K332E_K333E$ bound to Syntaxin-1a and inhibited SNARE complex formation like Munc18-1 $_{wt}$, in accordance with the published *in vivo* observations. The structure of Munc18-1 $K332E_K333E$ was solved recently as a homodimer (Wang et al., 2020). However, in contrast to Munc18-1 $P335A$ which oligomerizes, Munc18-1 $K332E_K333E$ in solution is a monomer. In this structure, helix 12 of domain 3a is indeed extended. It is possible that the P335A mutation also induces a similar extended conformation at lower concentrations than Munc18-1 $K332E_K333E$, which might cause it to oligomerize. In combination with the biochemically observed similarity between

Munc18-1_{wt} and Munc18-1_{K332E_K333E}, it became more and more evident that Munc18-1_{wt}, could undergo a conformational change, especially at domain 3a.

SNARE complex inhibition mechanism relies on two factors: *i.* the electrostatic interactions at the Munc18-1/Syntaxin-1a interface, and *ii.* through structural preclusion of the H3 motif when Syntaxin-1a is in closed conformation. According to my observations, SNARE complex formation was achieved when either, or both, of these factors was overthrown. This was suggested by the dissociation rates from Munc18-1_{P335A} and Munc18-1_{W28A} complexes. The off-rate for Munc18-1_{W28A} was at least 30x faster than Munc18-1_{wt}, while the off-rate for Munc18-1_{P335A} (0.061/s) was ~12x faster than Munc18-1_{wt}. Intriguingly, Munc18-1_{W28A} was much more inhibitory than Munc18-1_{P335A}, which was the least inhibitory mutant. Taken together, these two mutants highlight the fact that the observed loss of inhibition does not always correlate with reduction of the Munc18-1 affinity for Syntaxin-1a.

While baffling, this outcome made me speculate that the connecting point is the conformational flexibility of the Munc18-1/Syntaxin-1a pair. It is likely that the mutations at the tip of $\alpha 11\alpha 12$ of domain 3a allow for SNARE complex assembly by subtly destabilizing the Syntaxin-1a closed conformation. In this case, a looser conformation of Syntaxin-1a, while still tightly bound to Munc18-1, could set the SNARE N-terminus accessible to the interacting SNAREs. On the contrary, the N-peptide and Habc domain interactions of Syntaxin-1a are more crucial to sustain a tight binding to Munc18-1.

Evidently, the aforesaid idea is supported by the differences between the determined Syntaxin-1a off rates, when measured from position 1 (N-peptide) or position 186 (H3). This difference could also reflect local flexibility changes of the fluorophore at the different positions, which could proceed faster at the N-peptide region – after unbinding of the N-peptide, for example – than the H3 helix. Given that the differences were only observed for Syntaxin-1a $\Delta 161-182$, and not for Syntaxin-1a_{wt}, the findings suggest that the conformation by which Syntaxin-1a $\Delta 161-182$ is bound to Munc18-1 could be causing flexibility differences between positions 1 and 186. The off rate for Syntaxin-1a_{LE} (~0.026/s), determined as well from position 186, was the same as for Syntaxin-1a $\Delta 161-182$. Since the linker region is missing from Syntaxin-1a $\Delta 161-182$, it is conceivable that it binds to Munc18-1 with a somewhat “open”, or *looser*, conformation. Binding of Syntaxin-1a $\Delta 161-182$ to Munc18-1, therefore, could reflect the “open” conformation binding. Thus, it seems that when Syntaxin-1a is bound to Munc18-1 in a

Discussion

less closed conformation, the Syntaxin-1a N-peptide region is more flexible than H3. The flexibility caused at the N-peptide by the $\Delta 161-182$, or the LE mutations showed, once again, that the changes at the linker region are communicated to the N-peptide. Thence, how are these changes communicated?

I sought to understand how the two spatially distinct interaction sites are contribute to the tight interaction. My idea was to first test how depended on the interactions from both sites is the Munc18-1/Syntaxin-1a complex. To do this, I exploited my diverse collection of Munc18-1 and Syntaxin-1a mutants. I combined Munc18-1 mutants that carried mutations at domain 1, or domain 3a, with Syntaxin-1a linker, or N-terminus, mutants, respectively, and observed their stability. In most cases, these complexes were falling apart, suggesting that both sites are needed for the tight interaction. However, I observed an unstable complex when I combined two mutants of the same interacting site, e.g. Syntaxin-1a_{3x(11-26)} and Munc18-1_{w28A}. Nevertheless, this finding highlighted, once again, the importance of Munc18-1 domain 1/Syntaxin-1a N-terminus for sustaining the tight complex's interaction. It is likely that Syntaxin-1a remains bound to Munc18-1 after it Syntaxin-1a loosened.

As mentioned earlier, during the course of this study, two new SM structures (Vps45/Tlg2 and Munc18-1_{K332E_K333E}) became available (Eisenman 2020, Wang 2020). I gladly observed that these structures corroborated my experimental findings, which suggested conformational changes in domains 1 and 3a when Munc18 loosens its tight grip on Syntaxin. Probably, these switches in Munc18-1 are interconnected. Even more exciting was the observation of a loose Tlg2 while bound to Vps45. My working hypothesis during the course of my work was that the Munc18-1/Syntaxin-1a closed conformation structure was a snapshot of the most energetically favorable conformation and that the complex must somehow undergo a conformational change that enables the bound Syntaxin to engage in SNARE complex formation. In the Vps45/Tlg2 structure, the Tlg2 N-peptide remains bound to Vps45 domain 1 while its H3 loosens. In the structure, the N-terminal of H3 helix engages in limited interactions with the fully extended helical hairpin of domain 3a and does not interact with the Habc helices as observed for syntaxin in complex with Munc18. As a result, the N-terminus of H3 helix is rotated $\sim 120^\circ$ around the long axis, relative to the Munc18-1/Syntaxin-1a complex. The structure of the linker connecting the Tlg2 N-peptide to Habc was not resolved, probably because it is disordered like the corresponding region in the Munc18-1/Syntaxin-1a complex.

As outlined above, my biochemical observations suggested that the Munc18/syntaxin complex undergoes a conformational change that allows syntaxin to start engaging with its partner SNAREs while it is still bound by Munc18-1. A precise structural model of that state could not be gleaned from these observations, however. Fortunately, the newly available structures gave me the opportunity to model this elusive conformational state of the Munc18/syntaxin complex.

For homology modeling of the loose conformation of the Munc18-1/Syntaxin-a complex, the Vps45/Tlg2 structure was used as template. Although the sequence similarity of the two pairs is low, the models were created with high confidence. Future structural investigations are needed to corroborate the modeled structure. The conformational changes can be seen when comparing the crystal structure of the complex to the model. In the model, Syntaxin-1a is bound through N-peptide and Habc interactions to Munc18-1, with the H3 in an extended conformation. The H3 domain follows the helical extended hairpin region of domain 3a.

However, further investigations to evaluate the complex's stability are needed, thought. As such a state is not possible to be observed biochemically, the stability should be assessed *in silico*, i.e., through predictions of stability changes ($\Delta\Delta G$) between the model and the crystal structure and/or Molecular Dynamics simulations of the model. Vps45/Tlg2 complex structure and the model of the Munc18-1/Syntaxin-1a in loose conformation, show that the clasping of domain 1 persists while Syntaxin-1a is partly opening.

Munc18-1 is suggested to function as template of SNARE complex assembly (Baker et al., 2015, Sitarska et al., 2017, Lai et al., 2017, Jiao et al., 2018). The proposed mechanisms, however, by which the templating could occur differ. Baker et al., 2015 solved the structure of the R-SNARE Nyv1 interacting with the domain 3a of Vps33. Vps33 domain 3a binds the Qa-SNARE of Vam3 as well. Based on this observation, they suggested that Munc18-1 domain 3a could function as a template to align of R- and Qa-SNAREs. Sitarska et al., in 2017 suggested that Munc18-1 domain 3a could also interact with Synaptobrevin at the homologous position as observed for Vps33 and Nyv1. In their study, they suggested that two mutants at domain 3a, L348R (Parisotto et al., 2014) and D326K (designed to destabilize the $\alpha 11\alpha 12$ hairpin loop) impacted Synaptobrevin binding at opposite ways. L348R was suggested to interfere and D326K to promote putative Synaptobrevin binding (Sitarska et al., 2017). Surprisingly, my results did not

Discussion

confirm their findings. In my experiments, both mutants behaved like wt Munc18. It is worth noting, though, that Munc18-1_{L348R} had an increased propensity to precipitate. Therefore, the observations using this mutant could be influenced somewhat by this. Furthermore, I did not observe Synaptobrevin binding to Munc18-1_{wt}, despite multiple efforts using different approaches. Consequently, I was unable to probe for changes in the strength of synaptobrevin binding. the affinity of Munc18-1 for Synaptobrevin. The affinity between the two proteins is estimated to be in the μM range (Parisotto et al., 2014, Sitarska et al., 2017). This could explain why I did not Munc18-1/Synaptobrevin binding in my assays. Noteworthy, in some native gels, where I used Syb^{*28}, some degradation products appeared as non-specific smears after UV exposure (data not shown). It is possible that an unknown synaptobrevin degradation product could interact with Munc18-1. As the fluorescence label is attached to residues 28, a fluorescent synaptobrevin fragment could be shortened C-terminally, possibly missing the residues from 87 to 96, which are positively charged. Interestingly, this synaptobrevin region has been proposed to be interacting with the domain 3a of Munc18-1 (Parisotto et al., 2014). Therefore, I did not investigate this further as we thought that this might be an artifact. Newer studies, however, using liposome fusion assays (André et al., 2020) and single molecule force spectroscopy of (Jiao et al., 2018) indicated that Munc18-1 domain 3a interacts with Synaptobrevin from layers -4 to to +6 (residues 42-77). In my experiments, I mostly used Synaptobrevin 1-96. Indeed, several studies have shown that synaptobrevin residues 89 to 92 form a flexible hinge between the soluble and hydrophobic segments of the protein (Lindau et al., 2012, Ellena et al., 2009, Hu et al., 2021). Earlier studies in our lab demonstrated the importance of residues 77 to 90 for liposome fusion and the constitutive activity of Synaptobrevin in proteoliposomes and purified synaptic vesicles (Siddiqui et al., 2007). With this protein being intrinsically disordered, it is conceivable that in solution, C-terminus somehow autoinhibited the weak interaction with Munc18-1. It is possible that Synaptobrevin binding requires the MUN domain of Munc13 as suggested (Shu et al., 2020, Jiao et al., 2018, Wang et al., 2019). Additional experiments with shorter Synaptobrevin fragments and in higher concentrations, or in the presence of MUN domain, should thus be carried out to shed light on this apparent discrepancy.

Munc13 is an important regulator of synaptic release (Varoqueaux et al., 2002, Augustin et al., 1999b). Munc13-1 has been suggested to facilitate opening of Syntaxin-

1a through interactions of its MUN domain with the Munc18-1a/Syntaxin-1a complex at the domain 3a/linker region (Wang et al., 2017, Ma et al., 2013). The MUN domain is thought to act together with Munc18-1 in templating SNARE complex assembly (Lai et al., 2017, Jiao et al., 2018, Wang et al., 2019, Shu et al., 2020). Surprisingly, the MUN domain did not exhibit catalytic activity in my assays. Previous experiments suggested that MUN domain displays lower efficiency in catalyzing SNARE complex assembly in concentrations lower than 30 μ M (Wang et al., 2020, Wang et al., 2017, Yang et al., 2015). But even when used higher concentrations (40 μ M), I did not observe increase in the rate of SNARE complex formation. It is possible that the disagreement of my observations with the previously published studies constitutes a physiological feature of the interaction. As the affinity of MUN for the Munc18-1/Syntaxin-1 complex is supposed to be low (at the μ M range), it is possible that the high affinity interaction of Munc18-1/Syntaxin-1a prevented me from seeing a clear effect. On the other hand, it should not be ruled out that the effect does not exist or is produced indirectly through the interaction of the MUN domain with the C-terminal region of synaptobrevin as discussed above.

The affinity of the MUN domain for the Munc18-1/Syntaxin-1a complex is thought to be strengthened when membrane-anchored, as the C-terminal region of the MUN domain (subdomains C and D) is a possible membrane interaction site (Yang et al., 2015). The MUN catalytic activity observed at aforementioned studies was in most cases observed in reconstituted liposome-based assays. It is plausible that the lack of the lipids, hence membrane interaction, from my assays contributed to the absence of the proposed MUN activity.

My mutational scan showed a conformational switch of the Munc18-1/Syntaxin-1a complex can take place. This switch allows Syntaxin-1a to form a SNARE complex in the presence of Munc18-1, possible while still bound. The minor differences at the structures of other SM proteins indicate the existence of other conformations (Baker et al., 2015, Baker and Hughson, 2016). It has been discussed that the Munc18-1/Syntaxin-1a complex interaction is divergent from the rest (Eisemann et al., 2020), something special “at the pinnacle of the evolutionary path” (Shin, 2013). My findings suggest that the conformational transitions of the SM/Qa complex could explain the minor difference between the SM structures. It is possible that the minor differences between the other SM structures are a result of crystallization at different energetic minima. Therefore, the conformational transitions are rather conserved mode of the SM/Qa pairs, and not

divergent. At the Munc18-1/Syntaxin-1a complex, the tight interaction with Syntaxin-1a must be more energetically favorable, possibly to hold Syntaxin-1a blocked. The block could be lifted through a conformational transition of the complex could be triggered when Syntaxin-1a is needed to interact. pathway is conserved in other sm proteins but that different stages have been crystalized shows that for different sm proteins, the energy landscape of the pathway is changed a bit. For M18, the control (block) over syx is more important.

Whether the switch trigger would be a cofactor, or another interacting protein, was not identified in this study. The most extensively studied interacting partner is Munc13. It is possible that within the crowded cellular environment, Munc13 affinity to the complex might be higher due to the spatial confinement and limited diffusion. Increasing evidence suggest that liquid-liquid phase separation systems can regulate synapse organization (Milovanovic et al., 2018, Hayashi et al., 2021). In such systems, biomolecules (proteins and/or nucleic acids) condense into membraneless droplets. The concentration of a specific biomolecule this condensate/droplet is enriched, resulting in the lowering of the energetic barrier needed for the reactions to occur. Synapsin, a synaptic vesicle associated protein, was shown to organize the vesicle clusters through liquid liquid phase separation (Milovanovic et al., 2018). It is thus possible, that Munc18-1/Syntaxin-1a are regulated through interactions involving phase separation events, by Munc13 or other interacting partners.

For instance, Munc18-1 has been shown to interact with another protein, Mint. Mint interacts with Munc18-1 and CASK forming a tripartite complex (Zhang et al., 2020, Butz et al., 1998). Mint carries a Munc18-1 interacting domain, a CASK interacting domain and two PDZ domains. PDZ domains are often found in multi-domain scaffolding proteins of the synapse (Kim and Sheng, 2004), including RIM, a Munc13 interacting partner (Kaesler et al., 2011). PDZ domain containing proteins are components of membraneless condensates at the postsynaptic density assemblies and presynaptic active zone assemblies, which are now believed to form through phase separation mechanisms (Chen et al., 2020b). Hence, it is likely that the interaction of Munc18-1 with Mint interacts with Munc18-1 by organizing its spatiotemporal localization, by bridging interactions with other active zone proteins through scaffolding. However, the knowledge over the interaction of Munc18-1 with Mint is sadly limited.

Lastly, an example of a scarcely studied interaction is the one of Syntaxin-1a with the Kv2.1 potassium channel. (Yeh et al., 2019) showed that Syntaxin-1a N-terminus interacts with the intrinsically disordered C-terminus of Kv2.1 potassium channel. In fact, their molecular docking approaches suggest that the Kv2.1 potassium channel interacting region with Syntaxin-1a (Ha helix) is shared with Munc18-1. Of these, they identified that the Trp28/Phe34 interaction is competed by the interaction of Syntaxin-1a with this 9-residue long stretch of the potassium channel. Eventually, the interaction of the Kv2.1 channel with Syntaxin-1a Ha leads to cell death cascade, however, it serves a paradigm that Syntaxin-1a Ha can physiologically be accessible by other interactors. It is possible that this interaction is physiologically blocked by constitutive binding of Munc18-1 domain 1 to Syntaxin-1a Ha and only becomes accessible in non-physiological conditions.

The vagueness around the Munc18-1/Syntaxin-1 complex's interactors highlights the difficulty to recognize the trigger. Nevertheless, a conformational change involving the whole complex takes place allowing SNARE complex formation to occur while Syntaxin-1a is bound to Munc18-1. I did not manage to find upon what, but I did manage to see how.

6. Conclusion and Future directions

Soluble N-ethylmaleimide-sensitive factor Attachment protein Receptor (SNARE) proteins and Sec1/Munc18-1 (SM) proteins are important regulators of vesicular fusion. SNARE proteins are the core machinery driving fusion, which they exert by zippering into a 4-helical bundle, the SNARE complex. Neuronal SNARE proteins (Syntaxin-1a, SNAP25 and Synaptobrevin) facilitate fusion of neurotransmitter-loaded synaptic vesicles with the presynaptic plasma membrane. Interaction of the neuronal SM homologue, Munc18-1, with Syntaxin-1a is a crucial step for neurotransmitter release. Biochemically, Munc18-1/Syntaxin-1a interaction inhibits the latter from assembling into the SNARE complex. At the crystal structure of the complex Munc18-1 is bound to Syntaxin-1a, through interactions of the Syntaxin-1a N-peptide with the outer Munc18-1 domain 1, and the binding cavity formed by the inner surface of domains 1, 2 and 3a. Interaction of Munc18-1 with Syntaxin-1a is believed to lock the latter in closed conformation. In this conformation, the SNARE motif is bundling with the Habc domain, preventing it from assembling into the SNARE complex. Earlier studies have identified two Syntaxin-1a mutants that can escape the tight grip of Munc18-1; one lacking the N-peptide (Syntaxin-1a Δ N) and one bearing mutations at two residues of Syntaxin-1a linker helix (Syntaxin-1a $_{LE}$). Syntaxin-1a Δ N and Syntaxin-1a $_{LE}$ can both bind to Munc18-1, in a somewhat similar conformation to Munc18-1/Syntaxin-1a. However, they are both able to form SNARE complex in the presence of Munc18-1. Considering these findings, I sought to understand how Syntaxin-1a can escape the tight Munc18-1 grip and assembled into SNARE complex.

My mutational scan of the Munc18-1/Syntaxin-1a complex showed a conformational transition is possible and involves the synchronous transition of both proteins. I identified the Syntaxin-1a linker to be indispensable for the inhibition, yet, not necessary for the interaction with Munc18-1. All Syntaxin-1a linker mutants I studied maintained binding to Munc18-1. However, mutations at Syntaxin-1a linker impacted the inhibition to a different degree. Syntaxin-1a $_{LE}$ and Syntaxin-1a $_{L169A_E170A}$ impacted the inhibition at the maximum. I identified Pi-pi stacking interaction of Tryptophan 28 in the domain 1 of Munc18-1 domain 1 with Syntaxin-1a Phenylalanine 34 as the source of the observed increase of fluorescence emission upon Syntaxin-1a binding. Munc18-1 Tryptophan 28 is an important interaction contributor in the inner surface of domain 1. Mutation of this residue affected the inhibition and impacted greatly the dissociation rate of the complex.

I also found that the short stretch that connect the N-peptide to the Habc domain of Syntaxin-1a is very important for interactions with Munc18-1 domain 1. Removal of this region also impacted the inhibition. An even greater effect was observed when this region was extended. Their effects on the inhibition probably result in a slight destabilization of Munc18-1/Syntaxin-1 complex.

Munc18-1 domain 3a is another important interaction hub. Munc18-1 domain 3a interacts with Syntaxin-1a through the $\alpha11\alpha12$ helical hairpin as well the $\beta10\beta11$ beta hairpin. Interactions of the $\beta10\beta11$ beta hairpin with the Syntaxin-1a H3 have a subtle contribution to the inhibition. $\alpha11\alpha12$ helical hairpin interactions with Hc, linker, and H3 helices are important for the Munc18-1/Syntaxin-1a interaction and the inhibition.

All Munc18-1 domain 3a mutants formed a stable complex with Syntaxin-1a. Mutation P335A had the greatest impact of all Munc18-1 mutations on the inhibition. The dissociation rate for the Munc18-1_{P335A}/Syntaxin-1a complex, though, was found to be slower than the Munc18-1_{W28A}/Syntaxin-1a complex. Some other mutations at domain 3a residues had lesser or no effect. Interestingly, mutations at their Syntaxin-1a counter interacting residues (on Hc) affected at some degree the inhibition.

Mutations at the Syntaxin-1a linker increased the flexibility of its N-terminus. Dissociation rates of Syntaxin-1a_{Δlinker} and Syntaxin-1a_{LE} were somewhat higher when determined from position 1 than when determined from position 186. This was not observed for Syntaxin-1a_{wt} as the dissociation rates, when determined from both positions, were found the same. As these were determined by measuring fluorescence anisotropy decay, it is possible they reflect local flexibility changes of the tagged residues.

My biochemical and biophysical approaches showed that the mutations at two spatially distinct sites led to similar effects. This suggested that the Munc18-1/Syntaxin-1a complex is conformationally flexible, allowing for the changes to be communicated from one site to the second. Probably through conformational transitions when the two are in complex.

During my study, the structure of the homologous Vps45/Tlg2 complex was published. The syntaxin homologue Tlg2 was found in a more open conformation in the complex compared to Syntaxin 1a in complex with Munc18. The structural features of the Vps45/Tlg2 complex corroborated my biochemically investigations on the Munc18/syx complex, which had put forward the idea that a transition from a locked towards a more open syntaxin occurs while it is bound by Munc18.

Conclusion and Future directions

Together with the Protein Modelling Unit of UNIL, I created a model of the Munc18-1/Syntaxin-1a complex in a more loose conformation based on the Vps45/Tlg2 structure. In the model, the Munc18-1/Syntaxin-1a complex has undergone a larger conformational change in both proteins. Munc18-1 domain 1 and domain 3 have rotated to accommodate the less closed Syntaxin-1a. Syntaxin-1a H3 rotated and swung away from the Habc, following the extension of Munc18-1 domain 3a hairpin helices. This new model of the Munc18-1 bound Syntaxin-1a in a less closed conformation probably represents a snapshot of an intermediate, less stable conformation between the locked conformation observed in the Munc18-1/Syntaxin-1a and the SNARE crystal structures.

Altogether, my data suggest the Munc18-1/Syntaxin-1a undergo a conformational transition while bound to each other. Munc18-1 can remain bound while Syntaxin-1a is opening. It is likely that Munc18-1 does not have to leave Syntaxin-1a for the later to assemble into SNARE complex. SNARE complex assembly could initiate while Syntaxin-1a is bound to Munc18-1. By extending the hairpin structure of domain 3a, Munc18-1 can serve a template for SNARE complex assembly (Fig.6). The *in vitro* observed inhibition probably reflects an energetic minimum that cannot be crossed easily and thus constitutes a perfect target for external controlling factors.

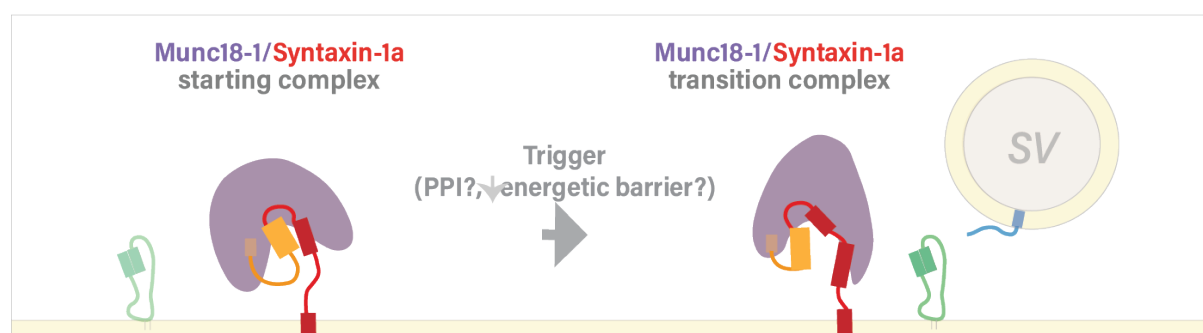


Figure 6: Syntaxin-1a and Munc18-1 undergo a conformational transition in complex. Upon trigger activation Munc18-1 and Syntaxin-1a undergo a conformational transition together as a complex. The transition might be depended on protein protein interactions (PPI) or local changes at the cell environment that lower the energetic barrier. The conformational transition can set Syntaxin-1a ready to interact with its SNARE partners.

Whether lowering of the energetic barrier is exerted through interactions with tethering proteins, or local changes of the cellular environment at the active zone needs to be further assessed. Munc13, and other scaffolding proteins, could facilitate the initiation of the transitioning events by bridging the necessary interacting partners. The model created during this study depicts a possible snapshot of the conformational transitions. Further biophysical investigations are needed to address what are the

energetic differences between the model and the crystal structure. Moreover, *in vivo* investigations of the novel mutants described in this study can provide further insights on how Munc18-1/Syntaxin-1a conformational transitions affect exocytosis. With the recent advances in cryo-electron tomography, it is worth attempting to observe the SNARE, SM, and tethering interactions *in vivo*, in different synapses. This can give us the additional spatiotemporal information to elucidate the steps governing synaptic release, and, in the long term, design targeted therapies for the neurodevelopmental disorders associated with these factors.

7. Bibliography

- ANDRÉ, T., CLASSEN, J., BRENNER, P., BETTS, M. J., DÖRR, B., KREYE, S., ZUIDINGA, B., MEIJER, M., RUSSELL, R. B., VERHAGE, M. & SÖLLNER, T. H. 2020. The Interaction of Munc18-1 Helix 11 and 12 with the Central Region of the VAMP2 SNARE Motif Is Essential for SNARE Templating and Synaptic Transmission. *eNeuro*, 7.
- ARCHBOLD, J. K., WHITTEN, A. E., HU, S. H., COLLINS, B. M. & MARTIN, J. L. 2014. SNARE-ing the structures of Sec1/Munc18 proteins. *Curr Opin Struct Biol*, 29, 44-51.
- AUGUSTIN, I., ROSENMUND, C., SÜDHOF, T. C. & BROSE, N. 1999a. Munc13-1 is essential for fusion competence of glutamatergic synaptic vesicles. *Nature*, 400, 457-461.
- AUGUSTIN, I., ROSENMUND, C., SÜDHOF, T. C. & BROSE, N. 1999b. Munc13-1 is essential for fusion competence of glutamatergic synaptic vesicles. *Nature*, 400, 457-61.
- BAKER, R. W. & HUGHSON, F. M. 2016. Chaperoning SNARE assembly and disassembly. *Nature reviews. Molecular cell biology*, 17, 465-479.
- BAKER, R. W., JEFFREY, P. D., ZICK, M., PHILLIPS, B. P., WICKNER, W. T. & HUGHSON, F. M. 2015. A direct role for the Sec1/Munc18-family protein Vps33 as a template for SNARE assembly. *Science*, 349, 1111-4.
- BAR-ON, D., NACHLIEL, E., GUTMAN, M. & ASHERY, U. 2011. Dynamic conformational changes in munc18 prevent syntaxin binding. *PLoS Comput Biol*, 7, e1001097.
- BARCLAY, J. W., ALDEA, M., CRAIG, T. J., MORGAN, A. & BURGOYNE, R. D. 2004. Regulation of the fusion pore conductance during exocytosis by cyclin-dependent kinase 5. *J Biol Chem*, 279, 41495-503.
- BASU, J., SHEN, N., DULUBOVA, I., LU, J., GUAN, R., GURYEV, O., GRISHIN, N. V., ROSENMUND, C. & RIZO, J. 2005. A minimal domain responsible for Munc13 activity. *Nat Struct Mol Biol*, 12, 1017-8.
- BOYD, A., CIUFO, L. F., BARCLAY, J. W., GRAHAM, M. E., HAYNES, L. P., DOHERTY, M. K., RIESEN, M., BURGOYNE, R. D. & MORGAN, A. 2008a. A random mutagenesis approach to isolate dominant-negative yeast sec1 mutants reveals a functional role for domain 3a in yeast and mammalian Sec1/Munc18 proteins. *Genetics*, 180, 165-78.
- BOYD, A., CIUFO, L. F., BARCLAY, J. W., GRAHAM, M. E., HAYNES, L. P., DOHERTY, M. K., RIESEN, M. L., BURGOYNE, R. D. & MORGAN, A. 2008b. A Random Mutagenesis Approach to Isolate Dominant-Negative Yeast sec1 Mutants Reveals a Functional Role for Domain 3a in Yeast and Mammalian Sec1/Munc18 Proteins. *Genetics*, 180, 165-178.
- BRENNER, S. 1974. The genetics of *Caenorhabditis elegans*. *Genetics*, 77, 71-94.
- BURKHARDT, P., HATTENDORF, D. A., WEIS, W. I. & FASSHAUER, D. 2008. Munc18a controls SNARE assembly through its interaction with the syntaxin N-peptide. *Embo j*, 27, 923-33.
- BUTZ, S., OKAMOTO, M. & SÜDHOF, T. C. 1998. A Tripartite Protein Complex with the Potential to Couple Synaptic Vesicle Exocytosis to Cell Adhesion in Brain. *Cell*, 94, 773-782.
- CHEN, W., CAI, Z. L., CHAO, E. S., CHEN, H., LONGLEY, C. M., HAO, S., CHAO, H. T., KIM, J. H., MESSIER, J. E., ZOGHBI, H. Y., TANG, J., SWANN, J. W. & XUE, M.

- 2020a. Stxbp1/Munc18-1 haploinsufficiency impairs inhibition and mediates key neurological features of STXBP1 encephalopathy. *Elife*, 9.
- CHEN, X., WU, X., WU, H. & ZHANG, M. 2020b. Phase separation at the synapse. *Nature Neuroscience*, 23, 301-310.
- CHRISTIE, M. P., WHITTEN, A. E., KING, G. J., HU, S.-H., JARROTT, R. J., CHEN, K.-E., DUFF, A. P., CALLOW, P., COLLINS, B. M., JAMES, D. E. & MARTIN, J. L. 2012. Low-resolution solution structures of Munc18:Syntaxin protein complexes indicate an open binding mode driven by the Syntaxin N-peptide. *Proceedings of the National Academy of Sciences*, 109, 9816-9821.
- COLBERT, K. N., HATTENDORF, D. A., WEISS, T. M., BURKHARDT, P., FASSHAUER, D. & WEIS, W. I. 2013. Syntaxin1a variants lacking an N-peptide or bearing the LE mutation bind to Munc18a in a closed conformation. *Proc Natl Acad Sci U S A*, 110, 12637-42.
- DEMIRCIOGLU, F. E., BURKHARDT, P. & FASSHAUER, D. 2014. The SM protein Sly1 accelerates assembly of the ER-Golgi SNARE complex. *Proc Natl Acad Sci U S A*, 111, 13828-33.
- DULUBOVA, I., SUGITA, S., HILL, S., HOSAKA, M., FERNANDEZ, I., SUDHOF, T. C. & RIZO, J. 1999. A conformational switch in syntaxin during exocytosis: role of munc18. *Embo j*, 18, 4372-82.
- DULUBOVA, I., YAMAGUCHI, T., WANG, Y., SÜDHOF, T. C. & RIZO, J. 2001. Vam3p structure reveals conserved and divergent properties of syntaxins. *Nat Struct Biol*, 8, 258-64.
- EISEMANN, T. J., ALLEN, F., LAU, K., SHIMAMURA, G. R., JEFFREY, P. D. & HUGHSON, F. M. 2020. The Sec1/Munc18 protein Vps45 holds the Qa-SNARE Tlg2 in an open conformation. *eLife*, 9, e60724.
- ELLENA, J. F., LIANG, B., WIKTOR, M., STEIN, A., CAFISO, D. S., JAHN, R. & TAMM, L. K. 2009. Dynamic structure of lipid-bound synaptobrevin suggests a nucleation-propagation mechanism for trans-SNARE complex formation. *Proceedings of the National Academy of Sciences*, 106, 20306-20311.
- FASSHAUER, D., SUTTON, R. B., BRUNGER, A. T. & JAHN, R. 1998. Conserved structural features of the synaptic fusion complex: SNARE proteins reclassified as Q- and R-SNAREs. *Proc Natl Acad Sci U S A*, 95, 15781-6.
- FURGASON, M. L. M., MACDONALD, C., SHANKS, S. G., RYDER, S. P., BRYANT, N. J. & MUNSON, M. 2009. The N-terminal peptide of the syntaxin Tlg2p modulates binding of its closed conformation to Vps45p. *Proceedings of the National Academy of Sciences*, 106, 14303-14308.
- GERBER, S. H., RAH, J.-C., MIN, S.-W., LIU, X., DE WIT, H., DULUBOVA, I., MEYER, A. C., RIZO, J., ARANCILLO, M., HAMMER, R. E., VERHAGE, M., ROSENMUND, C. & SÜDHOF, T. C. 2008. Conformational switch of syntaxin-1 controls synaptic vesicle fusion. *Science (New York, N.Y.)*, 321, 1507-1510.
- GIL-PISA, I., MUNARRIZ-CUEZVA, E., RAMOS-MIGUEL, A., URIGÜEN, L., MEANA, J. J. & GARCÍA-SEVILLA, J. A. 2012. Regulation of munc18-1 and syntaxin-1A interactive partners in schizophrenia prefrontal cortex: Down-regulation of munc18-1a isoform and 75 kDa SNARE complex after antipsychotic treatment. *International Journal of Neuropsychopharmacology*, 15, 573-588.
- GUIBERSON, N. G. L., PINEDA, A., ABRAMOV, D., KHAREL, P., CARNAZZA, K. E., WRAGG, R. T., DITTMAN, J. S. & BURRÉ, J. 2018. Mechanism-based rescue of Munc18-1 dysfunction in varied encephalopathies by chemical chaperones. *Nat Commun*, 9, 3986.

- HACKMANN, Y., GRAHAM, S. C., EHL, S., HÖNING, S., LEHMBERG, K., ARICÒ, M., OWEN, D. J. & GRIFFITHS, G. M. 2013. Syntaxin binding mechanism and disease-causing mutations in Munc18-2. *Proc Natl Acad Sci U S A*, 110, E4482-91.
- HAN, G. A., BIN, N. R., KANG, S. Y., HAN, L. & SUGITA, S. 2013. Domain 3a of Munc18-1 plays a crucial role at the priming stage of exocytosis. *J Cell Sci*, 126, 2361-71.
- HAN, G. A., PARK, S., BIN, N. R., JUNG, C. H., KIM, B., CHANDRASEGARAM, P., MATSUDA, M., RIADI, I., HAN, L. & SUGITA, S. 2014. A pivotal role for pro-335 in balancing the dual functions of Munc18-1 domain-3a in regulated exocytosis. *J Biol Chem*, 289, 33617-28.
- HANUKOGLU, I. 2015. Proteopedia: Rossmann fold: A beta-alpha-beta fold at dinucleotide binding sites. *Biochem Mol Biol Educ*, 43, 206-9.
- HAYASHI, T., MCMAHON, H., YAMASAKI, S., BINZ, T., HATA, Y., SUDHOF, T. C. & NIEMANN, H. 1994. Synaptic vesicle membrane fusion complex: action of clostridial neurotoxins on assembly. *Embo j*, 13, 5051-61.
- HAYASHI, Y., FORD, L. K., FIORITI, L., MCGURK, L. & ZHANG, M. 2021. Liquid-Liquid Phase Separation in Physiology and Pathophysiology of the Nervous System. *The Journal of Neuroscience*, 41, 834-844.
- HODGES, R. S., J. SODEK, L. B. SMILLIE, AND L. JURASEK 1973. Tropomyosin: Amino Acid Sequence and Coiled-Coil Structure. *Cold Spring Harbor Symp. Quant Biol* 1972, 37, 299-310.
- HU, S.-H., LATHAM, C. F., GEE, C. L., JAMES, D. E. & MARTIN, J. L. 2007. Structure of the Munc18c/Syntaxin4 N-peptide complex defines universal features of the N-peptide binding mode of Sec1/Munc18 proteins. *Proceedings of the National Academy of Sciences*, 104, 8773-8778.
- HU, S. H., CHRISTIE, M. P., SAEZ, N. J., LATHAM, C. F., JARROTT, R., LUA, L. H., COLLINS, B. M. & MARTIN, J. L. 2011. Possible roles for Munc18-1 domain 3a and Syntaxin1 N-peptide and C-terminal anchor in SNARE complex formation. *Proc Natl Acad Sci U S A*, 108, 1040-5.
- HU, Y., ZHU, L. & MA, C. 2021. Structural Roles for the Juxtamembrane Linker Region and Transmembrane Region of Synaptobrevin 2 in Membrane Fusion. *Frontiers in Cell and Developmental Biology*, 8.
- JAHN, R. & FASSHAUER, D. 2012. Molecular machines governing exocytosis of synaptic vesicles. *Nature*, 490, 201-7.
- JIAO, J., HE, M., PORT, S. A., BAKER, R. W., XU, Y., QU, H., XIONG, Y., WANG, Y., JIN, H., EISEMANN, T. J., HUGHSON, F. M. & ZHANG, Y. 2018. Munc18-1 catalyzes neuronal SNARE assembly by templating SNARE association. *eLife*, 7, e41771.
- KAESER, P. S., DENG, L., WANG, Y., DULUBOVA, I., LIU, X., RIZO, J. & SÜDHOF, T. C. 2011. RIM Proteins Tether Ca²⁺ Channels to Presynaptic Active Zones via a Direct PDZ-Domain Interaction. *Cell*, 144, 282-295.
- KASULA, R., CHAI, Y. J., BADEMOSI, A. T., HARPER, C. B., GORMAL, R. S., MORROW, I. C., HOSY, E., COLLINS, B. M., CHOQUET, D., PAPADOPULOS, A. & MEUNIER, F. A. 2016. The Munc18-1 domain 3a hinge-loop controls syntaxin-1A nanodomain assembly and engagement with the SNARE complex during secretory vesicle priming. *J Cell Biol*, 214, 847-58.
- KIM, E. & SHENG, M. 2004. PDZ domain proteins of synapses. *Nature Reviews Neuroscience*, 5, 771-781.
- KLOEPPER, T. H., KIENLE, C. N. & FASSHAUER, D. 2007. An elaborate classification of SNARE proteins sheds light on the conservation of the eukaryotic endomembrane system. *Mol Biol Cell*, 18, 3463-71.

- LAI, Y., CHOI, U. B., LEITZ, J., RHEE, H. J., LEE, C., ALTAS, B., ZHAO, M., PFUETZNER, R. A., WANG, A. L., BROSE, N., RHEE, J. & BRUNGER, A. T. 2017. Molecular Mechanisms of Synaptic Vesicle Priming by Munc13 and Munc18. *Neuron*, 95, 591-607.e10.
- LI, W., MA, C., GUAN, R., XU, Y., TOMCHICK, D. R. & RIZO, J. 2011. The crystal structure of a Munc13 C-terminal module exhibits a remarkable similarity to vesicle tethering factors. *Structure*, 19, 1443-55.
- LINDAU, M., HALL, BENJAMIN A., CHETWYND, A., BECKSTEIN, O. & SANSOM, MARK S. P. 2012. Coarse-Grain Simulations Reveal Movement of the Synaptobrevin C-Terminus in Response to Piconewton Forces. *Biophysical Journal*, 103, 959-969.
- MA, C., LI, W., XU, Y. & RIZO, J. 2011. Munc13 mediates the transition from the closed syntaxin-Munc18 complex to the SNARE complex. *Nat Struct Mol Biol*, 18, 542-9.
- MA, C., SU, L., SEVEN, A. B., XU, Y. & RIZO, J. 2013. Reconstitution of the vital functions of Munc18 and Munc13 in neurotransmitter release. *Science*, 339, 421-5.
- MARGITTAI, M., FASSHAUER, D., JAHN, R. & LANGEN, R. 2003. The Habc domain and the SNARE core complex are connected by a highly flexible linker. *Biochemistry*, 42, 4009-14.
- MARTIN, S., PAPADOPULOS, A., TOMATIS, VANESA M., SIERECKI, E., MALINTAN, NANCY T., GORMAL, RACHEL S., GILES, N., JOHNSTON, WAYNE A., ALEXANDROV, K., GAMBIN, Y., COLLINS, BRETT M. & MEUNIER, FREDERIC A. 2014. Increased Polyubiquitination and Proteasomal Degradation of a Munc18-1 Disease-Linked Mutant Causes Temperature-Sensitive Defect in Exocytosis. *Cell Reports*, 9, 206-218.
- MARTIN, S., TOMATIS, V. M., PAPADOPULOS, A., CHRISTIE, M. P., MALINTAN, N. T., GORMAL, R. S., SUGITA, S., MARTIN, J. L., COLLINS, B. M. & MEUNIER, F. A. 2013. The Munc18-1 domain 3a loop is essential for neuroexocytosis but not for syntaxin-1A transport to the plasma membrane. *J Cell Sci*, 126, 2353-60.
- MEIJER, M., BURKHARDT, P., DE WIT, H., TOONEN, R. F., FASSHAUER, D. & VERHAGE, M. 2012. Munc18-1 mutations that strongly impair SNARE-complex binding support normal synaptic transmission. *EMBO J*, 31, 2156-68.
- MEIJER, M., CIJSOUW, T., TOONEN, R. F. & VERHAGE, M. 2015. Synaptic Effects of Munc18-1 Alternative Splicing in Excitatory Hippocampal Neurons. *PLoS one*, 10, e0138950-e0138950.
- MEIJER, M., DORR, B., LAMMERTSE, H. C., BLITHIKIOTI, C., VAN WEERING, J. R., TOONEN, R. F., SOLLNER, T. H. & VERHAGE, M. 2018. Tyrosine phosphorylation of Munc18-1 inhibits synaptic transmission by preventing SNARE assembly. *Embo j*, 37, 300-320.
- MILOVANOVIC, D., WU, Y., BIAN, X. & DE CAMILLI, P. 2018. A liquid phase of synapsin and lipid vesicles. *Science*, 361, 604-607.
- MISURA, K. M., SCHELLER, R. H. & WEIS, W. I. 2000. Three-dimensional structure of the neuronal-Sec1-syntaxin 1a complex. *Nature*, 404, 355-62.
- MOREY, C. 2015. Role of Munc18c in SNARE mediated exocytosis. *University of Lausanne*, PhD thesis.
- MOREY, C., KIENLE, C. N., KLOPPER, T. H., BURKHARDT, P. & FASSHAUER, D. 2017. Evidence for a conserved inhibitory binding mode between the membrane fusion assembly factors Munc18 and syntaxin in animals. *J Biol Chem*, 292, 20449-20460.
- MORRIS, A. L., MACARTHUR, M. W., HUTCHINSON, E. G. & THORNTON, J. M. 1992. Stereochemical quality of protein structure coordinates. *Proteins*, 12, 345-64.
- MUNCH, A. S., KEDAR, G. H., VAN WEERING, J. R., VAZQUEZ-SANCHEZ, S., HE, E., ANDRE, T., BRAUN, T., SOLLNER, T. H., VERHAGE, M. & SORENSEN, J. B.

2016. Extension of Helix 12 in Munc18-1 Induces Vesicle Priming. *J Neurosci*, 36, 6881-91.
- MUNSON, M., CHEN, X., COCINA, A. E., SCHULTZ, S. M. & HUGHSON, F. M. 2000. Interactions within the yeast t-SNARE Sso1p that control SNARE complex assembly. *Nat Struct Biol*, 7, 894-902.
- NOVICK, P. & SCHEKMAN, R. 1979. Secretion and cell-surface growth are blocked in a temperature-sensitive mutant of *Saccharomyces cerevisiae*. *Proc Natl Acad Sci U S A*, 76, 1858-62.
- PARISOTTO, D., PFAU, M., SCHEUTZOW, A., WILD, K., MAYER, M. P., MALSAM, J., SINNING, I. & SOLLNER, T. H. 2014. An extended helical conformation in domain 3a of Munc18-1 provides a template for SNARE (soluble N-ethylmaleimide-sensitive factor attachment protein receptor) complex assembly. *J Biol Chem*, 289, 9639-50.
- PARK, S., BIN, N.-R., YU, B., WONG, R., SITARSKA, E., SUGITA, K., MA, K., XU, J., TIEN, C.-W., ALGOUNEH, A., TURLOVA, E., WANG, S., SIRIYA, P., SHAHID, W., KALIA, L., FENG, Z.-P., MONNIER, P. P., SUN, H.-S., ZHEN, M., GAO, S., RIZO, J. & SUGITA, S. 2017. UNC-18 and Tomosyn antagonistically control synaptic vesicle priming downstream of UNC-13 in *C. elegans*. *The Journal of Neuroscience*.
- PARK, S., BIN, N. R., MICHAEL RAJAH, M., KIM, B., CHOU, T. C., KANG, S. Y., SUGITA, K., PARSAUD, L., SMITH, M., MONNIER, P. P., IKURA, M., ZHEN, M. & SUGITA, S. 2016. Conformational states of syntaxin-1 govern the necessity of N-peptide binding in exocytosis of PC12 cells and *Caenorhabditis elegans*. *Mol Biol Cell*, 27, 669-85.
- PEI, J., MA, C., RIZO, J. & GRISHIN, N. V. 2009. Remote homology between Munc13 MUN domain and vesicle tethering complexes. *Journal of molecular biology*, 391, 509-517.
- PEVSNER, J., HSU, S.-C., BRAUN, J. E. A., CALAKOS, N., TING, A. E., BENNETT, M. K. & SCHELLER, R. H. 1994a. Specificity and regulation of a synaptic vesicle docking complex. *Neuron*, 13, 353-361.
- PEVSNER, J., HSU, S. C. & SCHELLER, R. H. 1994b. n-Sec1: a neural-specific syntaxin-binding protein. *Proc Natl Acad Sci U S A*, 91, 1445-9.
- PEVSNER, J., HSU, S. C. & SCHELLER, R. H. 1994c. n-Sec1: a neural-specific syntaxin-binding protein. *Proceedings of the National Academy of Sciences*, 91, 1445-1449.
- PIOVESAN, D., MINERVINI, G. & TOSATTO, S. C. 2016. The RING 2.0 web server for high quality residue interaction networks. *Nucleic Acids Res*, 44, W367-74.
- POBBATI, A. V., STEIN, A. & FASSHAUER, D. 2006. N- to C-terminal SNARE complex assembly promotes rapid membrane fusion. *Science*, 313, 673-6.
- RAMACHANDRAN, G. N., RAMAKRISHNAN, C. & SASISEKHARAN, V. 1963. Stereochemistry of polypeptide chain configurations. *J Mol Biol*, 7, 95-9.
- RAMOS-MIGUEL, A., HERCHER, C., BEASLEY, C. L., BARR, A. M., BAYER, T. A., FALKAI, P., LEURGANS, S. E., SCHNEIDER, J. A., BENNETT, D. A. & HONER, W. G. 2015. Loss of Munc18-1 long splice variant in GABAergic terminals is associated with cognitive decline and increased risk of dementia in a community sample. *Molecular Neurodegeneration*, 10, 65.
- SCHMITZ, S. K., KING, C., KORTLEVEN, C., HUSON, V., KROON, T., KEVENAAR, J. T., SCHUT, D., SAARLOOS, I., HOETJES, J. P., DE WIT, H., STIEDL, O., SPIJKER, S., LI, K. W., MANSVELDER, H. D., SMIT, A. B., CORNELISSE, L. N., VERHAGE, M. & TOONEN, R. F. 2016. Presynaptic inhibition upon CB1 or mGlu2/3 receptor activation requires ERK/MAPK phosphorylation of Munc18-1. *Embo j*, 35, 1236-50.

- SCHÖNICHEN, A., WEBB, B. A., JACOBSON, M. P. & BARBER, D. L. 2013. Considering Protonation as a Posttranslational Modification Regulating Protein Structure and Function. *Annual Review of Biophysics*, 42, 289-314.
- SHEN, M.-Y. & SALI, A. 2006. Statistical potential for assessment and prediction of protein structures. *Protein science : a publication of the Protein Society*, 15, 2507-2524.
- SHIN, Y.-K. 2013. Two gigs of Munc18 in membrane fusion. *Proceedings of the National Academy of Sciences*, 110, 14116-14117.
- SHU, T., JIN, H., ROTHMAN, J. E. & ZHANG, Y. 2020. Munc13-1 MUN domain and Munc18-1 cooperatively chaperone SNARE assembly through a tetrameric complex. *Proceedings of the National Academy of Sciences*, 117, 1036-1041.
- SIDDIQUI, T. J., VITES, O., STEIN, A., HEINTZMANN, R., JAHN, R. & FASSHAUER, D. 2007. Determinants of Synaptobrevin Regulation in Membranes. *Molecular Biology of the Cell*, 18, 2037-2046.
- SITARSKA, E., XU, J., PARK, S., LIU, X., QUADE, B., STEPIEN, K., SUGITA, K., BRAUTIGAM, C. A., SUGITA, S. & RIZO, J. 2017. Autoinhibition of Munc18-1 modulates synaptobrevin binding and helps to enable Munc13-dependent regulation of membrane fusion. *Elife*, 6.
- STAMBERGER, H., NIKANOROVA, M., WILLEMSSEN, M. H., ACCORSI, P., ANGRIMAN, M., BAIER, H., BENKEL-HERRENBRUECK, I., BENOIT, V., BUDETTA, M., CALIEBE, A., CANTALUPO, G., CAPOVILLA, G., CASARA, G., COURAGE, C., DEPREZ, M., DESTREE, A., DILENA, R., ERASMUS, C. E., FANNEMEL, M., FJAER, R., GIORDANO, L., HELBIG, K. L., HEYNE, H. O., KLEPPER, J., KLUGER, G. J., LEDERER, D., LODI, M., MAIER, O., MERKENSCHLAGER, A., MICHELBERGER, N., MINETTI, C., MUHLE, H., PHALIN, J., RAMSEY, K., ROMEO, A., SCHALLNER, J., SCHANZE, I., SHINAWI, M., SLEEGERS, K., STERBOVA, K., SYRBE, S., TRAVERSO, M., TZSCHACH, A., ULDALL, P., VAN COSTER, R., VERHELST, H., VIRI, M., WINTER, S., WOLFF, M., ZENKER, M., ZOCCANTE, L., DE JONGHE, P., HELBIG, I., STRIANO, P., LEMKE, J. R., MOLLER, R. S. & WECKHUYSSEN, S. 2016. STXBPI encephalopathy: A neurodevelopmental disorder including epilepsy. *Neurology*, 86, 954-62.
- SUDHOF, T. C. 2004. The synaptic vesicle cycle. *Annu Rev Neurosci*, 27, 509-47.
- SUTTON, R. B., FASSHAUER, D., JAHN, R. & BRUNGER, A. T. 1998. Crystal structure of a SNARE complex involved in synaptic exocytosis at 2.4 Å resolution. *Nature*, 395, 347-53.
- SÖLLNER, T., BENNETT, M. K., WHITEHEART, S. W., SCHELLER, R. H. & ROTHMAN, J. E. 1993. A protein assembly-disassembly pathway in vitro that may correspond to sequential steps of synaptic vesicle docking, activation, and fusion. *Cell*, 75, 409-18.
- TOONEN, R. F. & VERHAGE, M. 2003. Vesicle trafficking: pleasure and pain from SM genes. *Trends Cell Biol*, 13, 177-86.
- VARDAR, G., SALAZAR-LÁZARO, A., BROCKMANN, M., WEBER-BOYVAT, M., ZOBEL, S., KUMBOL, V. W.-A., TRIMBUCH, T. & ROSENMUND, C. 2021. Reexamination of N-terminal domains of syntaxin-1 in vesicle fusion from central murine synapses. *eLife*, 10, e69498.
- VAROQUEAUX, F. & FASSHAUER, D. 2017. Getting Nervous: An Evolutionary Overhaul for Communication. *Annu Rev Genet*, 51, 455-476.
- VAROQUEAUX, F., SIGLER, A., RHEE, J.-S., BROSE, N., ENK, C., REIM, K. & ROSENMUND, C. 2002. Total arrest of spontaneous and evoked synaptic transmission

- but normal synaptogenesis in the absence of Munc13-mediated vesicle priming. *Proceedings of the National Academy of Sciences*, 99, 9037-9042.
- VERHAGE, M., MAIA, A. S., PLOMP, J. J., BRUSSAARD, A. B., HEEROMA, J. H., VERMEER, H., TOONEN, R. F., HAMMER, R. E., VAN DEN BERG, T. K., MISSLER, M., GEUZE, H. J. & SUDHOF, T. C. 2000. Synaptic assembly of the brain in the absence of neurotransmitter secretion. *Science*, 287, 864-9.
- WANG, S., CHOI, U. B., GONG, J., YANG, X., LI, Y., WANG, A. L., YANG, X., BRUNGER, A. T. & MA, C. 2017. Conformational change of syntaxin linker region induced by Munc13s initiates SNARE complex formation in synaptic exocytosis. *The EMBO journal*, 36, 816-829.
- WANG, S., LI, Y., GONG, J., YE, S., YANG, X., ZHANG, R. & MA, C. 2019. Munc18 and Munc13 serve as a functional template to orchestrate neuronal SNARE complex assembly. *Nature Communications*, 10, 69.
- WANG, X., GONG, J., ZHU, L., WANG, S., YANG, X., XU, Y., YANG, X. & MA, C. 2020. Munc13 activates the Munc18-1/syntaxin-1 complex and enables Munc18-1 to prime SNARE assembly. *Embo j*, 39, e103631.
- WEBB, B. & SALI, A. 2016. Comparative Protein Structure Modeling Using MODELLER. *Curr Protoc Bioinformatics*, 54, 5.6.1-5.6.37.
- XU, Y., SU, L. & RIZO, J. 2010. Binding of Munc18-1 to synaptobrevin and to the SNARE four-helix bundle. *Biochemistry*, 49, 1568-76.
- YAMAGUCHI, T., DULUBOVA, I., MIN, S.-W., CHEN, X., RIZO, J. & SÜDHOF, T. C. 2002. Sly1 Binds to Golgi and ER Syntaxins via a Conserved N-Terminal Peptide Motif. *Developmental Cell*, 2, 295-305.
- YANG, X., WANG, S., SHENG, Y., ZHANG, M., ZOU, W., WU, L., KANG, L., RIZO, J., ZHANG, R., XU, T. & MA, C. 2015. Syntaxin opening by the MUN domain underlies the function of Munc13 in synaptic-vesicle priming. *Nature Structural & Molecular Biology*, 22, 547.
- YEH, C.-Y., YE, Z., MOUTAL, A., GAUR, S., HENTON, A. M., KOUVAROS, S., SALOMAN, J. L., HARTNETT-SCOTT, K. A., TZOUNOPOULOS, T., KHANNA, R., AIZENMAN, E. & CAMACHO, C. J. 2019. Defining the Kv2.1–syntaxin molecular interaction identifies a first-in-class small molecule neuroprotectant. *Proceedings of the National Academy of Sciences*, 116, 15696-15705.
- YU, I. M. & HUGHSON, F. M. 2010. Tethering factors as organizers of intracellular vesicular traffic. *Annu Rev Cell Dev Biol*, 26, 137-56.
- ZHANG, Y. & HUGHSON, F. M. 2021. Chaperoning SNARE Folding and Assembly. *Annu Rev Biochem*, 90, 581-603.
- ZHANG, Z., LI, W., YANG, G., LU, X., QI, X., WANG, S., CAO, C., ZHANG, P., REN, J., ZHAO, J., ZHANG, J., HONG, S., TAN, Y., BURCHFIELD, J., YU, Y., XU, T., YAO, X., JAMES, D., FENG, W. & CHEN, Z. 2020. CASK modulates the assembly and function of the Mint1/Munc18-1 complex to regulate insulin secretion. *Cell Discovery*, 6, 92.
- ŠALI, A. & BLUNDELL, T. L. 1993. Comparative Protein Modelling by Satisfaction of Spatial Restraints. *Journal of Molecular Biology*, 234, 779-815.

Appendix

Modeller Script 1: align2d.py

```
1 from modeller import *
2
3 env = Environ()
4 aln = Alignment(env)
5 mdl = Model(env, file='6xm1', model_segment=('FIRST:A','LAST:B'))
6 aln.append_model(mdl, align_codes='6xm1', atom_files='6xm1.pdb')
7 aln.append(file='M18Syx.ali', align_codes='M18Syx')
8 aln.align2d(max_gap_length=50)
9 aln.write(file='M18Syx-6xm1.ali', alignment_format='PIR')
10 aln.write(file='M18Syx-6xm1.pap', alignment_format='PAP')
11
```

Modeller Script 2: model-single.py

```
1 from modeller import *
2 from modeller.automodel import *
3 from modeller import soap_protein_od
4
5 env = Environ()
6 a = AutoModel(env, alnfile='M18Syx-6xm1.ali',
7               knowns='6xm1', sequence='M18Syx',
8               assess_methods=(assess.DOPE,
9                               soap_protein_od.Scorer(),
10                              assess.GA341))
11 a.starting_model = 1
12 a.ending_model = 100
13 a.make()
```

Modeller Script 3: evaluate_model.py

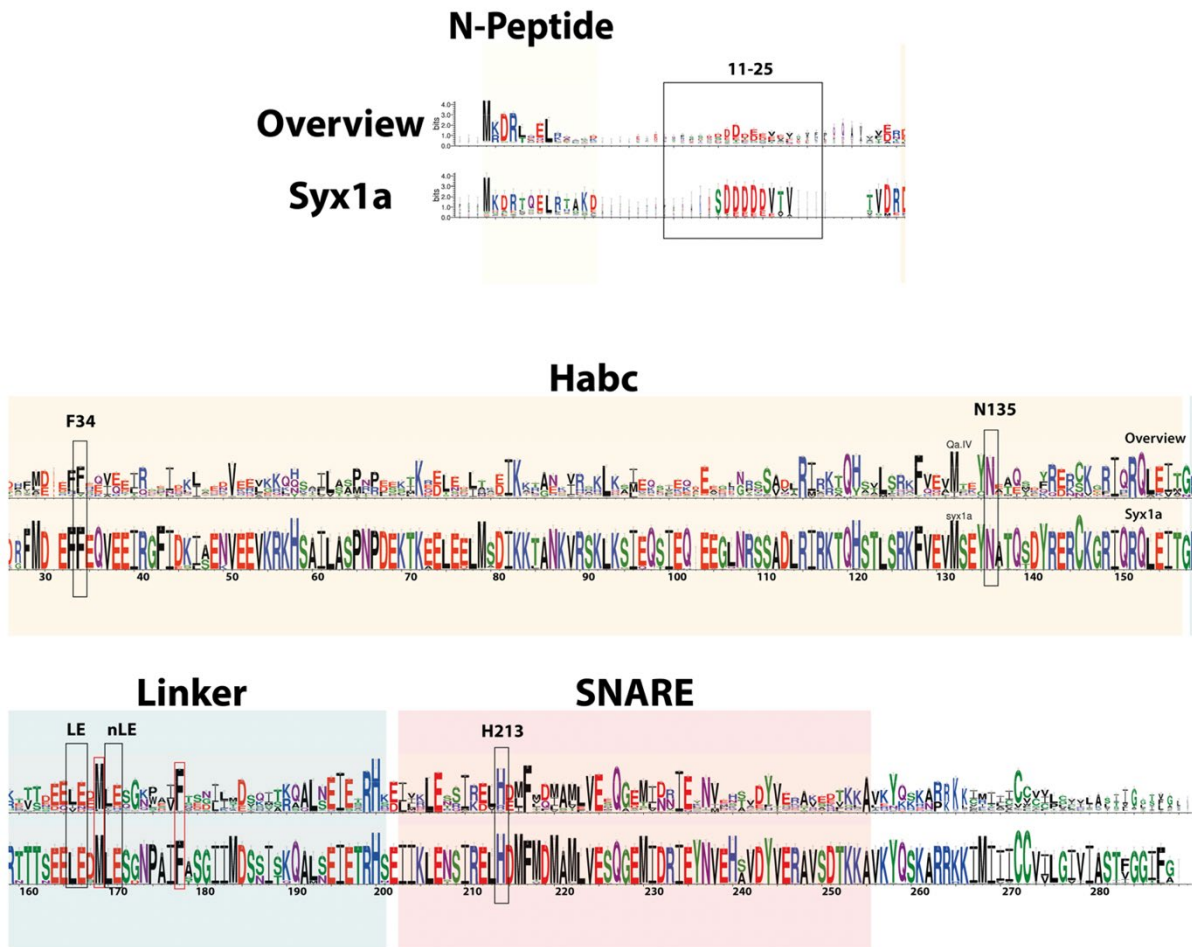
```
1 from modeller import *
2 from modeller.scripts import complete_pdb
3
4 log.verbose() # request verbose output
5 env = Environ()
6 env.libs.topology.read(file='${LIB}/top_heav.lib') # read topology
7 env.libs.parameters.read(file='${LIB}/par.lib') # read parameters
8
9 # read model file
10 mdl = complete_pdb(env, 'M18Syx.B99990080.pdb')
11
12 # Assess with DOPE:
13 s = Selection(mdl) # all atom selection
14 s.assess_dope(output='ENERGY_PROFILE NO_REPORT', file='M18.profile',
15              normalize_profile=True, smoothing_window=15)
16
```

Modeller Script 4: model-loop-define.py

```
1 from modeller import *
2 from modeller.automodel import *
3
4 log.verbose()
5 env = Environ()
6
7 env.io.atom_files_directory = ['.', '../atom_files']
8
9 # Create a new class based on 'LoopModel' so that we can redefine
10 # select_loop_atoms
11 class MyLoop(LoopModel):
12     # This routine picks the residues to be refined by loop modeling
13     def select_loop_atoms(self):
14         # Two residue ranges (both will be refined simultaneously)
15         return Selection(self.residue_range('616:B', '626:B'),
16                         self.residue_range('616:B', '626:B'),
17                         self.residue_range('769:B', '779:B'),
18                         self.residue_range('626:B', '636:B'))
19
20 a = MyLoop(env,
21           alnfile = 'M18Syx-6xm1.ali',      # alignment filename
22           knowns   = '6xm1',                # codes of the templates
23           sequence = 'M18Syx',              # code of the target
24           loop_assess_methods=assess.DOPE) # assess each loop with DOPE
25 a.starting_model= 1                        # index of the first model
26 a.ending_model  = 1000                     # index of the last model
27
28 a.loop.starting_model = 1                  # First loop model
29 a.loop.ending_model   = 2                  # Last loop model
30
31 a.make()                                   # do modeling and loop refinement
```

AFigure 1: Screenshots of Modeller scripts.

Screenshots of selected scripts for each method described (align2d.py, model-single.py, evaluate_model.py, model-loop-define.py) at the modeller protocol for the production of the homologous complexes.



AFigure 2: Weblogo representations for Syntaxin conservation from vertebrates.

The weblogos were constructed from the multiple sequence alignments of ~600 Syntaxin sequences from vertebrates. The weblogo for the total Syntaxin homologs (top) and Syntaxin-1a (bottom) are annotated with the domains - N-peptide, Habc and SNARE domains. Conserved aminoacids (F34, N135m L165, E166, M168, F177, and H213 and region 11-25 mentioned in this study are indicated. Alignment result by Dr. Nickias Kienle.

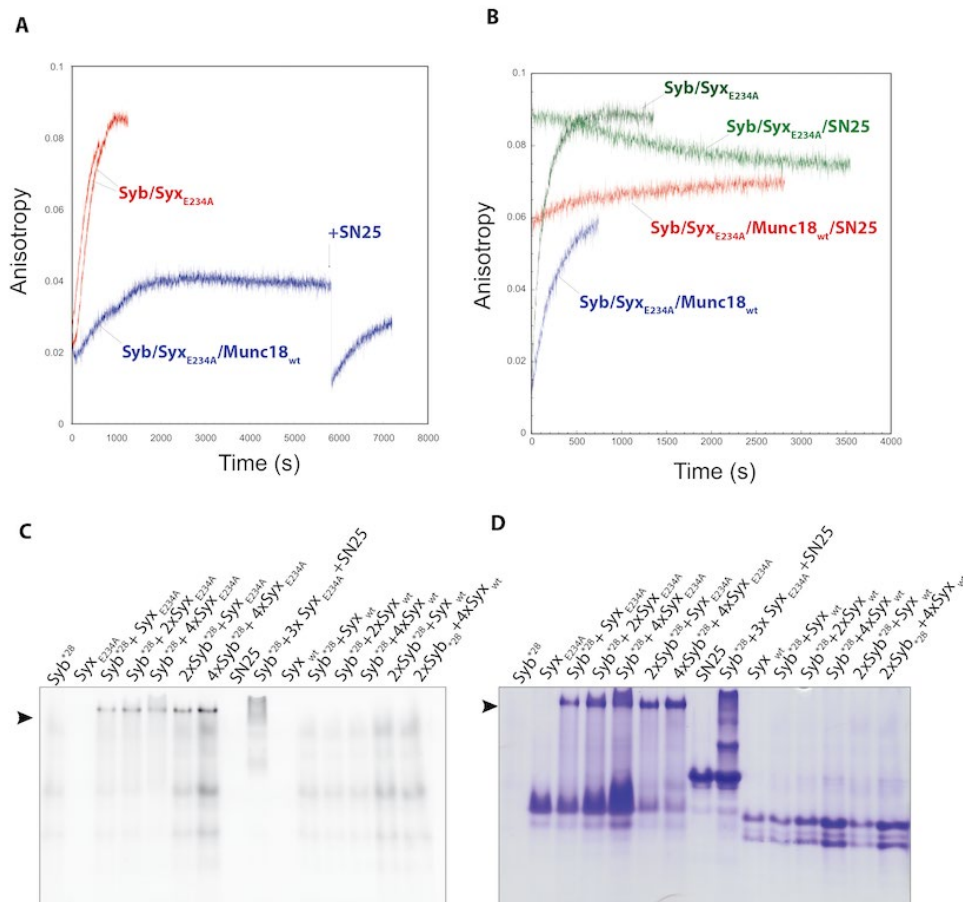


Figure 3: Syntactin_{E234A} forms a binary complex with Synaptobrevin. **A.** Syb^{*28} fluorescence anisotropy increases immediately when Syntactin_{E234A} is added to the cuvette (red traces). Presence of Munc18_{wt} is affecting the rate of increase (blue trace). Addition of SNAP25 causes a sudden change in the Synaptobrevin increase rate. **B.** Like (A), Syntactin_{E234A}/Syb^{*28} anisotropy rate changed when SNAP25 was added to the cuvette. **C-D.** Native gel electrophoresis of Syb^{*28}/Syntactin_{E234A} and Syb^{*28}/Syntactin_{wt} mixtures' gradients. After the electrophoresis, the gel was exposed to blue light (C) and stained with Coomassie (D). A band corresponding to the Syb^{*28}/Syntactin_{E234A} complex appeared, confirming the anisotropy measurements.

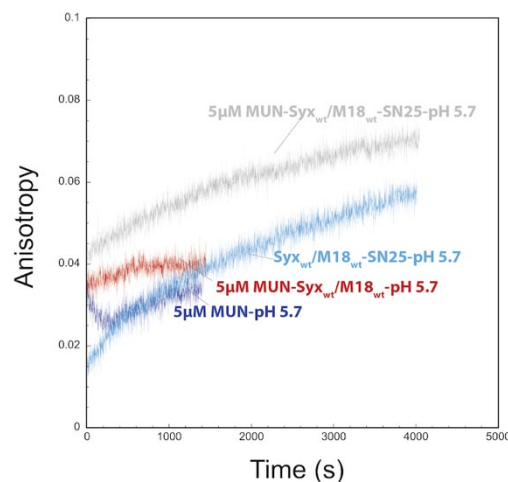


Figure 4: A. Synaptobrevin^{*28} fluorescence anisotropy at pH5.7 in the presence of 5µM MUN (blue), and Munc18_{wt}/Syntactin_{wt} (red), and after the addition of SNAP25 (grey).

IOANNA STEFANI

Mobile No: +41786940224
E-mail: ioanna.stefani@unil.ch
Mother tongue: Greek

Foreign languages: English (Fluent), German (B1), French (A2).

Nationality: Cypriot
DOB: 04 August, 1993

Education

2017 – (2022) PhD in Life Sciences

Dept: Fundamental Neuroscience & Computational Biology, University of Lausanne, Switzerland

2015 – 2016 Master by Research (MRes) in Protein Structure and Function

Grade: 65%

Dept: Biology and Biochemistry, University of Bath, UK

2011 – 2015 Ptychion (BSc Hons) in Molecular Biology and Genetics

Grade: 7.8/10

Dept: Molecular Biology and Genetics, Democritus University of Thrace, Greece

Research Experience

02/2017- University of Lausanne, Switzerland

Departments of Computational Biology and Fundamental Neuroscience,
Supervisor: Prof. Dirk Fasshauer
PhD student

Thesis title: "Probing the conformational flexibility of the Munc18-1/Syntaxin-1a pair."

Experimental design and performance of **biophysical**, **biochemical** and *in silico* experiments for **protein-protein interaction** studies. Hands on experience in design, optimization and performance of **recombinant protein expression and purification** (affinity and ion exchange **chromatography using FPLC (AKTA)** system), *in vitro* protein-protein interactions' investigation using binding assays (**Size exclusion chromatographies, Native and SDS PAGE, Fluorescence Spectroscopy, ITC, FRET**) as well as *in silico* study of conformational flexibility using **homology modelling**.

04/2016 -08/2016 University of Bath, United Kingdom

Department of Biology and Biochemistry,
Supervisor: Dr Julien Licchesi
MRes Project 2 student

Thesis title: "Development of a probing system for the localization of an E3 ubiquitin ligase"

Molecular cloning for the construction of a reporter and its **evaluation in established cell lines**.

10/2015 - 02/2016 University of Bath, United Kingdom

Department of Biology and Biochemistry,
Supervisor: Dr Christopher R Pudney
MRes Project 1 student

Thesis title: "Tryptophan as a probe: A study on the application and optimization of Site-Directed Mutagenesis for the labelling of NEMO (NF- κ B Essential Modulator) peptide with tryptophan residues."

Molecular cloning, Site directed mutagenesis and **recombinant protein expression**.

06/2014 - 08/2015 Democritus University of Thrace, Greece

Department of Molecular Biology and Genetics,
Supervisor: Giannoulis Fakis, D. Phil

Undergraduate dissertation student and undergraduate research placement

Thesis title: Effects of naturally-occurring polymorphisms on the recombinant expression levels and enzymatic activity of the Rhesus monkey arylamine N-acetyltransferase 1 (NAT1).

Molecular cloning, recombinant expression, colorimetric (DTNB) *in vitro* enzymatic activity assays, western blotting.

Scientific Skills and Achievements

Publications

(2022): **Stefani Ioanna**, Iwaszkiewicz Justyna, Zoete Vincent, Fasshauer Dirk, "Syntaxin-1a undergoes a conformational transition while in complex with Munc18-1. (In preparation)

2019: Boukouvala S, Chasapopoulou Z, Giannouri D, Kontomina E, Marinakis N, Rizou SV, **Stefani I**, Tsirka T, Veyssière C, Zaliou S, Sabbagh A, Crouau -Roy B, Fakis G. "Population variability of rhesus macaque (*Macaca mulatta*) NAT 1 gene for arylamine N-acetyltransferase 1: Functional effects and comparison with human." *Sci Rep.* 2019 Jul 29;9(1):10937. <https://doi.org/10.1038/s41598-019-47485-x>

Conference presentations

Oral presentations:

2022: Biophysics of the Brain Conference, 1-2/3/2022, Online

2020: 64th Annual Meeting of the Biophysical Society, February, San Diego, California.

2019, 2017, 2015: Symposium of Biology Students in Europe in Glasgow (UK), Lund (Sweden) and Alexandroupolis, (Greece) respectively.

Poster presentations:

2019: *i.*, September, 7th European Synapse Meeting, Lausanne, Switzerland, *ii.*, April, ADAS D.Day, Lausanne, Switzerland.

2018: DNF Symposium, Lausanne, Switzerland.

2016: Symposium of Biology Students in Europe, Vila Real, Portugal.

2015: 66th Annual Conference of the Greek Society for Biochemistry and Molecular Biology, Athens, Greece.

Prizes and Awards

Cyprus State Scholarship recipient for undergraduate studies (2011-2015) by the Cyprus State Scholarship Foundation with annual renewal upon fulfillment of merit requirements.

Teaching and Supervision

2017- 2021: Preparation and teaching of a two-day practical course on "Protein expression, purification assays for in vitro observations of protein-protein interactions" as part of the 6th semester course: "Dynamic Cell".

2015: Pedagogical and Didactic competence certification issued by Democritus University of Thrace after completion of respective courses' cycle (Marks: 9,4 out of maximal 10).

Supervision:

09/2018-12/2018: **Three-month** long supervision of **master** student Yasmine Genolet, for her first step research project in the programme of Molecular Life Sciences, UniL

07/2018-08/2018: **Two-month** long supervision of **undergraduate** student Akansha Mehta as part of the international Summer Undergraduate Research (SUR) programme of UniL.

In both cases supervision included **experimental design, teaching, guidance** in research, techniques, troubleshooting, writing and presentations.

Organizational and Communication Skills (Extracurricular activities)

Organizations:

2019-2020 Co-president of ADAS (Association of doctorate students and assistants of the Faculty of Biology and Medicine) committee.

Duties included the representation of PhD students and PostDocs at the University commissions, communication with the other associations, the doctoral school, the Faculty and the Direction. Also, organization of courses, seminars, events and social activities for the students.

2018-2021 Frequent member of the ADAS committee.

Contributed to the organization of D.Day 2019 as part of the abstract selection group. Represented the UniL to the annual meeting of Doctoral Schools of Europe (Orpheus) 2019 in Dublin. Also organized the ADAS Pubquiz 2019.

2015: Volunteer at the organization of SymbioSE (Symposium of Biology Students in Europe) 2015 in Alexandroupolis, Greece.

Main tasks included logistics and keeping up on schedule.

2009-2010: Member of the European Youth Parliament

Participated at 3 sessions (Larnaca, Cyprus 2010, Graz, Austria 2010 and Limassol, Cyprus 2009)

Public outreach:

07/2021: Protein 3D Shapes: Youtube outreach video <https://www.youtube.com/watch?v=IoT6eQeWMhs>

07/2020: Participation at the 3 Minutes Thesis online competition organized by the LMB-UNIGE 2020 Life Sciences Symposium.

02/2020: Guest blogger Annual Meeting of the Biophysical Society (<https://www.biophysics.org/blog/author/ioanna-stefani>)

2019-2020: Organizer of Café Scientifique Lausanne (Press release: <https://news.unil.ch/display/1580389409383>). Responsible for speaker selection, invitation and communication. Involved in advertising and outreach.

07/2019: Volunteer at We Scientists 2035 workshop at EPFL organized by the Swiss Academy of Sciences.

05/2019: Volunteer at the organization of Pint of Science Lausanne.

04/2017: Participant at FameLab-Talking Science Switzerland preliminaries.

12/2016: Volunteer at the 1st Cyprus Science Festival at UCLan Cyprus.

Responsible for the preparation and demonstration of the "DNA molecule of Life" station. Participants were introduced to the basics of DNA and isolated themselves DNA from bananas using household products.

11/2016: Volunteer at TEDxLimassol 2016

03-05/2014: Participant and finalist at FameLab Cyprus preliminaries and final.